moffatt & nichol

Carmel River Lagoon

Sediment Transport Study

PRODUCED FOR DENISE DUFFY & ASSOCIATES

FEBRUARY 2021

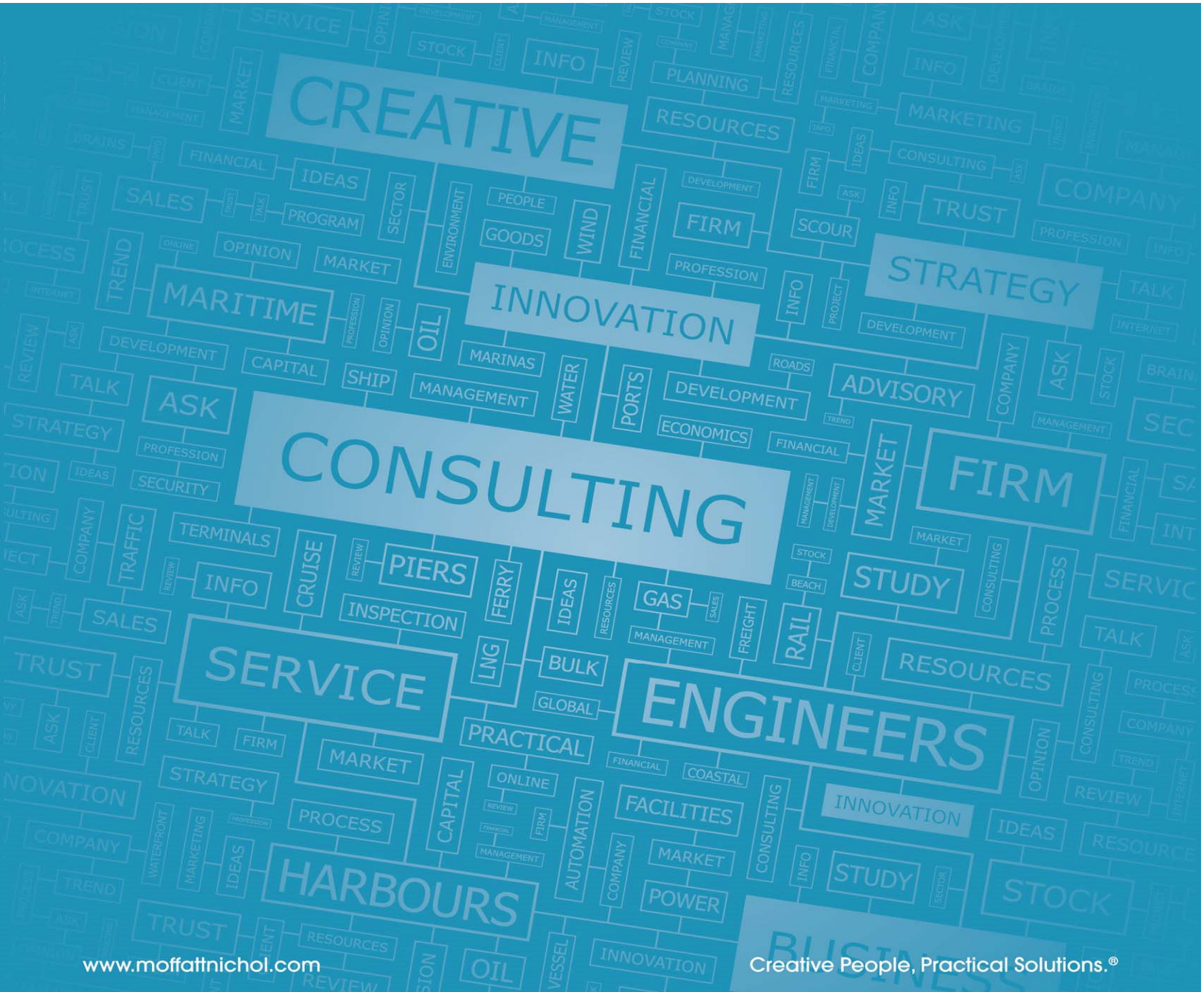

Document Verification

Client	Denise Duffy & Associates
Project name	Carmel River Lagoon
Document title	Sediment Transport Study
Document subtitle	
Status	Draft
Date	February 17, 2021
Project number	11132
File reference	

Revision	Description	Issued by	Date	Checked
0	Draft for Review	M. Jorgensen	February 17, 2020	R. Dornhelm

Produced by:
Moffatt & Nichol
2185 N. California Blvd., Suite 500
Walnut Creek, CA 94596-3500
T 925.944.5411
www.moffattnichol.com

Table of Contents

List of Figures

List of Tables

Glossary

AP	Arrowhead Point
BFE	Base Flood Elevation
CB	Carmel Beach
CRL	Carmel River Lagoon
CRSB	Carmel River State Beach
CRSB	Carmel River State Beach
DD&A	Denise Duffy & Associates
ENSO	El Niño Southern Oscillation
FEMA	Federal Emergency Management Agency
IPCC	International Panel on Climate Change
lat	Latitude
lon	Longitude
MB	Monastery Beach
MN	Moffatt & Nichol
NDBC	National Data Buoy Center
NGS	National Geodetic Survey
nm	Nautical miles
NOAA	National Oceanic and Atmospheric Administration
ONI	Oceanic Niño Index
OPC	{California} Ocean Protection Council
PP	Pescadero Point
SC	Stillwater Cove
SLR	Sea-Level Rise
SWEL	Stillwater Elevation
TAC	Technical Advisory Committee
USGS	United States Geological Survey
WC	Whaler's Cove

Executive Summary

The Carmel littoral cell extends from Cypress Point to Point Lobos, Figure 1-1. This report provides an overview of sediment transport patterns within the Carmel littoral cell and the beach morphology and sediment dynamics of Carmel River State Beach (CRSB) and the Carmel River Lagoon (CRL).

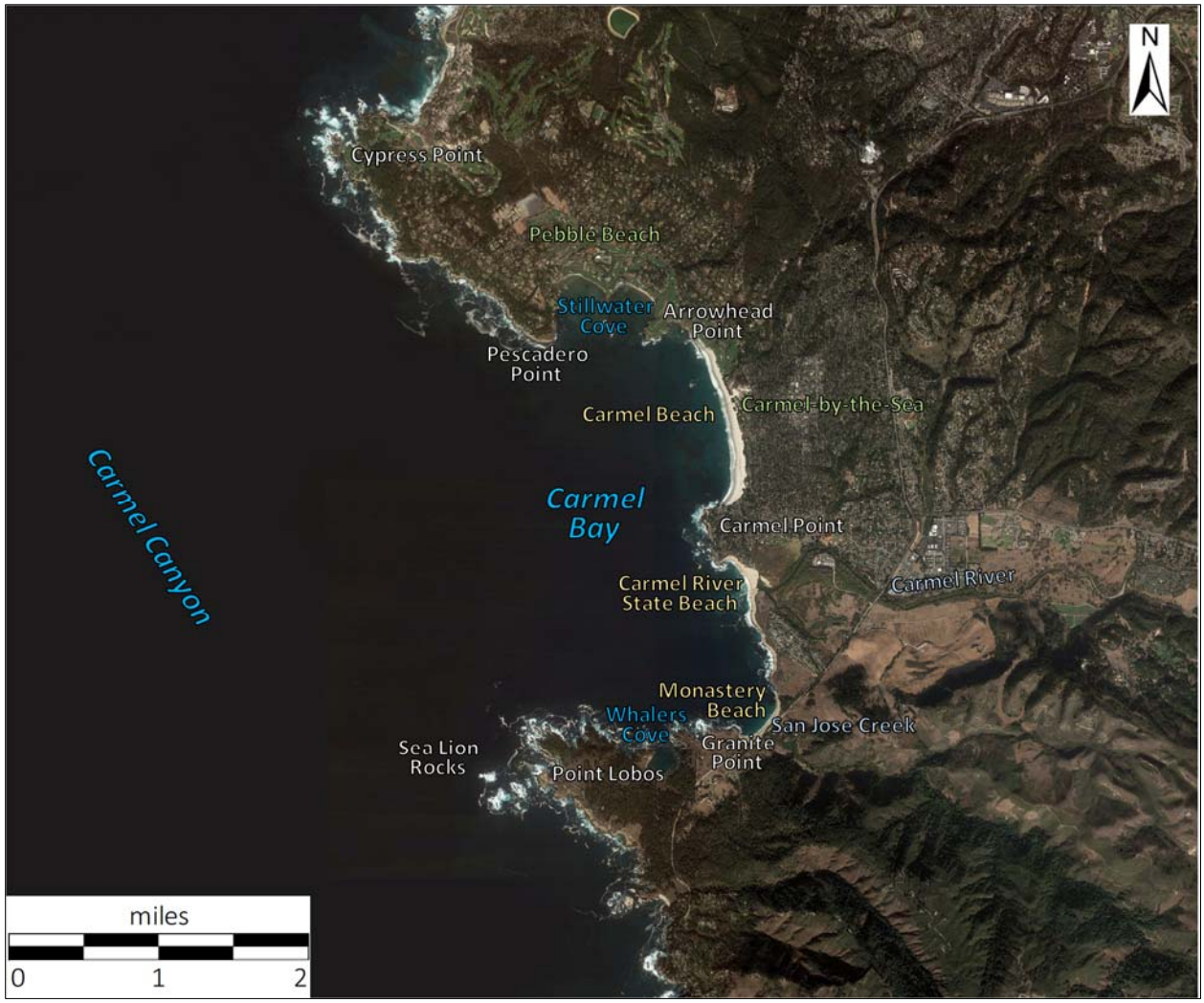

Figure 1-1: Overview of Carmel Bay.

The analysis finds the following:

Carmel Littoral Cell

The Carmel littoral cell is contained between Cypress Point and Point Lobos. The general littoral transport direction is from north to south. The main input of sediment to the system comes from

breakdown and erosion of the granodiorite rock formations along the coast. The Carmel River provides sand to the Carmel River State Beach. San Jose Creek similarly provides sand to Monastery Beach. Remining creeks and streams in the area provide limited input of sand to the shoreline. The pocket beaches and crenulate bay shaped sections of shoreline: Stillwater Cove (SC), Carmel Beach (CB), Carmel River State Beach (CRSB), Monastery Beach (MB), and Whaler's Cove (WC) comprise quasi-stable littoral sub-cells. However, waves during winter storms can be large enough to induce longshore sand transport between these cells in a southward direction. Such storm events are infrequent and highly episodic.

CRSB can therefore be characterized as a quasi-stable littoral sub-cell where the primary input of sand comes from the Carmel River and there is a secondary input of sand from Carmel Beach. Wave patterns at CRSB induce a circular pattern of sediment movement where the longshore transport at the shoreline is often in a northward direction, whereas the sediment transport direction in deeper is in a southward direction. This circular pattern of sediment movement works to maintain the beach, although sand episodically moves southward past Ribera Beach towards Monastery Beach. The majority of sand volumes transported south are lost from the CRSB sub-cell and do not return. The magnitude of sand retained in the system at CRSB is therefore dependent on the wave climate from year to year, the occurrence of intermittent northwesterly high wind-wave events (during which sand is lost from the sub-cell), and sand input from the Carmel River. The latter is the most important, as a decline in sediment output from the Carmel River will lead to depletion of sediment from the system; conversely an increase can aid in restoring the beach.

Carmel Submarine Canyon

The Carmel submarine canyon is a significant element of the Carmel Littoral Cell. Sand transport south along the coast is eventually lost to the submarine canyon in the area of Monastery Beach where the submarine canyon come closest to shore and is within the active portion of the beach profile. Several mechanisms of sand loss to the submarine canyon have been identified, including: wave- and current-induced downslope migration of sand, submarine slope failures along the edge of the canyon, and rip currents. In the broader area from Pescadero Point down to CRSB large wave events during winter storms are capable of mobilizing sand to greater depths, which causes a loss of sand to the submarine canyon. Specific to CRSB, bursts of outflow from the Carmel River can wash sediment into the submarine canyon as well. The canyon acts as a sink to littoral cell system, and sediment that enters the canyon is lost from the system.

Swell Waves

Swell waves approach the coast year-round. Swell waves originating from storm systems in the North Pacific primarily occur during the fall and winter months, while swell waves from storm systems in the Southern Hemisphere tend to occur over the summer months. Swell wave events follow a sequence where the longest waves roll in first followed by progressively shorter waves until the wave trains die out. Each episode of swell can last from hours to several days, depending on the magnitude and duration of the storm system of origin.

The Carmel submarine canyon has a pronounced effect on swell waves as they propagate towards the shoreline. The canyon overall acts as a lens which focuses wave action along the cliffs from Cypress Point to Pescadero Point, at Point Lobos, and to a lesser degree focuses waves propagating towards Carmel Beach. Incident waves traveling along the canyon axis tend to disperse at the canyon heads in Carmel Bay, at CRSB, and at Monastery Beach, which produces a milder wave climate in these areas. The wave transformation caused by the canyon is to such a degree that incident swell waves end up having nearly the same angle of incidence at the shoreline irrespective of whether the swell arrives from northwesterly or southwesterly directions offshore. Wave transformation due to the submarine canyon is more significant the longer the wave periods of the incident waves, and therefore has a greater effect on swell waves.

Wind-Waves

The Carmel submarine canyon does not transform wind-waves to the same degree as swell waves. This is because the wave periods of wind-waves are significantly shorter than for swell waves. Waves associated with high winds from northwesterly directions can therefore cause intermittent bursts of sediment transport southward along the shoreline. These infrequent events can produce an exchange of sediment between the quasi-stable sub-cells of the system (SC, CB, CRSB, MB, and WC). Episodic wind events from southwesterly directions produce northward sediment transport along the shoreline. However, these events do not replenish sand to the littoral sub-cells, but rather tend to shift sand to the north within each sub-cell.

Wave Climate Interaction with Lagoon Breaching

Field observations have established that the primary agent responsible for natural lagoon breaching is inflow to the Lagoon from the Carmel River. Swell waves play a key role in closing off the breaches, but only when the discharge from the river decreases to 10 cfs or less. The primary role of swell waves is in building up the sandbar between the lagoon and the ocean. Both swell waves and wind-waves can promote migration of the breach north or south of its initial location depending on the incident wave direction; wind-waves probably more so than swell waves.

The magnitude of swell wave and wind-wave action increases in November and December around the time when initial lagoon breaching often takes place. Because the wind/wave climate is episodic, it is not possible to predict if the breach will migrate north or south, and when an initial breach may close. Swell waves combined with diminishing outflow from the Carmel River in June to July of average years result in closure of the lagoon for the season.

Sea-Level Rise Hazards

The CRSB and lagoon appear to be resilient to SLR hazards in the near-term as the Carmel River provides sufficient sediment annually to compensate for the sediment deficit caused by sea-level rise. However, it is evident that the beach is dependent on the Carmel River sediment supply. So, to the extent that climate change alters the sediment supply, the effect on the beach could be substantial.

1. Introduction

The present sediment transport study is in support of the Draft Environmental Impact Report (DEIR), DD&A (2016), for the *Carmel Lagoon Ecosystem Protective Barrier, Scenic Road Protection Structure, and Interim Sandbar Management Plan.*

The overall goal of the *Carmel Lagoon Ecosystem Protective Barrier, Scenic Road Protection Structure, and Interim Sandbar Management Plan* is to improve habitat for threatened and endangered species in the lower Carmel River and Lagoon, improve natural floodplain function, and protect public infrastructure, while maintaining flood protection to existing developed areas. There is a need to improve, and if possible, restore the natural breaching regime in the Lagoon while providing flood protection to low-lying areas. The intent is to try to reduce the current level of active management of the lagoon and reduce the necessity for mechanical breaching of the sandbar.

1.1.1. Summary of Draft Environmental Impact Report

The DEIR, DD&A (2016), identified a need to achieve the following objectives in order to meet the overall goal of the project:

- Reduce the necessity for mechanical breaching of the sandbar to the greatest extent practicable;
- Maintain the current level of flood protection for existing public facilities and private structures in the low-lying developed areas located immediately to the north of and within the Lagoon;
- Protect Scenic Road embankment and the California Department of Parks and Recreation's (State Parks') restroom, interpretive, and parking facilities from scour resulting from a northerly aligned Lagoon outflow channel that may result from a reduction in mechanical breaching;
- Protect the Scenic Road embankment from the increasing risk of erosion resulting from ocean storm surge and high tides, which could increase in severity due to climate change; and
- Allow for interim management of the sandbar while the design and construction of the other project components proceed;
- Design and construct project elements within the permitted timeframe; and
- Minimize infrastructure that could detract from the function and value of the natural environment.

To this end, the (DD&A, 2016) DEIR identified a Proposed Project and explored and evaluated a wide range of options and alternatives in the context of the objectives listed above.

1.2. Scope of Work

Moffatt & Nichol was retained by Denise Duffy & Associates to develop a sediment transport study for Carmel River State Beach and the Carmel Lagoon.

The intent of the study is to gain a better understanding of how much sand is in the system, how much moves by fluvial action (Carmel River) and under what flow condition, how much moves by ocean waves and currents, and where it moves to. The overall sand movement within the Carmel littoral cell is presented in the form of a sediment budget. Beach morphology and sediment dynamics of the Carmel River State Beach and Carmel Lagoon are analyzed using a simulation model.

A multi-year simulation of waves and flows was conducted to evaluate beach profile shapes, shoreline location, sandbar elevation, and beach width, including the distance from the edge of the lagoon to the shoreline.

1.2.1. TAC Review Panel

The work was conducted with input and peer reviewed by a Technical Advisory Committee (TAC) consisting of the following panel members:

1. Dr. Mara Orescanin, Professor of Coastal Oceanography at the Naval Postgraduate School (NPS). Dr. Orescanin has experience with the morphology of coastal lagoons, sandbar build-up, erosion, and sediment transport, and familiarity with CRL gained from field work on the beach and lagoon.

2. Dr. Doug Smith, Professor of Hydrology and watershed restoration at California State University, Monterey Bay (CSUMB). Dr. Smith has experience in Lagoon and river flooding cycles, river sediment transport and flow, and familiarity with the Carmel River and CRL.

3. Larry Hampson, (retired) engineer and consultant for the Monterey Peninsula Water Management District (MPWMD). Mr. Hampson has expertise with flood management, and sandbar management and longstanding experience with the historical setting of the CRL and on the ground knowledge gained from observations and field visits.

4. Jeff Hagar, consultant for Hagar Environmental Science. Mr. Hagar specializes in water resource management and aquatic species conservation, and has experience with monitoring of salmonoid habitat in lagoon ecosystems on the central coast, and specific expertise with steelhead trout on the San Lorenzo River at Santa Cruz, CA.

2. Site Information

2.1. Carmel River Lagoon

The Carmel River drains approximately 250 square miles of the Santa Lucia and Sierra de Salinas Mountains into Carmel Bay. The Carmel River watershed has historically experienced large variations in seasonal and yearly discharge rates. A complex dynamic exists between the Carmel River Lagoon (CRL) and the Pacific Ocean. Figure 2-1 shows the location of the CRL and general east-west orientation of the Carmel River. Figure 2-2 provides closeups of the CRL and Carmel River State Beach (CRSB) based on historical aerial imagery from 1929 and present.

During times of low or no river flow, waves build up the sandbar to form a berm along the CRSB shoreline that closes off the mouth of the lagoon. Groundwater exchange helps supply the lagoon, but some amount of outflow from the lagoon to the ocean occurs via groundwater seepage through the sandbar. The lagoon also loses water due to evapotranspiration. Eventually, a condition of dynamic equilibrium sets in and the lagoon water surface elevation reaches a base elevation typically seen over the dry summer months.

When river flows increase, the water level in the lagoon can rise rapidly and potentially reach or exceed the defined flood stage. This can occur at times from late fall to early spring.

Management of the lagoon water level has therefore been implemented to mitigate flood hazards to properties along the north side of the lagoon. The management practices include monitoring of the lagoon water level and projected river inflows to the lagoon, and mechanical breaching of the lagoon. If inflows to the lagoon do not pose a flood hazard, no management action is carried out and the lagoon can breach naturally. Following a breach event (mechanical or natural), depending on the wave climate, the incident waves will close the beach and reform the sandbar. This can occur progressively or quite rapidly depending on the wave characteristics and river outflows. When the annual rainy season ends, and depending on whether or not the breach has closed naturally, the decision is made to close the lagoon outlet before the river inflow subsides in order to maximize the volume of water in the lagoon heading into the dry season.

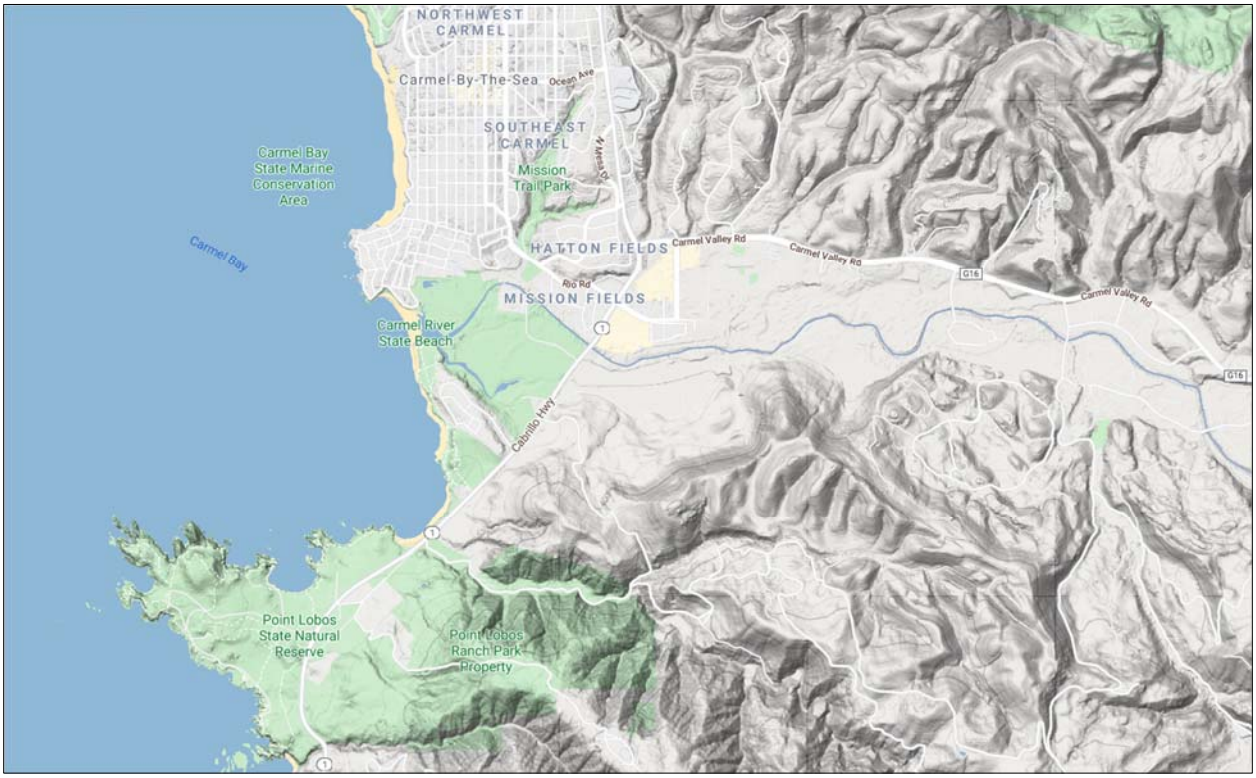

Figure 2-1: Carmel River State Beach site location.

Figure 2-2: Carmel River State Beach and Carmel River 1929 (left) and 2020 (right).

3. Basis of Analysis

3.1. Water Levels

Ocean water levels affecting the site include astronomical tides, storm surge, and wave action as described in the following sections.

3.2. Base Flood Elevations

Flood levels in the area of the Carmel River Lagoon are influenced by coastal flooding as well as fluvial flooding. The coastal Stillwater Elevation (SWEL) is around El. +8.2 feet NAVD88. The Coastal Base Flood Elevation (BFE) including wave runup ranges from El. +27 to +28 feet NAVD88 along Carmel River State Beach, per FEMA (2018). The fluvial BFE in the area of the sandbar is El. +16 feet NAVD88, increasing to El. +18 feet NAVD88 in the area of the Wastewater Treatment Facility (WTF) operated by the Carmel Area Wastewater District.

For reference, Table 3-1 summarizes discharge data for the Carmel River from FEMA (2017).

Table 3-1: Carmel River Percent Annual Chance Peak Discharge.

Percent Annual Chance	10%	2%	1%	0.2%
Recurrence Interval (every)	10 years	50 years	100 years	500 years
Discharge	9,800 cfs	19,000 cfs	23,300 cfs	33,500 cfs

3.3. Tides and Storm Surge

Coastal water level datums at the project site are summarized in Table 3-2 based on data from NOAA Station 9413450 at Monterey, NOAA (2020a). The values in the upper and lower part of the table reflect water level extremes due to a combination of astronomical tide and meteorological effects producing storm surge (positive or negative). The values in the center portion of the table indicate datums for astronomical tides only. Conversion between the older NGVD29 datum and NAVD88 datum was done based on the NGS (2020) datum shift.

Table 3-2: Water Level Datums.

Water Level Datum	Feet MLLW	Feet NAVD88	Description
100-yr	+8.08	+8.22	1% annual chance high water level.
50-yr	+7.92	+8.06	2% annual chance high water level.
10-yr	+7.59	+7.73	10% annual chance high water level.
5-yr	+7.42	+7.56	20% annual chance high water level.
HAT	+7.04	+7.18	Highest Astronomical Tide
KT	+6.90	+7.04	King Tide

Water Level Datum	Feet MLLW	Feet NAVD88	Description
MHHW	+5.34	+5.48	Mean Higher High Water
MHW	+4.64	+4.78	Mean High Water.
MTL	+2.87	+3.01	Mean Tide Level.
MSL	+2.83	+2.97	Mean Sea Level.
NGVD29	+2.59	+2.73	National Geodetic Vertical Datum of 1929.
MLW	+1.09	+1.23	Mean Low Water.
MLLW	0.00	+0.14	Mean Lower Low Water.
NAVD88	-0.14	0.00	North American Vertical Datum of 1988.
LAT	-1.91	-1.77	Lowest Astronomical Tide.
5-yr	-1.99	-1.85	20% annual chance low water level.
10-yr	-2.12	-1.98	10% annual chance low water level.
50-yr	-2.29	-2.15	2% annual chance low water level.
100-yr	-2.35	-2.21	1% annual chance low water level.

3.3.1. Astronomical Tides

Figure 3-1 summarizes the terminology used to describe tides. Tides at Carmel are semi-diurnal, which means that two high tides and two low tides occur each lunar day (in the figure, the higher high tides occurring at 24 hours and 24 hours later, and the lower low tides at 6 hours). The highest tides are referred to as “Higher high water” while the intermediate high tides are referred to as “Lower high water”. A similarly terminology is used for the low tides, where the lowest tides are referred to as “Lower low water” and the intermediate low tides “Higher low water”.

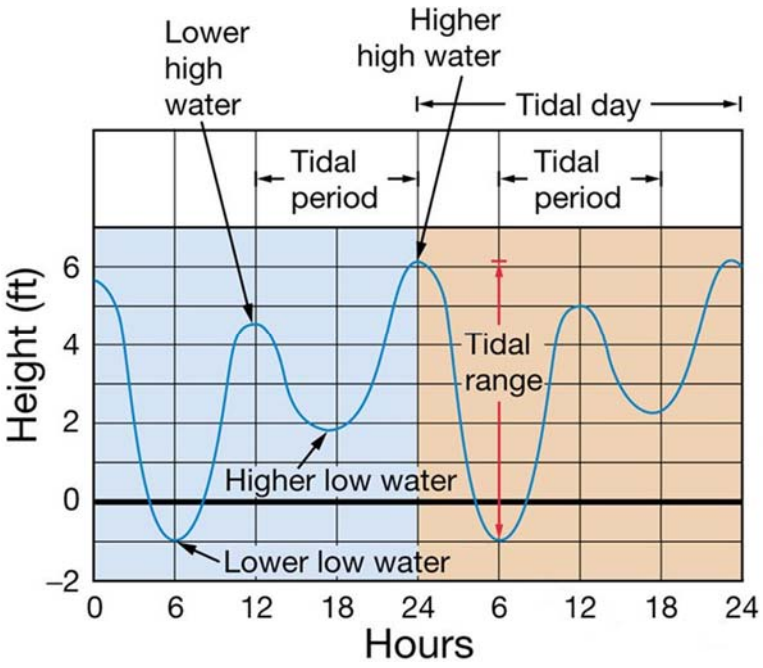

Figure 3-1: Terminology used to describe astronomical tides.

Tides occur due to the gravitational pull of the moon and the sun and vary over the cycle of a lunar day. A lunar day is approximately 24 hours and 50 minutes. The tidal period is the time between consecutive high tides or low tides. The tidal range is the difference in height between the low tide and the high tide.

3.3.2. El Niño Southern Oscillation

The El Niño Southern Oscillation (ENSO) reflects irregular variations of the sea surface temperature in the Eastern Pacific. The warming phase is termed El Niño while the cooling phase is named La Niña.

When warming of the ocean exceeds +0.5˚C El Niño conditions prevail. If the ocean temperature cools below -0.5˚C La Niña conditions are present. Within the range of+/-0.5˚C, conditions are termed ENSO-neutral. The ENSO cycle affects temperatures and rainfall worldwide.

El Niño and La Niña cycles typically last 9 to 12 months. They often commence in June or August and reach their peak during December through April, and subsequently, decay over May through July of the following year. Their periodicity is irregular, occurring every 3 to 5 years on average.

When El Niño conditions are present, ocean wave heights can be larger by 1 to 4 feet. Storms associated with El Niño effects typically approach from the west or southwest and may produce local littoral drift to the north, counter to the predominant southerly transport. The warming of the ocean that occurs during El Niño also produces a rise of the mean sea level which can be on the order of 10 to 12 inches. ENSO can therefore be considered as a form of temporary sea-level rise. Shorelines often experience severe erosion during El Niño storms.

During La Niña periods in the winter months, ocean wave heights are larger by 0.3 to 1.3 feet. When La Niña occurs in the summer months, ocean waves are slightly smaller than average.

Table 3-3 groups years categorized as having very strong, strong, moderate, or weak El Niño or La Niña conditions.

Table 3-3: Years with Very Strong, Strong, Moderate and Weak El Niño / La Niña Conditions.

El Niño				La Niña		
Very Strong	**Strong**	**Moderate**	**Weak**	**Weak**	**Moderate**	**Strong**
1972-73	1957-58	1951-52	1950-51	1950-51	1970-71	1955-56
1982-83	1965-66	1956-57	1952-53	1953-54	1971-72	1973-74
1997-98	1987-88	1963-64	1953-54	1954-55	1974-75	1975-76
2015-16	1991-92	1968-69	1958-59	1956-57	1983-84	1988-89
	2009-10	1986-87	1964-65	1963-64	1984-85	1998-99
		1994-95	1969-70	1964-65	1987-88	1999-00
		1996-97	1971-72	1966-67	1995-96	2007-08
		2002-03	1976-77	1967-68	2011-12	2010-11
		2014-15	1977-78	1972-73	2017-18	
			1979-80	1980-81		
			1981-82	1985-86		
			1990-91	1996-97		
			1992-93	2000-01		
			2001-02	2005-06		
			2004-05	2008-09		
			2006-07	2009-10		
			2018-19	2016-17		
			2019-20			

Extreme-Value Analysis (EVA) was utilized to assess return periods for the recurrence of El Niño and La Niña events. The data is summarized in Figure 3-2 and Figure 3-3. The results show that very strong El Niño conditions occur every 14 years on average (Oceanic Niño Index > 2.0). Return periods for Strong, Moderate, Weak, and Neutral conditions are indicated along the horizontal axis in Figure 3-2.

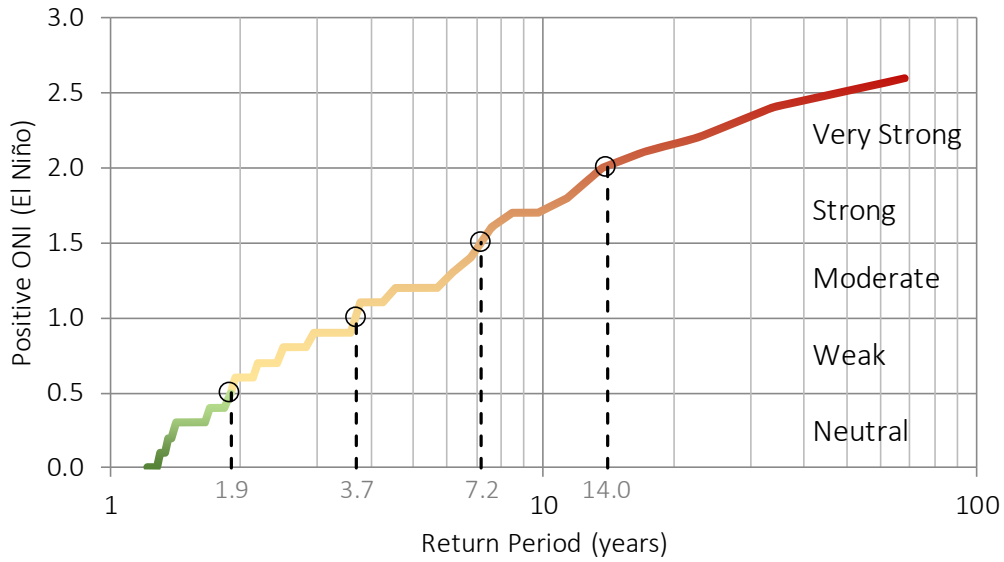

Figure 3-2: Recurrence interval of El Niño Conditions.

Recurrence intervals for La Niña conditions are shown in Figure 3-3, where Strong La Niña conditions are estimated to occur every 8 years on average (Oceanic Niño Index < -1.5). Very Strong La Niña conditions have so far not been observed.

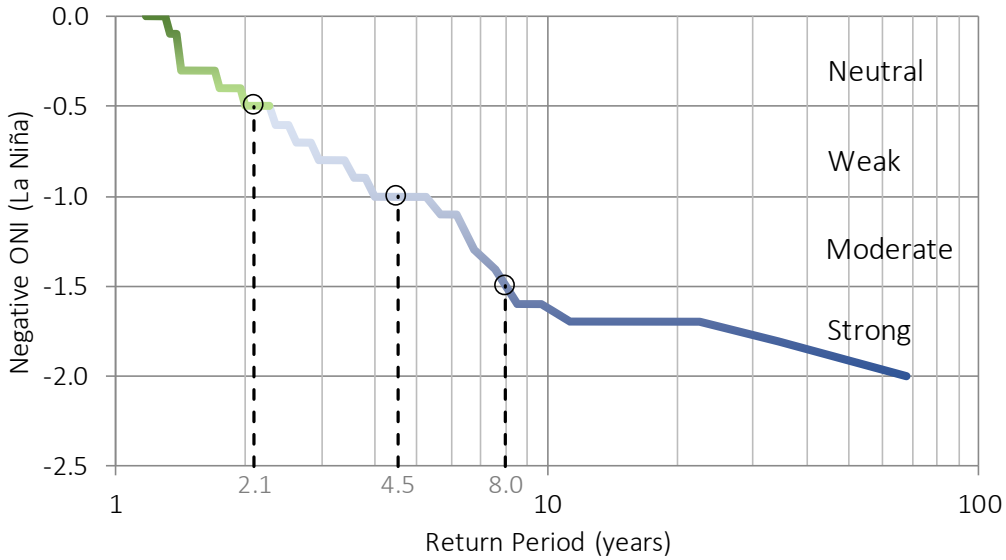

Figure 3-3: Recurrence Interval of La Niña Conditions.

3.4. Sea Level Rise

Current guidance for California recommends evaluation of sea-level rise (SLR) impacts using a scenario-based analysis. This method is founded on the approach by the Intergovernmental Panel on Climate Change (IPCC) to understand how sea-level rise and other drivers interact to threaten health, safety, and resources of coastal communities.

IPCC climate change scenarios are expressed in terms of Representative Concentration Pathways (RCPs). RCP 8.5 projects a future with the highest greenhouse gas emissions, high population and relatively slow income growth with modest rates of technological change and energy intensity improvements, leading in the long term to high energy demand and greenhouse gas (GHG) emissions. Some estimates of current emissions are tracking close to RCP 8.5.

The best available science and most recent guidance is summarized in *OPC (2018)* and has been adopted for this assessment. The guidance relies on the best available science to identify a range of sea-level rise scenarios including median, likely, 1-in-20 chance, and 1-in-200 chance projections, taking into account regional factors such as El Niño and extreme storm events that affect ocean levels, precipitation, and storm surge. This approach allows planners to understand the full range of possible impacts that can be reasonably expected based on the best available science, and build an understanding of the overall risk posed by potential future sea-level rise

Table 3-4 summarizes sea-level rise scenarios from *OPC (2018)* for Monterey which are applicable to Carmel. The columns outlined in dark blue reflects the OPC guidance for risk levels, which include low risk aversion, medium to high risk aversion, and extreme risk aversion.

Table 3-4: Sea-Level Rise Projections for Monterey, *OPC (2018)*.

		Probabilistic Projections (in feet) (based on Kopp et al. 2014)					H++ scenario (Sweet et al. 2017) *Single scenario
		MEDIAN	LIKELY RANGE		1-IN-20 CHANCE	1-IN-200 CHANCE	
		50% probability sea-level rise meets or exceeds...	66% probability sea-level rise is between...		5% probability sea-level rise meets or exceeds...	0.5% probability sea-level rise meets or exceeds...	
				Low Risk Aversion		Medium - High Risk Aversion	Extreme Risk Aversion
High emissions	2030	0.4	0.3 -	0.5	0.6	0.8	1.0
	2040	0.6	0.4 -	0.8	0.9	1.2	1.7
	2050	0.8	0.5 -	1.1	1.3	1.9	2.7
Low emissions	2060	0.9	0.5 -	1.2	1.5	2.3	
High emissions	2060	1.0	0.7 -	1.4	1.8	2.6	3.8
Low emissions	2070	1.0	0.6 -	1.4	1.9	3.0	
High emissions	2070	1.3	0.9 -	1.8	2.3	3.4	5.1
Low emissions	2080	1.2	0.7 -	1.7	2.3	3.8	
High emissions	2080	1.6	1.1 -	2.3	2.9	4.4	6.6
Low emissions	2090	1.3	0.8 -	2.0	2.7	4.6	
High emissions	2090	2.0	1.3 -	2.8	3.5	5.5	8.2
Low emissions	2100	1.5	0.9 -	2.3	3.1	5.5	
High emissions	2100	2.3	1.5 -	3.3	4.3	6.9	10.1
Low emissions	2110*	1.6	1.0 -	2.4	3.3	6.1	
High emissions	2110*	2.5	1.7 -	3.4	4.4	7.2	11.8
Low emissions	2120	1.7	1.0 -	2.7	3.8	7.3	
High emissions	2120	2.8	2.0 -	4.0	5.2	8.5	14.0
Low emissions	2130	1.9	1.1 -	3.0	4.2	8.3	
High emissions	2130	3.1	2.2 -	4.5	5.9	9.9	16.4
Low emissions	2140	2.0	1.1 -	3.2	4.7	9.5	
High emissions	2140	3.5	2.4 -	5.1	6.7	11.3	18.9
Low emissions	2150	2.1	1.1 -	3.6	5.3	10.8	
High emissions	2150	3.8	2.6 -	5.7	7.6	12.9	21.8

Notes:

- MEDIAN. Mean sea-level rise taken as an average of probabilistic scenarios.
- LIKELY RANGE. Median projection with 66% confidence limits. The upper range (outlined by blue box) is applicable to facilities and infrastructure with a low risk aversion to sea-level rise.
- 1-IN-20 CHANCE. 5% probability that sea-level rise meets or exceeds this projection (1 in 20 chance).
- 1-IN-200 CHANCE. 0.5% probability that sea-level rise meets or exceeds this projection (1 in 200 chance). This projection (outlined by a blue box) is representative of medium to high risk aversion and is applicable to facilities and infrastructure that are vulnerable to sea-level rise impacts.
- H++ Scenario. Worst case scenario representative of rapid ice sheet loss and accelerated sea-level rise. This projection is applicable to facilities with extreme risk aversion to sea-level rise hazards. For example critical infrastructure or facilities that are extremely sensitive to sea-level rise hazards and unable to adapt to sea-level rise.

3.5. Wind Statistics

Figure 3-4 summarizes annual wind data for the Monterey Regional Airport for the years from 1996 to 2019. The wind rose shows that high winds can occur over the sector from west-southwest (WSW) to northwest (NW).

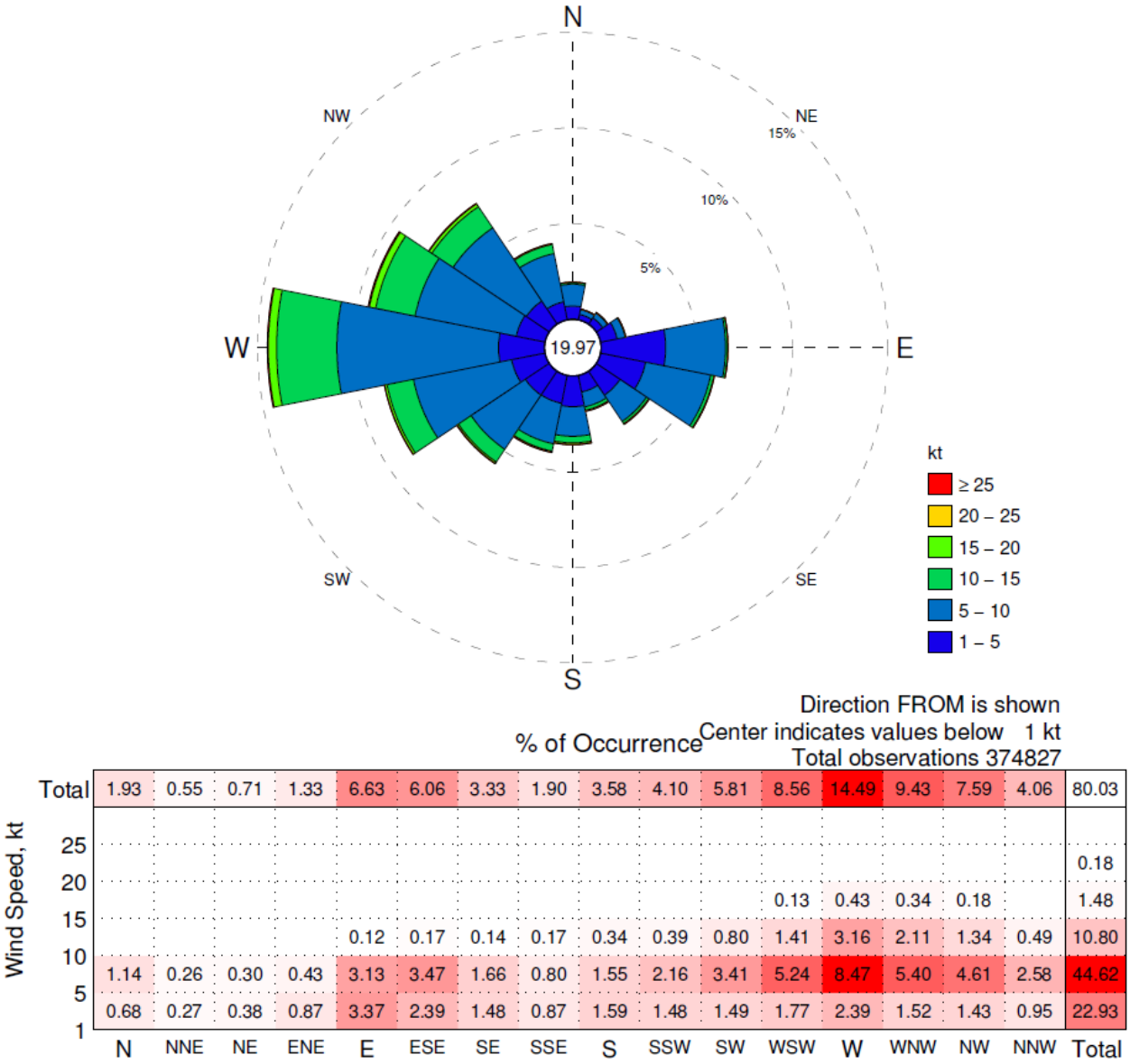

Figure 3-4: Wind rose for Monterey Regional Airport.

Figure 3-5 summarizes wind speeds offshore, recorded at the National Oceanic and Atmospheric (NOAA) National Data Buoy Center (NDBC) wave buoy 46042 located 27 nm west of Monterey Bay at latitude: 36.785°N, longitude 122.398°W. The data collected covers the years from 1987 through 2019.

Comparing with Figure 3-4 it can be seen that the offshore wind speeds are generally higher in terms of wind speed with the most frequent winds from northwesterly (NW) and north-northwesterly directions (NNW). High wind speeds can also occur from southeasterly (SE) to southerly (S) directions. An uptick in wind speeds from easterly (E) directions is also noticeable, which compares with the wind direction observed over land, Figure 3-4. Refer to Appendix A for wind roses by month.

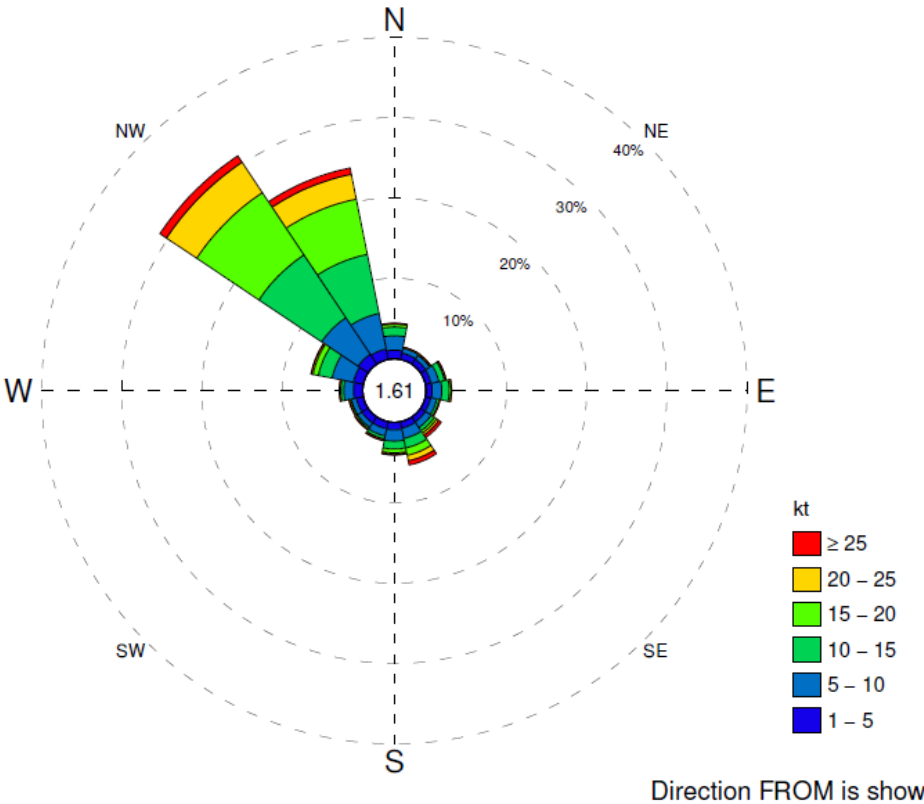

% of Occurrence
Direction FROM is shown
Center indicates values below 1 kt
Total observations 262090

Wind Speed, kt	N	NNE	NE	ENE	E	ESE	SE	SSE	S	SSW	SW	WSW	W	WNW	NW	NNW	Total
Total	4.40	1.50	1.48	2.58	3.13	1.80	3.04	5.46	4.04	2.38	1.89	1.78	2.86	6.61	31.17	24.27	98.39
25							0.37	0.53							0.97	0.80	2.91
20	0.10						0.32	0.70	0.19					0.21	4.54	3.15	9.44
15	0.34			0.18	0.25		0.33	0.94	0.47	0.17	0.11		0.14	0.69	9.34	7.02	20.18
10	1.09		0.16	0.72	0.92	0.32	0.48	1.20	0.98	0.37	0.23	0.19	0.38	1.74	9.41	7.51	25.79
5	1.80	0.62	0.59	1.00	1.20	0.77	0.85	1.32	1.39	0.91	0.64	0.63	1.19	2.71	5.47	4.51	25.58
1	1.04	0.77	0.70	0.66	0.72	0.63	0.69	0.76	0.91	0.86	0.87	0.83	1.11	1.21	1.44	1.28	14.49
	N	NNE	NE	ENE	E	ESE	SE	SSE	S	SSW	SW	WSW	W	WNW	NW	NNW	Total

Figure 3-5: Offshore wind speeds for NDBC Buoy 46042 Monterey.

The offshore wind climate with a predominance of winds from WNW to NNW directions (occurring 62% of the time) means that Carmel Bay sees frequent wind-waves from northwesterly directions.

The offshore wave climate is described further in the following section.

4. Wave Climate

The Carmel shoreline is exposed to wind-waves generated by local storm systems as well as swell waves originating from distant storms over the Pacific. Figure 4-1 shows the general angles of wave incidence based on NOAA/NDBC wave data.

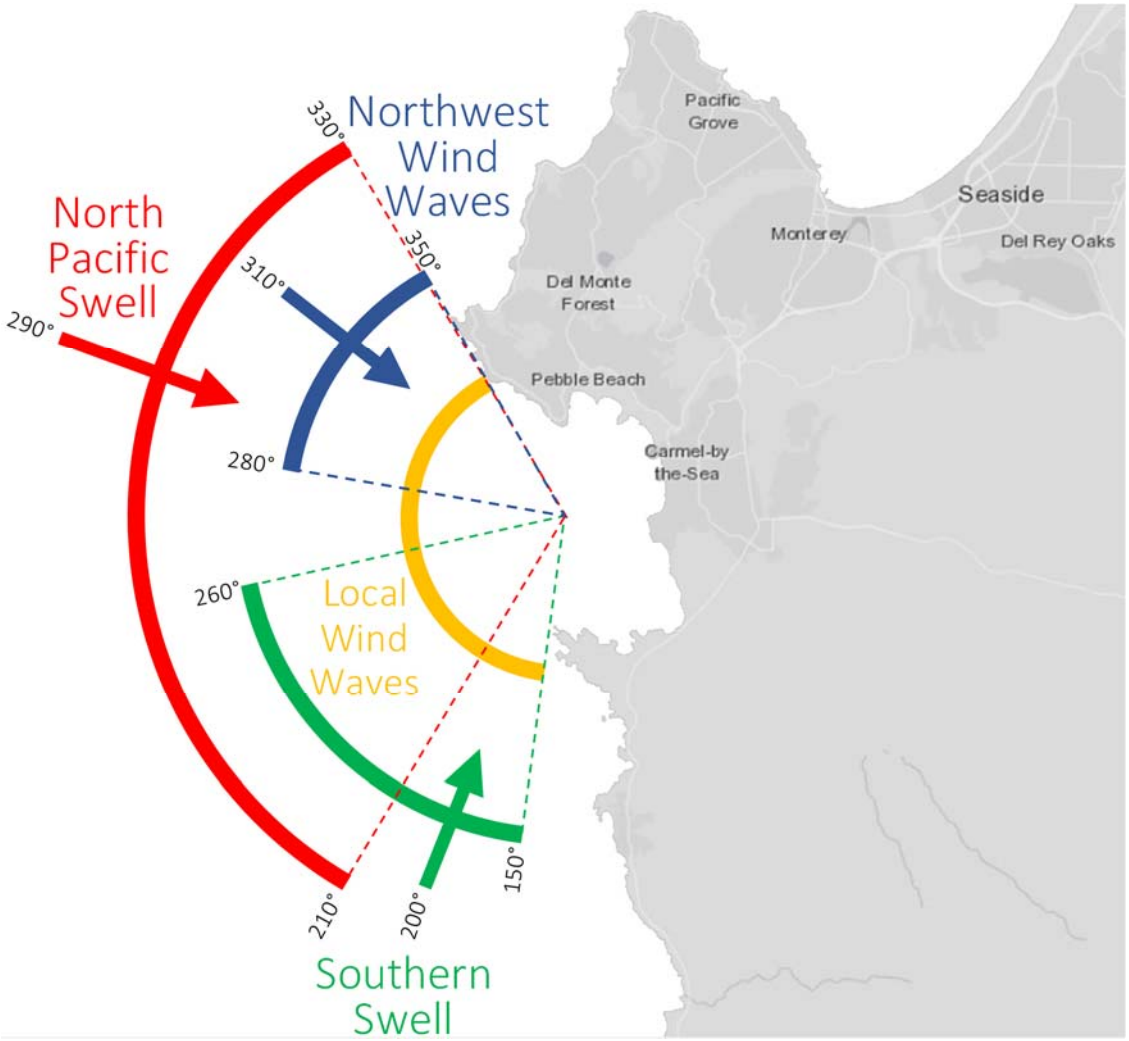

Figure 4-1: Angles of wave incidence at Carmel, adopted from USGS (2006).

There are four different wave systems that affect Carmel Bay: 1) North Pacific swell waves originating from distant storms over the North Pacific, 2) Southern swell originating from distant storms in the South Pacific, 3) Northwest wind waves generated by regional wind systems, and 4) Local wind waves which can occur from any direction over open water. North Pacific swell waves are generated by extra-tropical storm systems, mid-latitude low-pressure systems, and cold fronts over the North Pacific, USGS (2006). Southern swell is generated by storms in the Southern Hemisphere and occurs in the summertime. Swell waves are characterized by long wave periods, typically from 8 to 18 seconds. Northwest wind waves are generated by daily sea-breeze conditions and are more pronounced in the

spring and early summer months, USGS (2006). Wind waves are generated by regional and local wind conditions and produce waves with shorter periods, typically from 3 to 8 seconds. Local storms can occur from October through April.

4.1. Wave Statistics

Wave statistics reflecting the annual average conditions are presented in the following.

4.1.1. Wind-Waves

Wind-waves are waves generated by local storm systems. The most significant storms typically occur over the winter months from directions over the sector from south to northwest. Table 4-1 summarizes statistics for wave conditions for these storms, based on data from NDBC (2020) for the LLNR 297 wave buoy located 27 nm west of Monterey Bay, Station 46042, at lat/lon 36.785°N 122.398°W in a water depth of 5,400 feet (1,645.9 m).

Table 4-1: Distribution of wind-waves by significant wave height and direction.

H_S (feet)	SE	SSE	S	SSW	SW	WSW	W	WNW	NW	NNW	Total
0 - 2								0.0%	0.0%		0.0%
2 - 4	0.0%	0.0%	0.03%	0.0%	0.01%	0.2%	0.3%	2.4%	6.7%	0.5%	10.1%
4 - 6	0.0%	0.6%	0.7%	0.1%	0.1%	0.3%	0.5%	5.9%	39.1%	2.6%	50.0%
6 - 8	0.0%	0.9%	1.2%	0.3%	0.2%	0.1%	0.2%	2.6%	22.2%	1.6%	29.3%
8 - 10		0.7%	1.4%	0.3%	0.1%	0.1%	0.1%	0.7%	3.8%	0.2%	7.4%
10 - 12		0.5%	0.8%	0.11%	0.02%	0.0%	0.0%	0.1%	0.7%	0.02%	2.2%
12 - 14		0.2%	0.3%	0.0%	0.02%	0.0%	0.0%	0.01%	0.10%	0.0%	0.7%
14 - 16		0.06%	0.06%		0.0%				0.02%		0.1%
16 - 18		0.01%	0.01%	0.0%							0.0%
Total	**0.1%**	**3.0%**	**4.5%**	**0.9%**	**0.4%**	**0.7%**	**1.2%**	**11.7%**	**72.6%**	**4.9%**	**100%**

Table 4-2 summarizes peak wave periods for wind-waves by significant wave height and direction.

Table 4-2: Average peak period of wind-wave periods (in seconds) by significant wave height and direction.

H_S (feet)	SE	SSE	S	SSW	SW	WSW	W	WNW	NW	NNW
0 - 2								4.3	6.7	
2 - 4	5.3	4.5	4.3	4.3	7.2	6.9	7.2	6.8	6.5	5.0
4 - 6	5.2	5.2	5.3	5.8	6.7	7.2	7.3	6.9	6.8	6.1
6 - 8	6.1	5.8	6.0	6.5	7.3	7.3	7.3	7.2	7.3	7.1
8 - 10		6.6	6.7	7.1	7.2	7.2	7.5	7.4	7.5	7.4
10 - 12		7.1	7.2	7.2	7.2	7.5	7.0	7.4	7.6	7.5
12 - 14		7.5	7.4	7.3	7.7	7.7	7.7	7.7	7.7	7.7
14 - 16		7.7	7.6		7.7				7.7	
16 - 18		7.7	7.7	7.7						

4.1.2. Swell Waves

Swell waves are characterized by long wave periods, exceeding 8 seconds. At Carmel the primary direction of swell waves incidence is from west-northwest to northwest, Table 4-3. Swell waves from these directions are representative of North Pacific Swell (Figure 4-1). There is also a smaller percentage of swell arriving from southerly to south-southwesterly directions, representative of Southern Swell (Figure 4-1).

Incidence of swell waves can last from hours to several days, depending on the magnitude and duration of the storm system of origin. During an episode of swell, the waves with the longest wave periods will arrive first, followed by waves with progressively shorter periods, for example initial swell waves with 18 second periods, transitioning to swell with 15 second periods, then 13 second periods and so forth until the swell front dies down.

Table 4-3: Distribution of swell waves by significant wave height and direction.

H_S (feet)	SE	SSE	S	SSW	SW	WSW	W	WNW	NW	NNW	Total
0 - 2			0.0%	0.006%	0.002%	0.001%	0.001%	0.005%	0.0%		0.023%
2 - 4	0.0%	0.2%	1.7%	2.1%	0.9%	0.5%	1.2%	2.3%	1.5%	0.06%	10.5%
4 - 6	0.017%	0.3%	2.1%	2.2%	0.9%	0.8%	3.5%	9.1%	8.6%	0.3%	27.8%
6 - 8	0.002%	0.0%	0.4%	0.4%	0.2%	0.4%	3.0%	10.0%	11.2%	0.4%	26.0%
8 - 10		0.01%	0.1%	0.1%	0.1%	0.2%	1.9%	7.3%	7.6%	0.2%	17.4%
10 - 12	0.0%	0.02%	0.06%	0.03%	0.05%	0.1%	1.0%	4.1%	4.2%	0.06%	9.7%
12 - 14		0.03%	0.06%	0.03%	0.02%	0.06%	0.6%	2.1%	2.1%	0.03%	5.0%
14 - 16		0.03%	0.04%	0.01%	0.009%	0.04%	0.3%	0.9%	0.8%	0.01%	2.1%
16 - 18		0.02%	0.02%	0.004%	0.003%	0.020%	0.1%	0.4%	0.3%	0.01%	0.9%
18 - 20		0.006%	0.01%	0.000%	0.001%	0.007%	0.05%	0.2%	0.1%	0.0%	0.3%
20 - 22		0.003%	0.002%	0.0%		0.005%	0.05%	0.1%	0.0%	0.0%	0.2%
22 - 24			0.0%			0.004%	0.03%	0.02%	0.01%		0.1%
24 - 26						0.0%	0.013%	0.01%	0.000%		0.02%
26 - 28							0.0%	0.00%	0.000%		0.01%
28 - 30							0.0%	0.002%	0.000%		0.009%
30 - 32							0.0%	0.000%			0.001%
32 - 34							0.0%	0.0%			0.001%
34 - 36							0.0%				0.000%
Total	**0.0%**	**0.6%**	**4.4%**	**4.8%**	**2.1%**	**2.1%**	**11.8%**	**36.4%**	**36.6%**	**1.1%**	**100%**

The data summarized in Table 4-3 shows that around 70% of the offshore waves have significant wave heights in the range from 4 to 10 feet, and 99% of all waves are within the range from 2 to 16 ft significant wave height. Outside of these cases, the data indicates that the largest wave heights can be around 32 to 36 feet in height and will occur from westerly (W) and west-northwesterly directions (WNW).

Table 4-4 summarizes peak wave periods for swell waves by significant wave height and direction. The data shows that the largest (32 to 36 ft) waves indicated in Table 4-3 will have peak wave periods around 17.4 to 19.1 seconds. Aside from these, the data in the table shows that the peak wave period

is generally related to the wave height with smaller waves having shorter periods and larger waves having longer periods.

It should be noted that there is a group of data in Table 4-4 where long peak wave periods from 13 to 18.9 seconds occur for small to moderate wave heights. This is seen for waves from SE to SW having significant wave heights from 2 to 8 feet. Waves in this group are characteristic of Southern Swell, i.e. swell waves with long decay distance originating from distant storm systems. Swell waves of this type have a relatively small wave steepness (ratio of wave height to wave length). Larger waves from the same directions, SE to SW, with significant wave heights in the range from 10 to 24 feet characterize swell waves originating from storm systems further north in the Southern Hemisphere. Waves from these storm systems have a shorter decay distance and greater wave steepness.

Table 4-4: Average peak period of swell waves (in seconds) by significant wave height and direction.

H_S (feet)	SE	SSE	S	SSW	SW	WSW	W	WNW	NW	NNW
0 - 2			13.0	13.3	14.0	12.7	12.5	10.3	9.3	
2 - 4	16.8	14.5	14.4	14.7	14.4	13.1	12.3	11.2	9.7	10.1
4 - 6	15.7	14.6	15.3	15.6	15.0	13.4	12.8	12.0	10.0	10.0
6 - 8	18.9	14.8	15.8	16.1	14.0	12.5	13.2	12.9	10.5	9.7
8 - 10		10.9	12.5	13.2	10.7	11.6	13.5	13.4	11.1	9.9
10 - 12	10.5	9.1	9.4	9.5	9.8	12.2	13.9	14.0	11.8	11.0
12 - 14		9.2	8.8	9.1	10.3	12.8	14.0	14.4	12.5	11.2
14 - 16		9.1	9.1	9.3	10.8	13.4	14.6	14.7	13.1	11.8
16 - 18		9.5	9.5	10.0	10.8	14.4	15.2	15.1	13.2	11.2
18 - 20		10.0	9.7	10.0	12.1	15.3	15.4	15.6	13.1	12.0
20 - 22		10.1	9.5	9.8		16.3	15.8	16.0	13.8	11.9
22 - 24			9.1			17.7	16.1	16.6	14.0	
24 - 26						17.2	16.1	16.4	13.8	
26 - 28							16.6	17.2	14.8	
28 - 30							17.2	16.7	14.8	
30 - 32							19.1	19.1		
32 - 34							17.4	19.1		
34 - 36							19.1			

4.2. Wave Model Development

Coastal processes in Carmel Bay and at CRSB are primarily wave-driven, and include erosion, accretion, cross-shore sediment transport, and longshore sediment transport driven by wind- and swell waves and by wave-induced currents.

The Danish Hydraulic Institute (DHI) MIKE-21 Spectral Wave (SW) model was utilized to develop a regional wave model covering the area of Monterey Bay, Carmel, and Big Sur. The SW model simulates wave transformation of deep-water waves propagating to nearshore areas. Wave transformation effects resolved by the model include wave propagation by speed and direction, wave growth due to wind shear, shoaling and refraction due to variation of the seabed, diffraction and

reflection near structures, wave breaking in the surf zone, wave dissipation, and interaction between waves and currents.

4.2.1. Model Domain and Bathymetry

To account for the full offshore wave exposure outlined in Figure 4-1, the SW model domain extends approximately 20 miles west of Carmel Bay and 60 miles in the north-south orientation. Figure 4-2 shows the location of metocean gauges within the model domain outlined in blue.

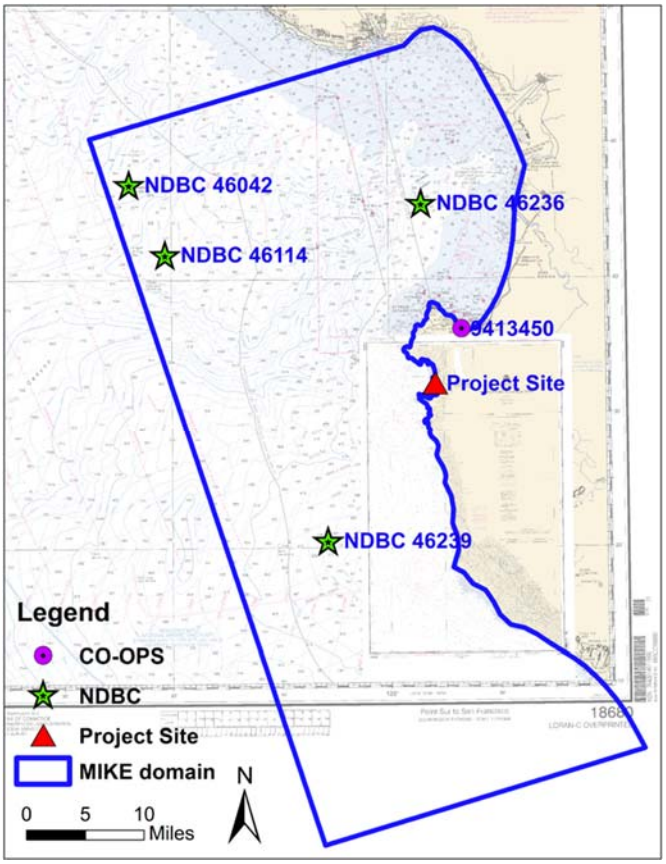

Figure 4-2: Metocean gauges and SW model domain.

Bathymetry data was obtained from NOAA's 1/3 arc-second (e.g. 10-meter resolution) coastal Digital Elevation Model (DEM) and was originally developed based on multi-agency hydrographic surveys (NOAA, 2012). The model bathymetry is referenced to the North American Vertical Datum of 1988 (NAVD88) datum. Figure 4-3 illustrates the regional seabed bathymetry (left) and the bathymetry in the vicinity of Carmel Bay (right). One of the main features of the regional bathymetry is the Monterey Bay Submarine Canyon, which is indicated by the undulating shape of darker blue colors in the figure on the left. Carmel Bay also features a submarine canyon, the Carmel Canyon, which is a spur off the Monterey Submarine Canyon. Within Carmel Bay, there is a segment of the canyon headed northeast towards Carmel Beach, while another segment is aligned southeast with a canyon head at CRSB and another at Monastery Beach. The canyon head at Monastery Beach comes close to shore and is said

to be literally a stone's throw from the beach. The submarine canyon heads have a major impact on sediment transport processes at Carmel as they effectively trap and remove sediment from the nearshore system.

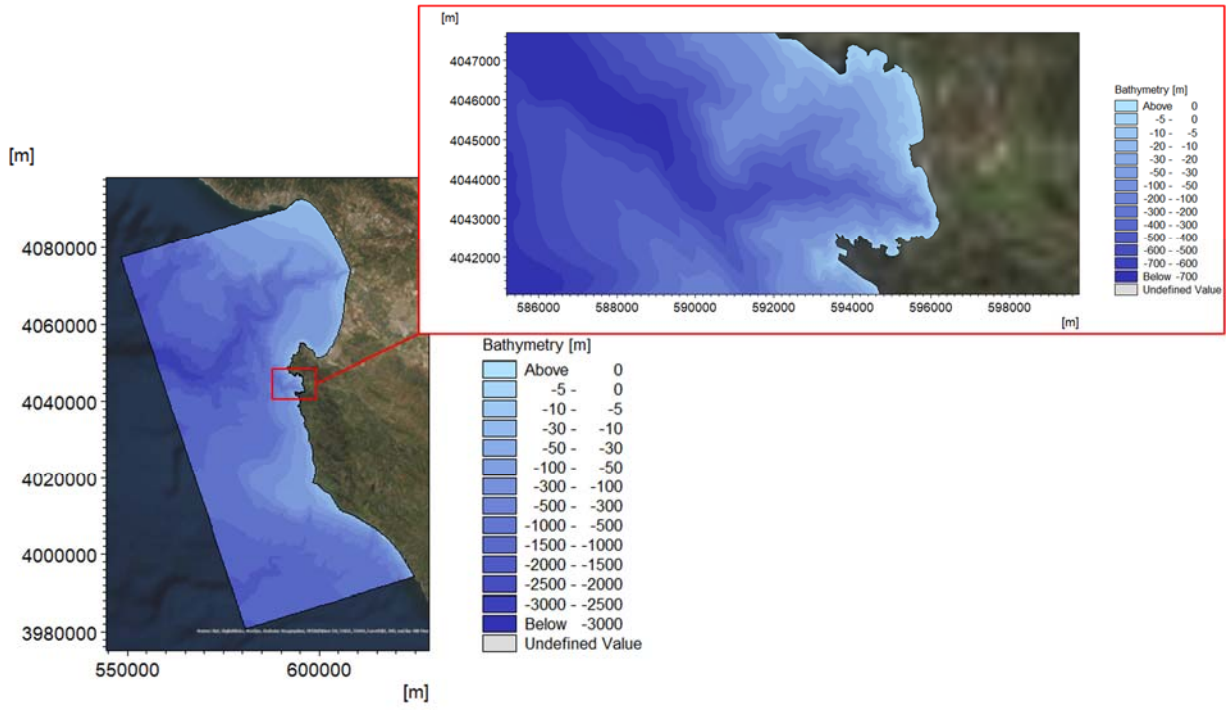

Figure 4-3: Regional model bathymetry (left), and local bathymetry (right).

4.2.2. SW Model Verification

Field measurements from wave buoys were utilized to evaluate the performance of the SW model. The SW model was run using wave measurements from NDBC wave buoy 46042 as the boundary condition. Within the model domain, the simulated significant wave heights and peak wave periods were compared with the measurements from other NDBC buoys (e.g. 46114, 46236, and 46239). The model verification included the period around December 2015. This winter can be characterized as a "very strong El Niño". Figure 4-4 through Figure 4-6 indicate that the SW model performs well in comparison with the field measurements. In these figures, the blue x's represent data recorded at NDBC wave boys while the red curves reflect data obtained via model simulation. The data shows that there is good agreement between observed and simulated data.

Following this model verification phase, the SW model was employed for multi-year simulation of wave data to support analysis of coastal processes at CRSB.

4.2.3. Conducted Wave Scenarios

Wave data recorded at NDBC wave buoy 46042 was used to characterize the offshore wave environment. A total of 156 scenarios was identified, accounting for approximately 94.5% of the total swell wave data recorded at the buoy.

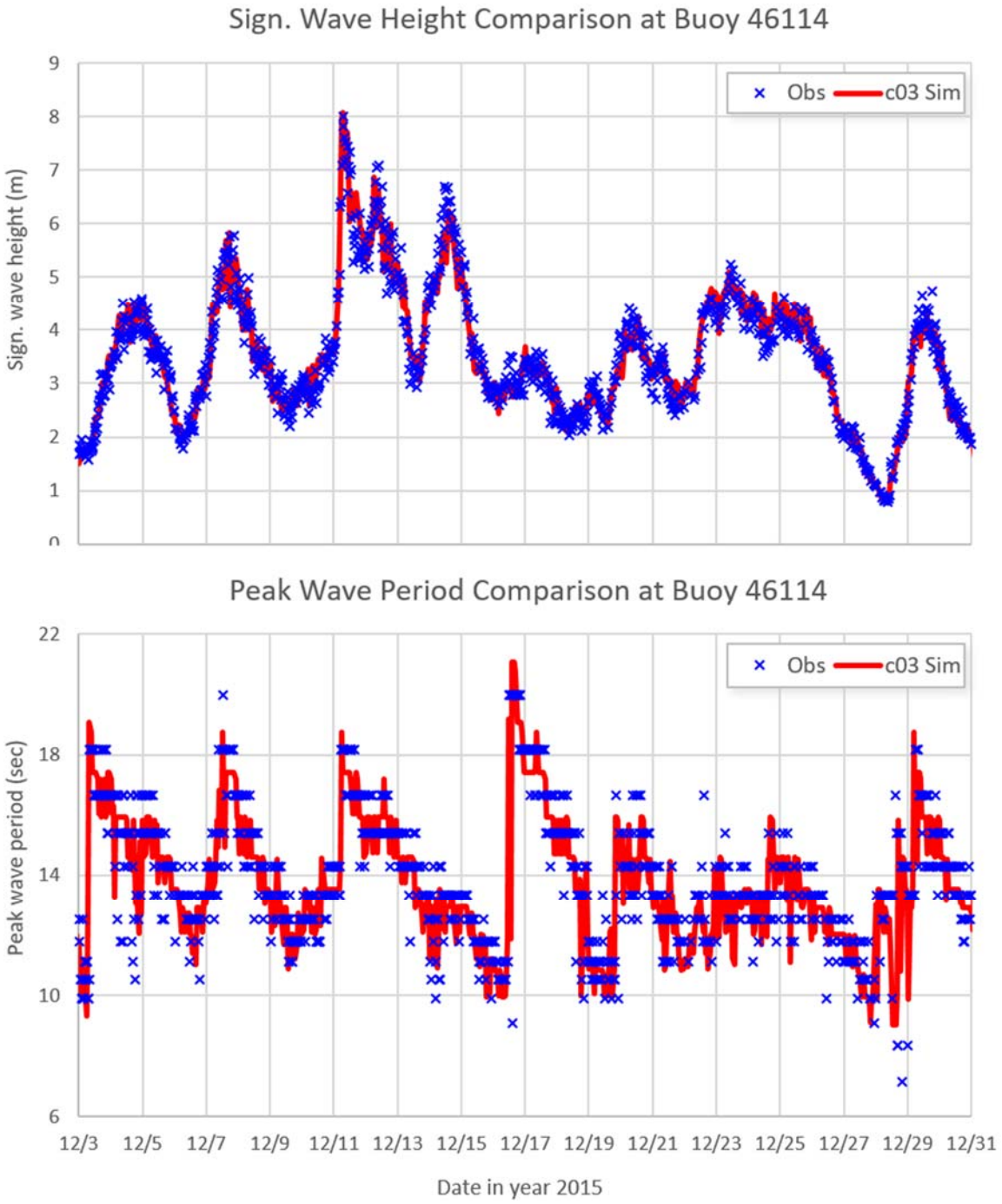

Figure 4-4: Comparison of simulated wave parameters with data from NBDC wave buoy 46114.

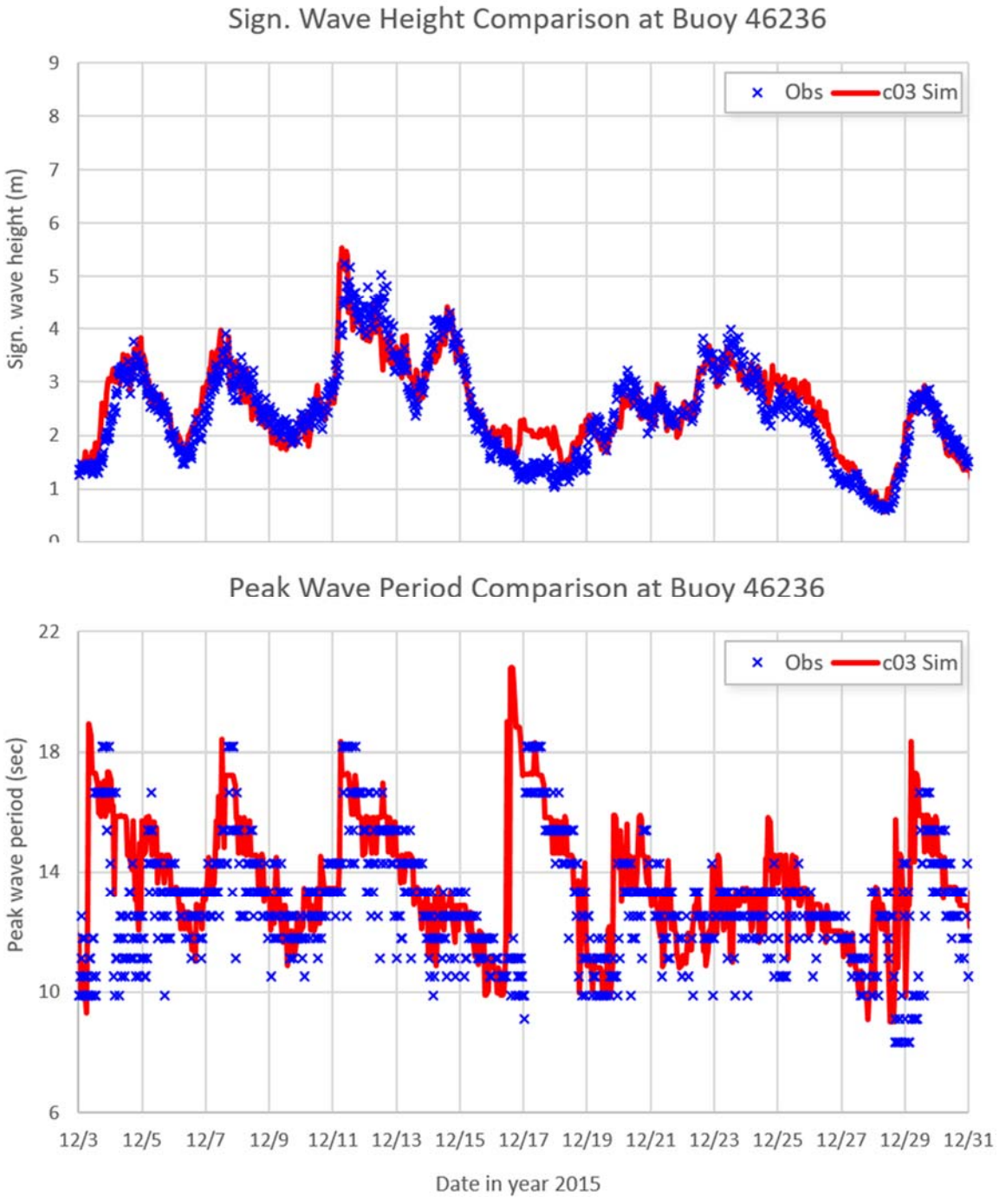

Figure 4-5: Comparison of simulated wave parameters with data from NDBC wave buoy 46236.

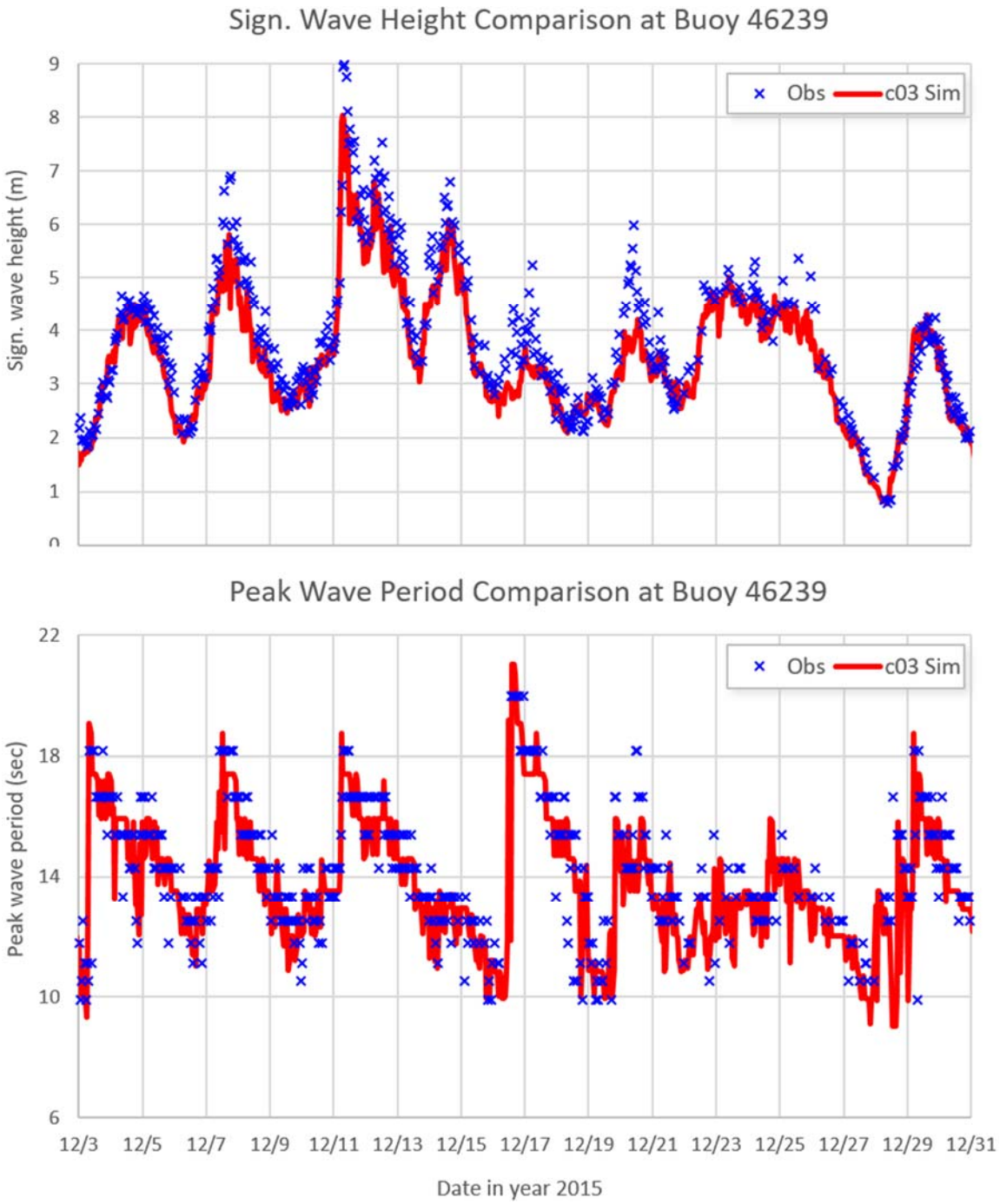

Figure 4-6: Comparison of simulated wave parameters with data from NDBC wave buoy 46239.

4.3. Wave Transformation

Figure 4-7 through Figure 4-9 illustrate three examples of regional swell wave transformation simulated with the SW model for swell waves from the northwest, west, and southwest.

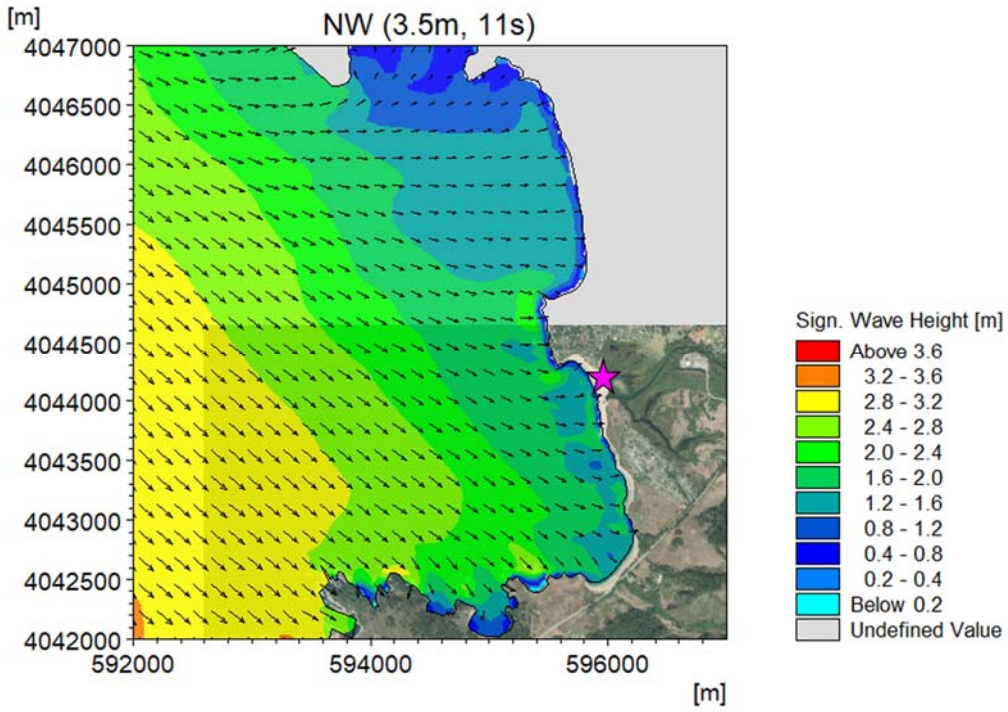

Figure 4-7: Illustration of swell wave transformation (offshore H_S=3.5m, T_P=11s, Northwest).

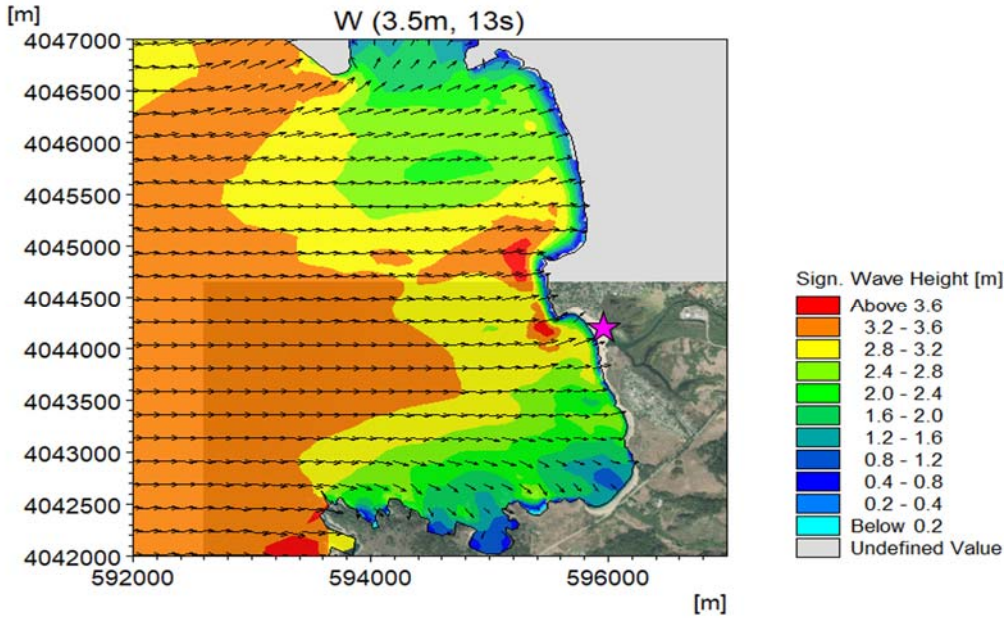

Figure 4-8: Illustration of swell wave transformation (Offshore H_S=3.5m, T_P=13s, West).

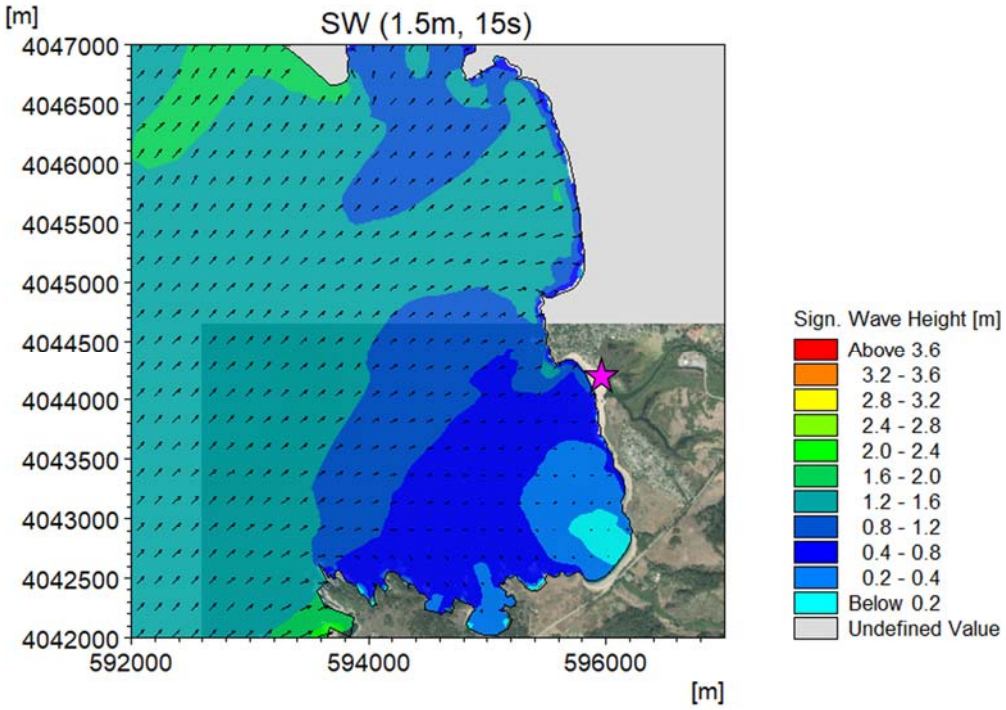

Figure 4-9: Illustration of swell wave transformation (Offshore H_S=1.5m, T_P=15s, Southwest).

The Carmel submarine canyon plays a significant role in how waves are transformed as the propagate from offshore waters to the shoreline, which is explained in the following.

Figure 4-10 shows wave transformation patterns for swell waves from directions approximately northwest to west-northwest, which has the highest percentage of occurrence per Table 4-3. Swell waves from this direction interval occur 36.6% + 36.4% = 73% of the time.

In the figure, blue colors are representative of wave crests while gray colors indicate wave troughs. Dark blue and dark gray hues indicate larger waves, while light blue and gray transitioning to white indicates decreasing wave heights. The distance between consecutive wave crests (or troughs) give an indication about wave lengths. Wave lengths are longer in deeper water and become gradually shorter as waves propagate into shallow water. Outlines of depth contours of the Carmel Canyon are indicated in black, which shows how the submarine canyon affects the incident swell waves.

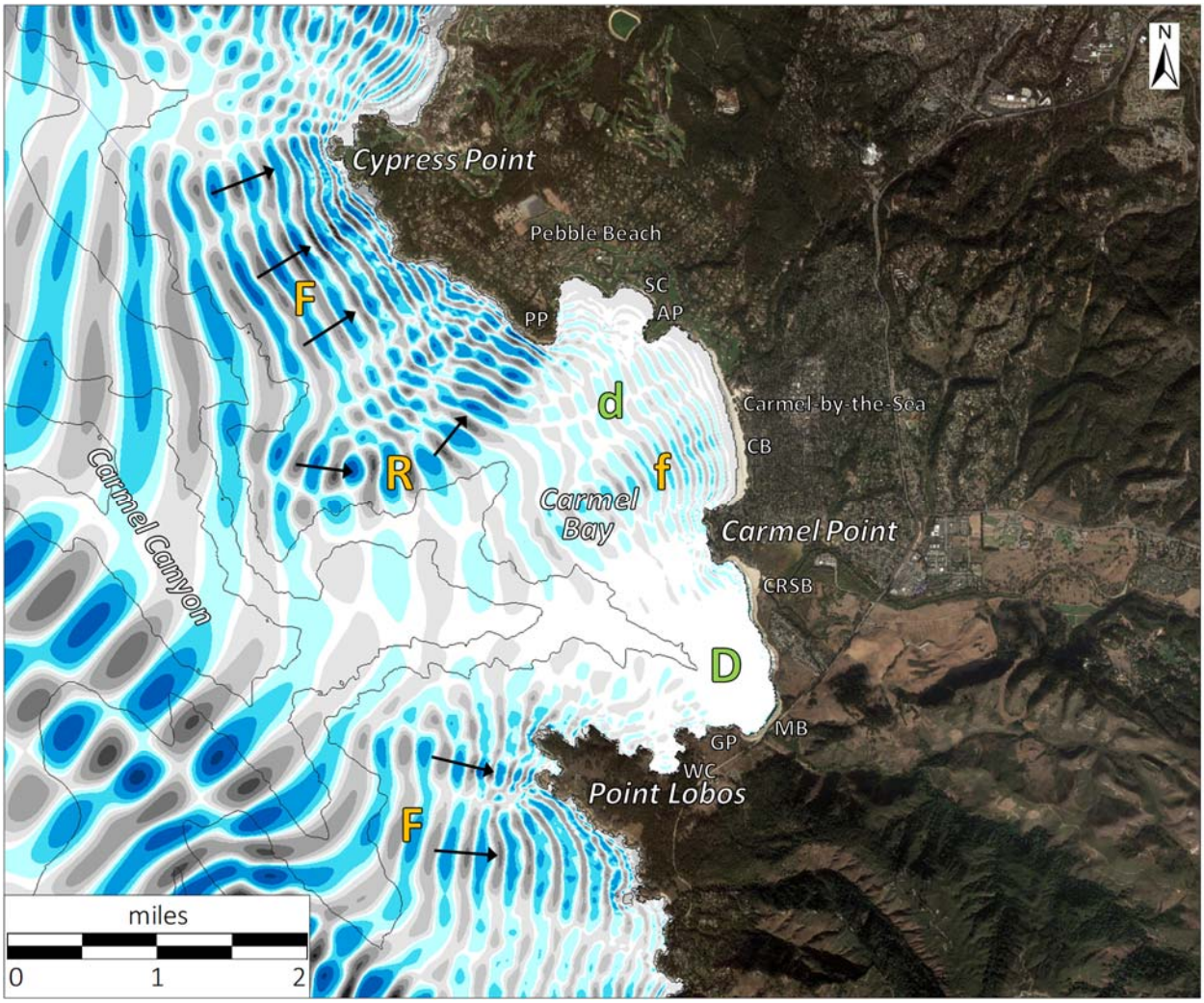

Figure 4-10: Transformation of swell waves arriving from northwest by west.

The figure shows that despite the direction of wave incidence being from northwest to west-northwest, wave refraction causes offshore waves to turn towards the cliffs between Cypress Point and Pescadero Point (PP) and also causes a focusing “F” of wave energy along this section of the coast. Incident waves also tend to converge on Point Lobos at the South end of Carmel Bay.

There is also an effect that wave energy reflects off the submarine canyon “R” and is directed towards Pescadero Point. The incident waves will tend to travel along the alignment of the submarine canyon. At the canyon heads waves tends to disperse. This occurs for waves propagating towards Arrowhead Point (AP), see “d” in the figure, and for waves propagating towards Carmel River State Beach and Monastery Beach at “D”. A slight focusing of waves occurs at Carmel Beach at “f”.

Figure 4-11 shows wave transformation patterns for swell waves from southerly to south-westerly directions. In this case the incident waves propagate across the submarine canyon in deeper water

and focus “F” on the shoreline between Cypress Point and Pescadero Point. Incident waves propagating along the south side of the canyon are reflected off the canyon wall where it turns into Carmel Bay at “R”, which causes focusing of waves towards Point Lobos by “F”. Waves propagating within the canyon become subject to dispersal in Carmel Bay near Arrowhead point at “d”, and in the area of CRSB and Monastery Beach at “D”. Slight focusing of incident wave energy occurs towards Carmel Beach at “f”.

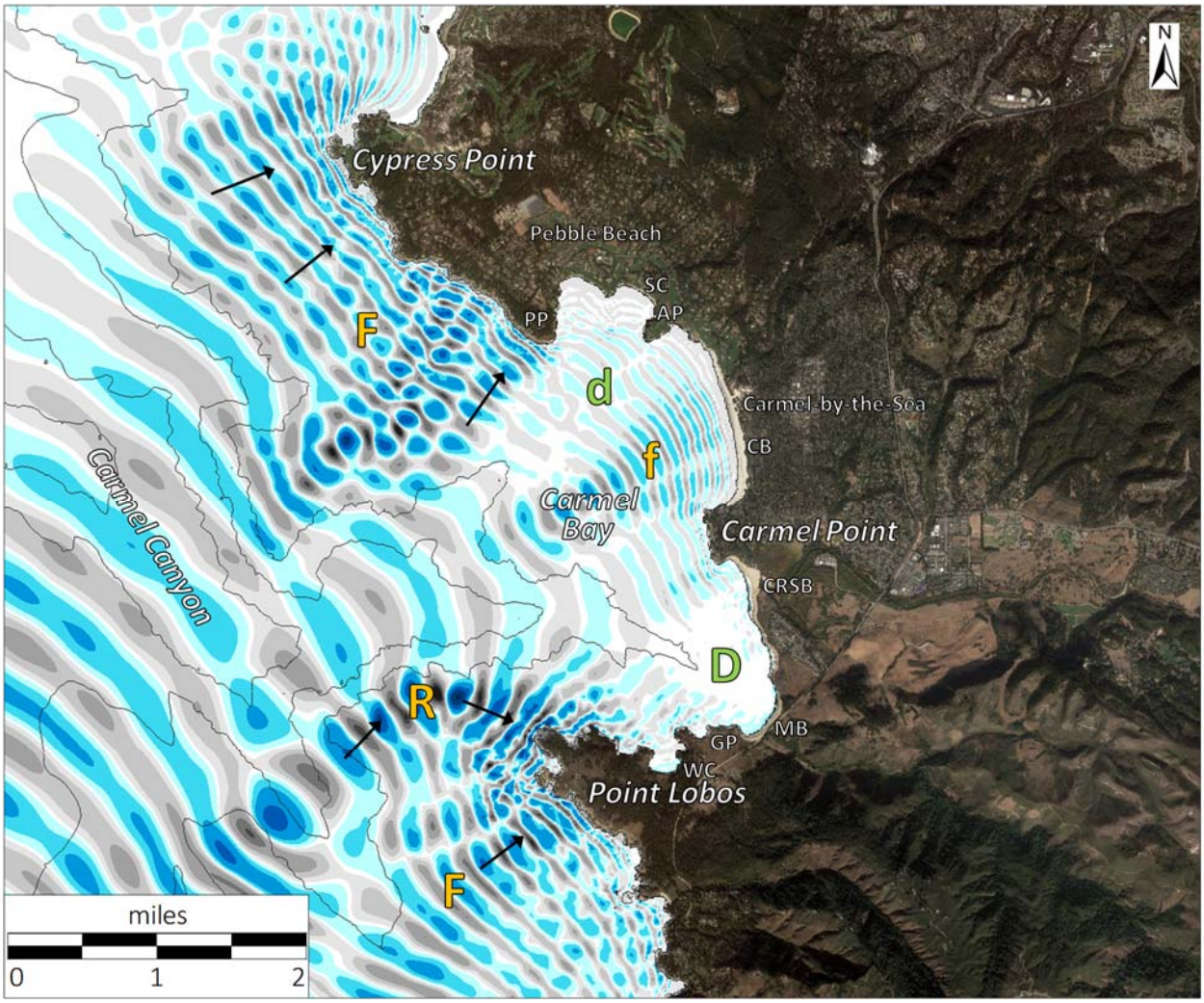

Figure 4-11: Transformation of swell waves arriving from south by west.

The ability of the submarine canyon to impact wave transformation is remarkable in that much the same effects result irrespective of whether the offshore waves arrive from northwesterly or southwesterly directions.

The focusing “F” of wave energy along the shoreline between Cypress Point and Pescadero Point is likely the explanation why this portion of the coast is particularly rugged. Conversely, the dispersal of

waves coming to the head of the canyon in Carmel Bay and towards Monastery Beach, means that the wave climate in these areas is much more calm than further offshore.

4.3.1. Focusing and Dispersal of Waves

How depth refraction transforms incident waves is illustrated in Figure 4-12. The black arrows indicate the direction of wave propagation. The two locations marked “D” can be taken as an idealized representation of the canyon heads shown in Figure 4-10 and Figure 4-11. The depth refraction patterns show that wave energy disperses at the canyon heads “D”. Conversely, there is a focusing “F” of wave energy between the canyon heads. The reason that the wave climate is more calm over the submarine canyon is that waves propagating through the canyon will tend to turn (refract) towards the side walls of the canyon. Consequently, the overall effect of the canyon is that it attenuates offshore waves as they enter Carmel Bay.

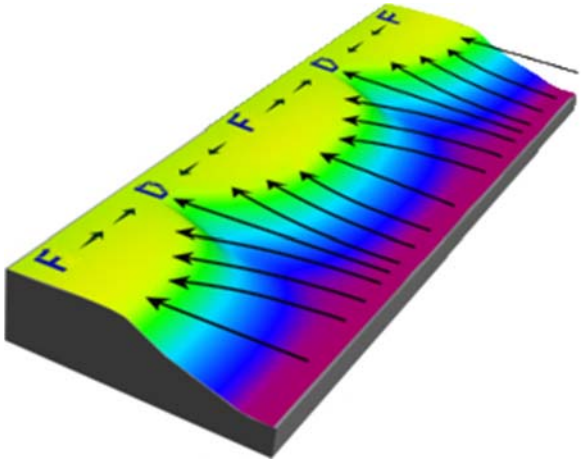

Figure 4-12: Refraction by a submarine canyon.

Table 4-5 shows how waves are affected by the submarine canyon in terms of their wave period, which translates to wave length. The table summarizes the ratio of water depth to wave length (h/L). Yellow color indicates shallow-water waves, which occur when $h/L < 0.04$. The solid blue color indicates deep water wave conditions when $h/L > 0.5$. The shading between yellow and blue indicates transitional conditions: $0.04 < h/L < 0.5$. In deep water, waves are not affected by the seafloor and are not subject to depth refraction and shoaling. As waves enter intermediate water depths, they begin to undergo wave transformation related to changes in water depth. These include depth-refraction, shoaling, and depth-limited wave breaking.

Table 4-5 shows that over the deeper part of the submarine canyon at water depths from 1,000 to 3,000 feet deep water wave conditions prevail, i.e. the incident waves propagate over the canyon and are not affected by it. In the shallower part of the canyon and near the canyon edge, swell waves transition to intermediate water depths where they become subject to refraction and shoaling. Wind-waves can propagate over the canyon without being affected. As waves propagate into the shallow areas near the shoreline and beach areas, they eventually become subject to shallow-water wave transformation effects including refraction, shoaling and depth-limited wave breaking.

Table 4-5: Influence of water depth on wave characteristics.

Zone	Water Depth (ft)	Wave Period (seconds)									
		Wind-Waves				Swell Waves					
		2	4	6	8	10	12	14	16	18	20
Beach to Intermediate depths	3	0.2	0.1	0.1	0.04	0.03	0.03	0.02	0.02	0.02	0.02
	30	1.5	0.4	0.2	0.1	0.1	0.1	0.1	0.1	0.1	0.05
	100	4.9	1.2	0.5	0.3	0.2	0.2	0.1	0.1	0.1	0.1
canyon edge	200	9.8	2.4	1.1	0.6	0.4	0.3	0.2	0.2	0.2	0.1
	300	14.6	3.7	1.6	0.9	0.6	0.4	0.3	0.3	0.2	0.2
submarine canyon interior	500	24.4	6.1	2.7	1.5	1.0	0.7	0.5	0.4	0.3	0.3
	1,000	48.8	12.2	5.4	3.1	2.0	1.4	1.0	0.8	0.6	0.5
	2,000	97.6	24.4	10.8	6.1	3.9	2.7	2.0	1.5	1.2	1.0
	3,000	146.5	36.6	16.3	9.2	5.9	4.1	3.0	2.3	1.8	1.5

4.3.2. Reflection by the Carmel Submarine Canyon

Per AGU (2005), wave reflection, R, and transmission, T, at a marine canyon can be described by:

$$R = \sqrt{\frac{\gamma}{1+\gamma}} \quad , \qquad T = \sqrt{\frac{1}{1+\gamma}}$$

and

$$\gamma = \left(\frac{h^2 l^2 - h_c^2 l_c^2}{2hlh_c l_c}\right)^2 sin^2(l_c W)$$

Where R and T are the ratios of reflected and transmitted wave energy, h is the water depth outside the canyon, h_c is the water depth inside the canyon, l and l_c represent the cross-canyon wave number outside and inside the canyon, and W is the width of the canyon.

These equations predict that when waves approach the submarine canyon at an oblique angle, nearly all of the wave energy is reflected. The critical angle, θ, for total reflection can be estimated as:

$$|\theta| = arcsin\left(\sqrt{h/h_c}\right)$$

For the Carmel submarine canyon, θ is in the range of 25° to 30°. This means that when waves approach the canyon at angles below this range they will be reflected off the canyon. When waves approach at oblique angles higher than θ there will be components of both reflection and transmission of wave energy across the canyon.

The above equations are derived for a box approximation of the canyon. In reality, the water depths outside and inside of the canyon vary, as does the width of the canyon and the angle of wave incidence. The wave-canyon interaction is therefore much more complex, as e.g. illustrated in Figure 4-10 and Figure 4-11.

5. Cliff Retreat Rates

Degradation and erosion of coastal cliffs at Carmel Bay an important role in the overall sediment budget. Cliff erosion is the second largest contributor of sediment to the littoral cell after the fluvial input from the Carmel River and San Jose Creek.

Figure 5-1 summarizes estimates of cliff retreat rates from USGS (2020). In the region from Cypress Point to Point Lobos cliff retreat rates are on the order of 4 to 8 inches per year (0.1 to 0.2 m/year), with the highest rates occurring along the most exposed areas of the coast (refer to areas where focusing of incident wave energy occurs marked with “F” in Figure 4-10 and Figure 4-11).

Figure 5-1: Overview of cliff erosion data, USGS (2020).

6. Shoreline Change

Shoreline change is another phenomenon that affects the overall sediment budget at Carmel Bay. While most of the pocket beaches and crenulate-shape bays are relatively stable, long-term shoreline recession has the effect of adding sand to the overall system. Beaches are subject to a seasonal (cyclical) variation where they tend to build up and widen in the summer and become narrower in the winter. Via this variation sediment is added to the littoral cell in the summer and released during the winter. The aggregate effect is a temporary storage of sediment within the littoral cell system. However, long-term shoreline recession will produce a net loss of sediment from the system.

Shoreline change at CRSB was evaluated based on historical aerial imagery. Figure 6-1 summarizes shoreline locations derived from aerial imagery recorded over the years from 1929 to 2020. The respective years included in the analysis are listed in Table 6-1. The table also indicates the color codes used to denote the shoreline locations in Figure 6-1.

Table 6-1: Aerial imagery dates and color code.

Date	Color Code	Source
1929-08-01		UCSB (2020)
1941-11-22		UCSB (2020)
1945-10-24		UCSB (2020)
1961-04-14		UCSB (2020)
1986-09-28		CCRP (2020)
1993-04-19		CCRP (2020)
2001-05-30		UCSB (2020)
2005-10-04		MCPW (2014)
2006-04-18		MCPW (2014)
2016-04-28 a)		NOAA (2020c)
2020-05-16		NM (2020)
a) El Nino year.		

The variety of the shoreline locations in Figure 6-1 reflect the seasonal and intra-annual variation of the shoreline as well as the long-term shoreline recession. The long-term recession rates were determined as the mean trend across the data for 58 transects along the shoreline at 50-ft spacing.

It is evident that the fluctuation of the shoreline location is smaller at the north end of the beach than at the south end. Removing the long-term recession trend from the data, the fluctuation of the shoreline varies from about 45 feet at the north, to 75 feet at the central location of the lagoon breach, to 150 feet at the south end.

This variation is not surprising, as the north end of the beach is more sheltered in the lee of Carmel Point and is therefore more stable. The portion of the beach fronting the river mouth is somewhat less

sheltered and exposed to larger waves and therefore exhibits more variation in the plan location of the shoreline. The shoreline segment located south of the river mouth is further exposed to wave action and also subject to significantly larger changes in sand volumes as pulses of sand deposited from the river move southward conveyed by the littoral transport.

Figure 6-1: Shoreline locations (1929 to 2020).

Figure 6-2 summarizes estimates of long-term shoreline change at Carmel River State Beach. The shoreline recession rates were developed based on aerial photography dating back to 1929. Refer to Table 6-1 for the specific dates.

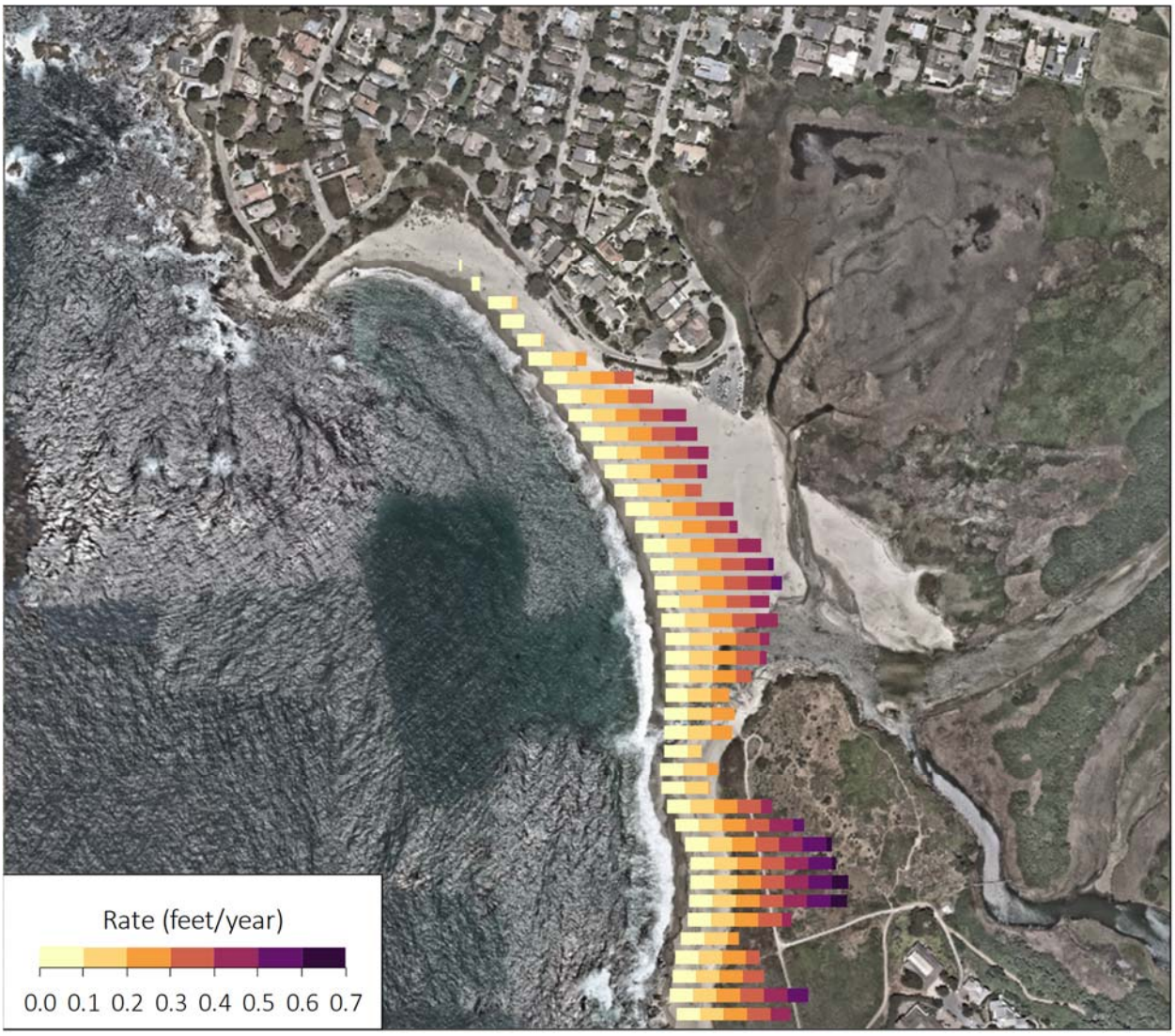

Figure 6-2: Long-term shoreline recession rates at Carmel River State Beach.

The results show that the northern part of the beach appears to be stable over the long-term. In this area, the beach is sheltered by the promontory at Carmel Point. It is conceivable that the long-term rate of shoreline recession in this area is tied to the cliff recession rate, which is on the order of a few inches per year. Moving south along the beach, it can be seen that the shoreline recession rate increases progressively, on the order of 0.4 to 0.5 feet per year at the river mouth, increasing to nearly 0.7 feet per year at the transition between Carmel River State Beach and Ribera Beach.

The shoreline recession trends shown in Figure 6-2 are consistent with estimates from USGS (2006, 2020), which are on the order of 0.3 to 0.9 feet per year (0.1 to 0.3 m/year). Figure 6-3 summarizes

the transects for which USGS estimates shoreline recession rates based on shoreline data for years (1876, 1933, 1945, and 1998).

Figure 6-3: Shoreline change transects from USGS (2020).

7. Sediment Grain Sizes

Sediment samples were acquired in connection with the studies reported in NPS (1972) and MG (2000). Table 7-1 provides a summary of the mean grain sizes determined from field samples. Note, phi-values converted to average diameter, d_{50}, per the Wentworth Classification Scale, Appendix B.

Figure 7-1 shows the variation of grain sizes with distance from the shore. It can be seen that the sediment gets coarser going from north to south from the north end of CRSB to Monastery Beach. The variation with water depth shows coarser sediment on the beaches and nearshore, decreasing in size as the water depth increases with the distance from the shore.

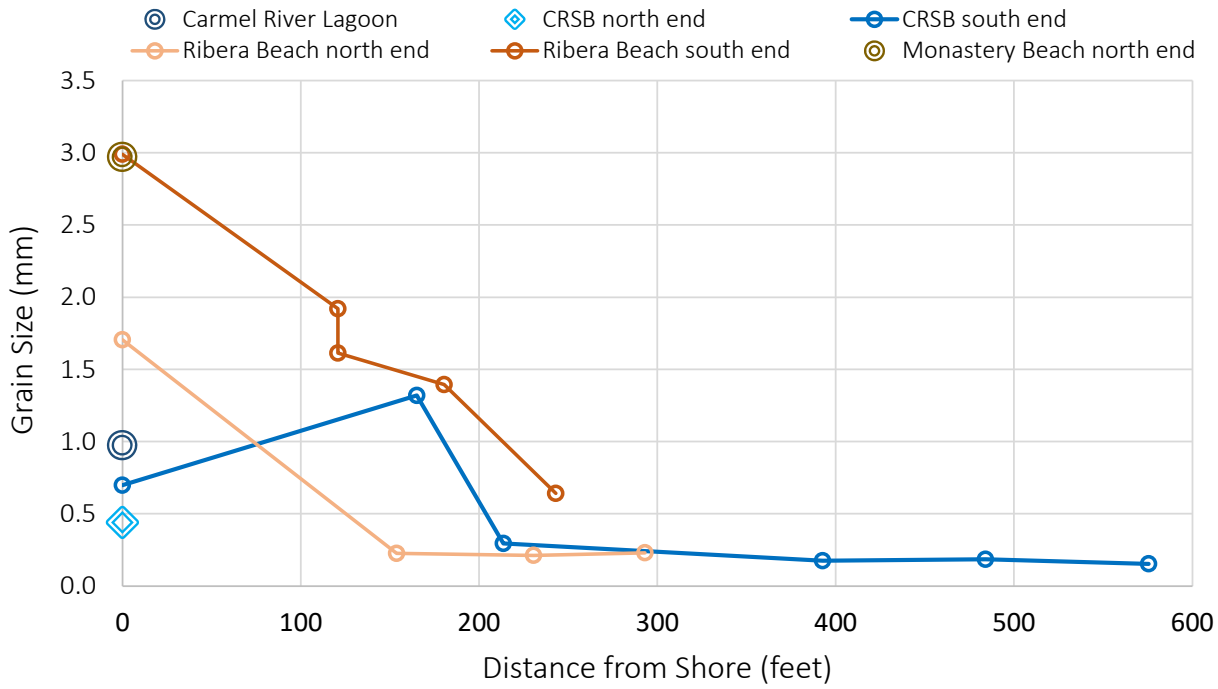

Figure 7-1: Overview of grain size samples from NPS (1972).

Figure 7-2 and Figure 7-3 shows examples of beach sand from Carmel River State Beach sampled on October 30, 2020. The sand grains are rounded, ranging from fine and medium sand to coarse sand with a few very fine pebbles (Figure 7-2) medium sand with fine pebbles (Figure 7-3).

Figure 7-2: CRSB beach sand.

Figure 7-3: CRSB beach sand.

Table 7-1: Sediment grain size based on sampling and sieve analysis.

Location	Sample/ Site #	Distance from shore (feet)	Water Depth (feet)	φ	Mean Grain Size d_{50} (mm)	Classification	Reference
Carmel River Lagoon	18	On beach	-	0.04	0.97	coarse sand	NPS (1972)
CRSB north end	13	On beach	-	1.18	0.44	medium sand	
CRSB south end	14	On beach	-	0.52	0.70	coarse sand	
	5	165.2	20	-0.40	1.32	very coarse sand	
	4	213.6	40	1.76	0.30	medium sand	
	3	392.6	60	2.52	0.17	fine sand	
	2	484.1	80	2.44	0.18	fine sand	
	1	575.5	95	2.71	0.15	fine sand	
Ribera Beach north end	15	On beach	-	-0.77	1.71	very coarse sand	
	8	153.7	26	2.15	0.23	fine sand	
	7	230.6	40	2.24	0.21	fine sand	
	6	293.1	65	2.12	0.23	fine sand	
Ribera Beach south end	16	On beach	-	-1.58	2.99	very fine pebbles	
	12	120.8	30	-0.94	1.92	very coarse sand	
	11	120.8	30	-0.69	1.61	very coarse sand	
	10	180.5	50	-0.48	1.39	very coarse sand	
	9	243.0	70	0.64	0.64	coarse sand	
Monastery Beach north end	17	0	0	-1.57	2.97	very fine pebbles	
Stillwater Cove, Pebble Beach	20	On beach	-	1.74	0.30	medium sand	MG (2000)
Carmel Beach (north)	21	On beach	-	0.57	0.67	coarse sand	
Carmel Beach (south)	22	On beach	-	1.87	0.27	medium sand	
CRSB (north)	23	On beach	-	0.68	0.62	coarse sand	
CRSB (central)	24C	On beach	-	0.96	0.51	coarse sand	
CRSB (south)	24S	On beach	-	-0.87	1.83	very coarse sand	
Monastery Beach	25	On beach	-	-0.66	1.58	very coarse sand	

Location	Sample/ Site #	Distance from shore (feet)	Water Depth (feet)	φ	Mean Grain Size d_{50} (mm)	Classification	Reference
Ribera Beach, south end	115	On beach	-	-1.04	2.06	very fine pebbles	NPS (1968)
Monastery Beach, north end	106	Back beach	-	-0.93	1.91	very coarse sand	
	107	Mid beach	-	-0.5	1.41	very coarse sand	
	108	Shoreline	-	-1.31	2.48	very fine pebbles	
Monastery Beach, central	109	Back beach	-	-0.74	1.67	very coarse sand	
	110	Mid beach	-	-0.82	1.77	very coarse sand	
	111	Shoreline	-	-1.09	2.13	very fine pebbles	
Monastery Beach, south end	112	Back beach	-	-1.02	2.03	very fine pebbles	
	113	Mid beach	-	-0.59	1.51	very coarse sand	
	114	Shoreline	-	-0.93	1.91	very coarse sand	

8. Carmel Littoral Cell

A littoral cell is a section along the coast where sediment processes are isolated from neighboring shoreline segments. A littoral cell exhibits a complete cycle of sedimentation including sources, losses, and transport paths. The Carmel littoral cell extends from Cypress Point to Point Lobos as illustrated in Figure 8-1. The net direction of sediment transport within the littoral cell is from north to south, GM (2000). North of Cypress Point the bluff is oriented approximately perpendicular to the average direction of incident waves. This means that material produced due to erosion of the cliffs in this area tends to move north towards Monterey or south into the Carmel littoral cell depending on how the incident waves deviate from the mean wave direction. The Carmel littoral cell terminates at Point Lobos around Monastery Beach (MB), where material is lost to the Carmel submarine canyon.

8.1. Sub-Cells

Within the Carmel littoral cell are sub-cells comprised of the pocket beaches and crenulate-shaped bays found along the shoreline. These features are located between rocky headlands which prevents sediment within these cells from moving along the coast. These coastal features are not true littoral cells, but exhibit a similar function by being able to retain sediment within a stable or quasi-stable cell. Examples of these are Carmel Beach (CB), Carmel River State Beach (CRSB), Monastery Beach (MB), Stillwater Cove (SC), and Whaler's Cove (WC).

Sediment transport patterns within the littoral cell, and sources and losses of sediment are described in the following.

8.2. Sediment Transport

Figure 8-1 provides an overview of the Carmel Littoral Cell and sub-cells within it. Seafloor elevation contours are indicated by the blue color bands with shallow water being light blue and deeper water dark blue. Within the littoral cell, sediment can be transported by waves, currents, streamflow, runoff, and by wind.

The arrows in Figure 8-1 indicate the predominant direction of the littoral transport. Yellow arrows indicate longshore transport, and red arrows indicate loss of sediment, while the black arrow indicates storage of sand via dune formation. The blue curves indicate streams that supply sediment to the shoreline areas.

Apart from the Carmel River, which is described later, sediment transported via streamflow, runoff, and wind comprises a smaller part of the overall system. Wave action is the most significant driver for movement of sediment within the littoral cell. Wave action contributes to erosion, cross-shore movement of sand onto beaches and movement of sand offshore, and longshore transport along the shoreline due to wave runup and rundown, and in the surf-zone via wave-induced currents.

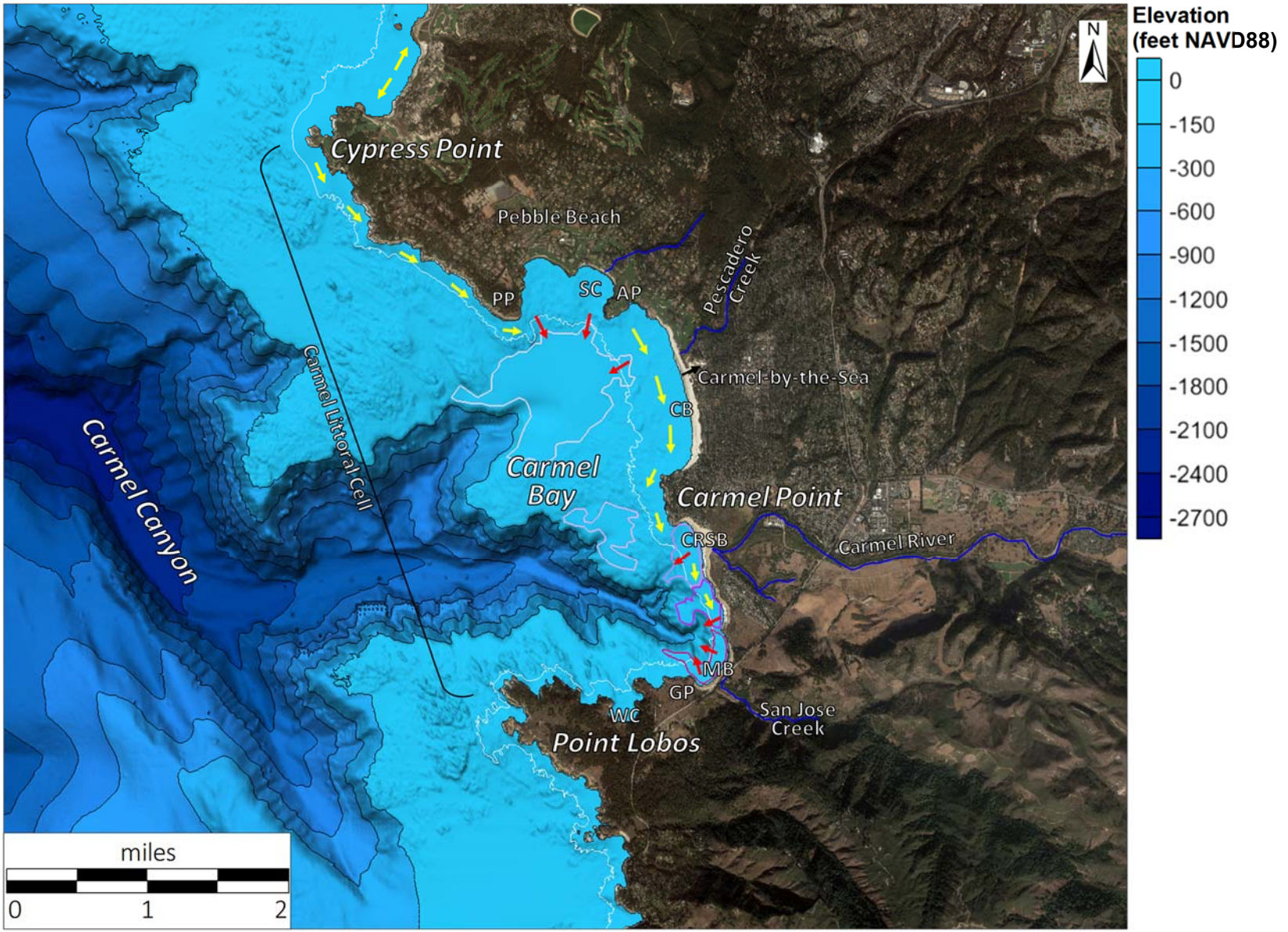

Figure 8-1: Overview of Carmel Littoral Cell.

Figure 8-2 illustrates the movement of sand particles along the shore due to wave-induced processes.

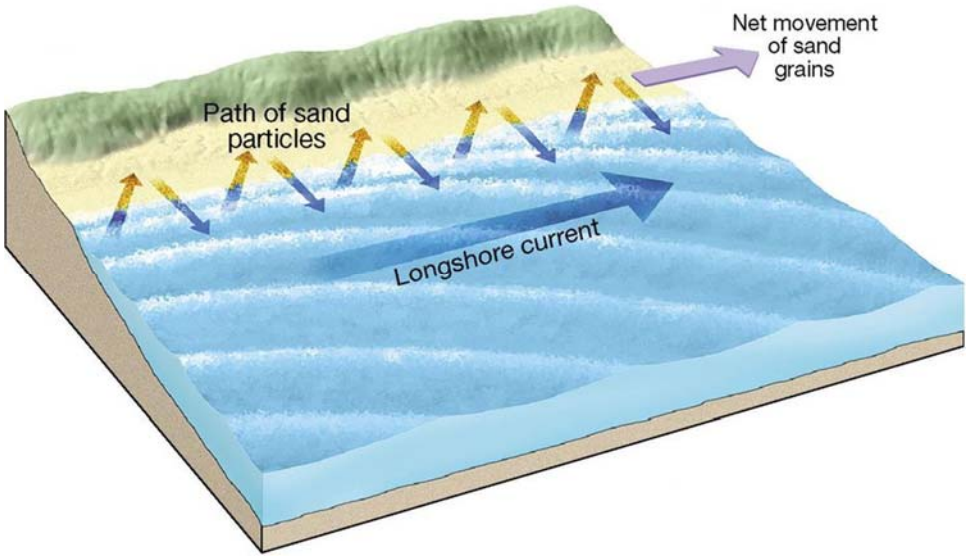

Figure 8-2: Wave-driven sediment transport along the shore.

In deep water, waves are unable to mobilize sediment on the seafloor. The depth at which this occurs is termed the closure depth. Figure 8-3 provides a summary of coastal terms and definition of the closure depth.

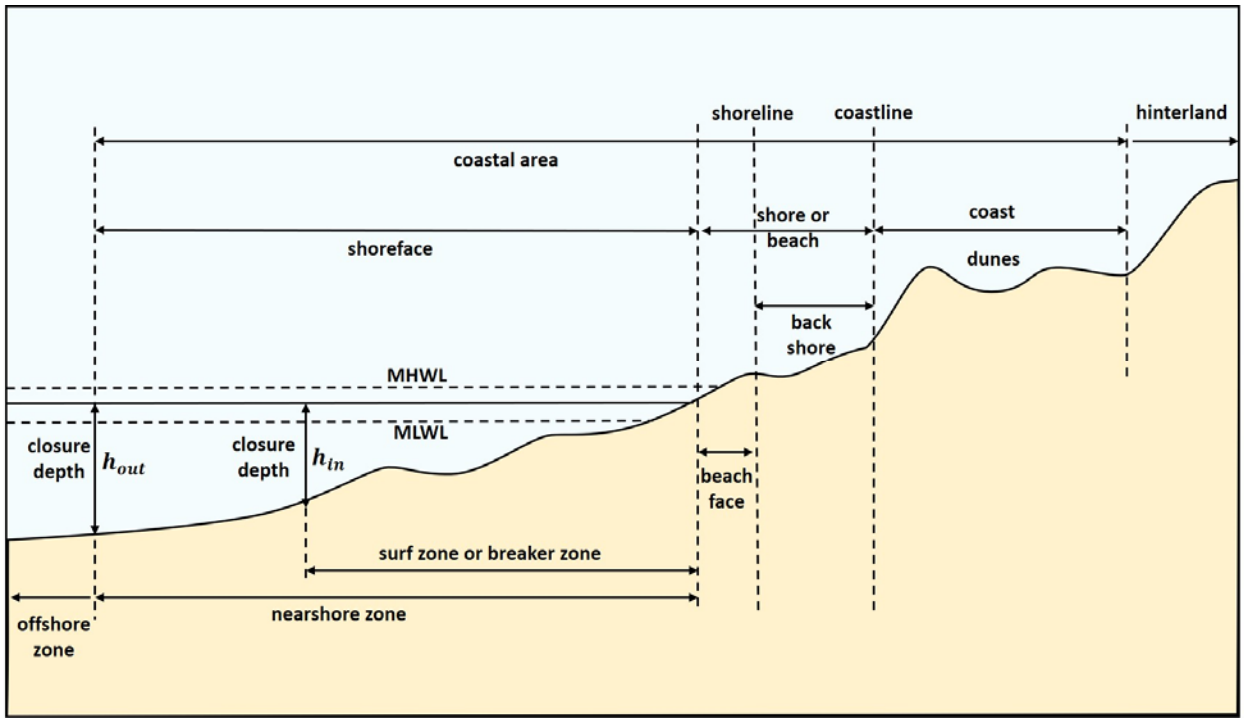

Figure 8-3: Definition of coastal terms and closure depth, adapted from SPM (1984).

Hallermeier (CEM, 2011), defines the closure depth as:

$$h_c = 2.28H_e - 68.5\left(\frac{H_e^2}{gT_e^2}\right)$$

Where H is effective significant wave height and T the effective wave period based on conditions exceeded only 12 hours per year (0.14% of the time). Birkemeier (CEM, 2011) suggested a simpler relationship given by:

$$h_c = 1.57H_e$$

The closure depth is indicated by the white line along the shore in Figure 8-1. At Carmel Bay the closure depth approximately follows the -45 to -50 feet NAVD88 elevation contour. The predominant zone of wave-induced longshore transport is between this line and the shoreline. Wave-driven sediment transport is limited seaward of the closure depth where water depths are so deep that waves cannot mobilize sediment on the seabed. In areas where the closure depth contour comes close to the shoreline, there is a limited potential for sand movement between adjacent areas. In these areas sediment exchange is sporadic and typically occurs during significant storm events.

8.3. Sand Sources and Loss of Sediment

The primary sources of sand input to the littoral cell include:

1. Sediment from gully erosion.
2. Sediment from sea cliff and bluff erosion.
3. Sand supplied by small streams, Pescadero Creek, San Jose Creek, and the Carmel River.
4. Onshore transport of sand, e.g. seasonal beach profile buildup due to swell waves.
5. Dune erosion, e.g. wind-blown sand transported from dunes to beach areas and surf zone.

Loss of sand from the littoral cell is due to the following mechanisms:

1. Longshore transport out of the system.
2. Offshore transport of sand, e.g. seasonal beach profile variation due to winter waves.
3. Offshore loss of sand to the Carmel Submarine Canyon.
4. Dune growth (on Carmel Beach).
5. El Niño effects. The warming (and expansion) of the ocean water produces a temporary rise of the mean sea level, which when coinciding with winter storms can produce widespread shoreline recession and beach narrowing (similar to sea-level rise).

6. Sea-level rise, e.g. shoreline recession and beach narrowing due to rise in water level.

The competing mechanisms of accretion and erosion produces a dynamic equilibrium of sediment within the littoral cell.

Elements of the Carmel Littoral Cell are described in the following.

8.4. Coastal Cliffs from Cypress Point to Pescadero Point

This portion of the coast consists of craggy coastal cliffs. There are a limited number of access points to the water and isolated pocket beach areas. The majority of the shoreline is rocky and swept free of sand. Due to reflection of long period swell waves as they pass over the Carmel submarine canyon, a portion of the incident waves are directed towards the coastal cliffs. This occurs for waves incident from both northwesterly and southerly directions, and means that the shoreline is continually exposed to wave action. Material dislodged from the cliffs by wave action and natural decomposition of the rock is transported southeast along the cliffs toward Pescadero Point and ultimately provides input of beach sand to Carmel Beach.

8.5. Stillwater Cove

Stillwater Cove is a sheltered inlet consisting of two pocket beaches perched between Pescadero Point and Arrowhead Point. Stillwater Cove is the moniker for the pocket beach to the east, which is sheltered by the Pescadero Rocks fronting the inlet. The pocket beach to the west is open to the bay and receives a higher degree of wave exposure. The shoreline in this area is rocky and consists of sections of steep bluff interspersed by narrow beaches and is aptly named Pebble Beach.

The primary source of sediment with Stillwater Cove comes from erosion of the bluff along the golf course. A ravine with a small inland drainage area has an outlet at the beach, but does not contribute a significant input of sediment to the beach.

Sediment coming from erosion of the cliffs between Cypress Point and Pescadero Point will tend to move along the bluff towards Stillwater Cove. A fraction of this material may enter the cove, but most of it is probably lost to the deeper portion of the bay at the entrance to the cove (refer to the two red arrows in Figure 8-1. The deposit of sand offshore from Stillwater Cove can be seen in the figure as a smooth appearance of the seafloor, as opposed to the irregular seabed within the cove which is indicative of a rocky substrate. Sediment lost to the deeper water outside of the cove will tends to migrate downslope towards the north arm of the submarine canyon where it is ultimately lost from the system. In this regard, the submarine canyon acts as a sediment trap, and sediment entering the canyon can be considered as lost from the littoral cell.

8.6. Carmel Beach

Carmel Beach is a crenulate-shaped bay suspended between Arrowhead Point and Carmel Point. The beach is approx. 400 feet wide and has an abundance of white sand. The characteristic white color of

the sand comes from the source of the material which is the granodiorite rock formations in the bay. Pescadero Creek also has an outlet on the beach via Pescadero Canyon. The drainage area for the creek is estimated to be around 567 acres and the sediment supply to the beach from this drainage area is therefore limited. There is enough sand on Carmel Beach that wind-blown sand transport has created an area of dunes along the beach of approximately 10 acres in size. Wind-blown sediment contributing to growth of the dunes is considered a loss of sediment from the littoral cells. Conversely, sand that is eroded from the dunes provides an input to the system.

The alignment of the beach is generally perpendicular to the average incident wave direction. During significant wave events, the surf zone can extend out past Carmel Point and sediment can be transported from Carmel Beach to the Carmel River State Beach area.

Over the summer months when the wave climate is mild, incident swell waves will transport sand onto the beach which can widen by around 200 feet over this period. Winter waves pull sand away from the beach out into deeper water and the beach can therefore become quite narrow in the winter months.

8.7. Carmel River State Beach

Carmel River State Beach features sweeping views of the beach and coastal cliffs. One of the most prominent features of the area is the lagoon formed at the outlet of the Carmel River.

The beach extends from the prominent headland at Carmel Point at the north and tapers out along the rocky shoreline to the south.

The sand at Carmel River State Beach is variable in color and size. Fine white sand is likely sand originating from Carmel Beach and breakdown of granodiorite formations along the shore. The coarser and more yellow sand is indicative of fluvial deposits coming down the Carmel River.

The Carmel River is a significant source of sediment to the littoral cell. Estimates of the sediment output from the river are on the order of 62,000 CY/year on average. The sediment output from the river varies seasonally and from year to year depending on rainfall amounts.

As indicated by the red arrow in Figure 8-1, sand at the Carmel River State Beach may be lost due to downslope migration to the Carmel submarine canyon. The north arm of the canyon comes close to shore in this area, in proximity to the closure depth contour. There is evidence that significant wave events and outflow currents cause sediment to be transported into the submarine canyon. The mechanisms that can cause this to happen include:

1. Winter storm wave events, which draw sand away from the beach out into deeper water and over the edges of the submarine canyon.
2. Seepage flow from the Carmel River.
3. Flushing events when the Carmel River Lagoon breaches out into the bay.
4. Rip-currents producing strong outflows away from the beach, which carry sand offshore and into the canyon.

The net sediment transport direction at Carmel River State Beach is from the north to the south. However, incident swell can cause the littoral transport direction to be northerly, NPS (2019). Major pulses of sediment move south during storms from northwesterly directions, GM (2000).

8.8. Ribera Beach

Ribera Beach is a short stretch of beach between Carmel River State Beach and Monastery Beach. This beach runs along Ribera Road and is also referred to as the Middle Beach. The headlands framing the beach don't protrude as much out from shore and the beach is therefore relatively narrow with rock outcrops. The beach is perched against a narrow 300 ft long shore-parallel granodiorite outcrop on the seafloor, NPS (1972). The sand in this area is very coarse.

There is evidence of sand being transported along the shoreline in the form of sand chutes carved into the rock outcrops. These manifest as branching, rounded chutes carved into the rock terrace. The chutes are filled with sand and vary in width from 2 to 3 inches up to 10 feet wide, NPS (1968).

Diver surveys have identified a sand fall in this area, NPS (1968), which consists of a river of very coarse sand on the seabed aligned in a southwest direction towards the submarine canyon head. The sand river formation is the result of the longshore littoral transport being diverted seaward by the rock outcrop at the south end of the area, at the transition to Monastery Beach.

8.9. Monastery Beach

Monastery Beach (MB) is a pocket beach framed between the rocky shoreline to the north and Granite Point (GP) at its south end. The orientation of the beach is perpendicular to the average direction of incident waves. A key feature of the area is San Jose Creek which has a meandering outlet at the beach. The sand at this beach is likely a mix of sand from granodiorite decomposition, sand from the Carmel River transported along the shore, and sediment output from San Jose Creek. The net direction of sediment transport along Monastery Beach is to the north as indicated by the northward migration of San Jose Creek on the beach.

The Carmel Littoral Cell generally terminates at Monastery Beach by Granite Point. Only a very limited amount of sand is transported west past Granite Point. Evidence to this is the fact that Whaler's Cove contains very little sand. The majority of the shoreline in Whaler's Cove consists of rocky cliffs with very narrow patches of sandy beach at the back of the cove.

At Monastery Beach, the primary loss of sand is to the south arm of the Carmel submarine canyon, which comes close to shore in this area. The mechanisms that can convey sediment from shore out to the submarine canyon include:

1. Winter storm wave events, which draw sand away from the beach out into deeper water and into the canyon.
2. Outflow from San Jose Creek, which may produce turbidity flows out to the canyon.
3. Rip-currents producing strong outflows away from the beach, which carry sand offshore and into the canyon. Rip currents have been observed to achieve enough speed to break through

the surf zone, NPS (1968). Rip-currents can occur at the rocky headland formations and along the beach. Cusp formations along the beach, which are known to occur at Monastery Beach are often indicative of rip-currents.

4. Sand chutes, consisting of rounded channels carved in the rock terrace have been observed around the canyon head, NPS (1968). These have an orientation perpendicular to shore suggesting that these have formed due to abrasion associated with wave-induced oscillation of the coarse sand on the seabed.

5. Sand falls consisting of rivers of very coarse sand on the seafloor, directed towards the head of the submarine canyon. Sand falls have been identified at the headland features at the north and south end of Monastery Beach, NPS (1968).

8.10. Carmel Canyon

The Carmel submarine canyon is the end destination of sediment transported out of the Carmel Littoral Cell. Once sediments enter the canyon, they will not reenter the system.

Several processes have been identified that document transport of sand from the seabed into the canyon in the area of Carmel River State Beach and Monastery Beach. These include:

1. Tidal circulation patterns, which may drive a net drift of fine sediment into the canyon.

2. Runnels in the bedrock of the seafloor. These are believed to be carved by abrasion from sand particles moving with the orbital motion of incident waves during significant wave events. The downslope grade of the seafloor produces a net flow of sediment towards and into the canyon.

3. Outflow events during Carmel River Lagoon breaching and/or during significant discharges from the Carmel River and San Jose Creek. In these cases, sediment can be flushed out into deeper water via hypopycnal and hyperpycnal flows (Figure 8-4). Hypopycnal flows occur during smaller outflow events and/or when the transported sediment consists of coarse material, which causes the material to be deposited in the deeper water fronting the beach. The freshwater outflow may initially consist of a lens atop the heavier seawater. Hyperpycnal flows can occur during significant outflow events. In this case, the sediment flows as a turbidity current downslope over the seabed towards the canyon.

4. Mass wasting along the edges of the canyon due to oversteepening of sediment deposits.

5. Seismic activity, which causes submarine landslides into the canyon. Earthquakes can also cause landslides on the seafloor, which subsequently move as turbidity flows downslope towards the canyon.

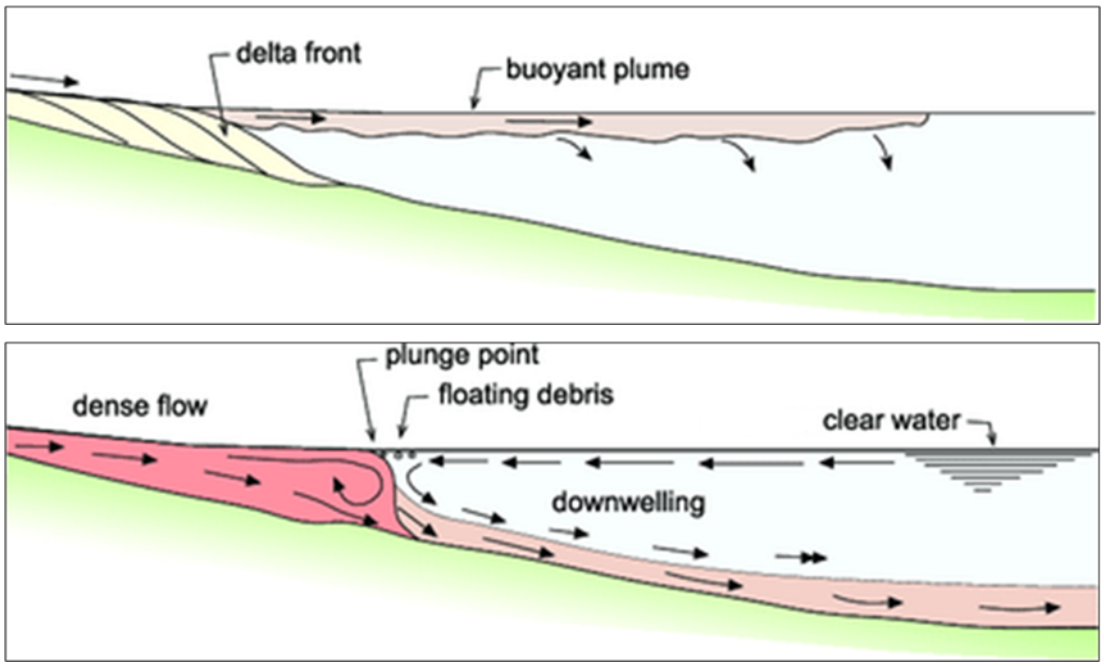

Figure 8-4: Illustrations of hypopycnal flow (upper) and hyperpycnal flow (lower).

8.11. Sediment Budget

Figure 8-5 presents an idealized version of the Carmel coast, summarizing sediment input and losses from the littoral cell. The littoral cell can be considered as a control volume along the shoreline. Sediment input to the system is denoted by arrows going into the cell marked with a “+” symbol. Sediment losses are indicated by arrows going out of the cell marked with a “÷” symbol.

The arrow on the left side indicates littoral transport into the cell, which is small to negligible where the littoral cell starts at Cypress Point. Likewise, the littoral transport leaving the system (arrow on the right) is also small where the littoral cell terminates at Point Lobos.

There is longshore littoral transport within the cell which can be to the north and south depending on winter storm and wave patterns, but with a net transport to the south (left to right in the figure).

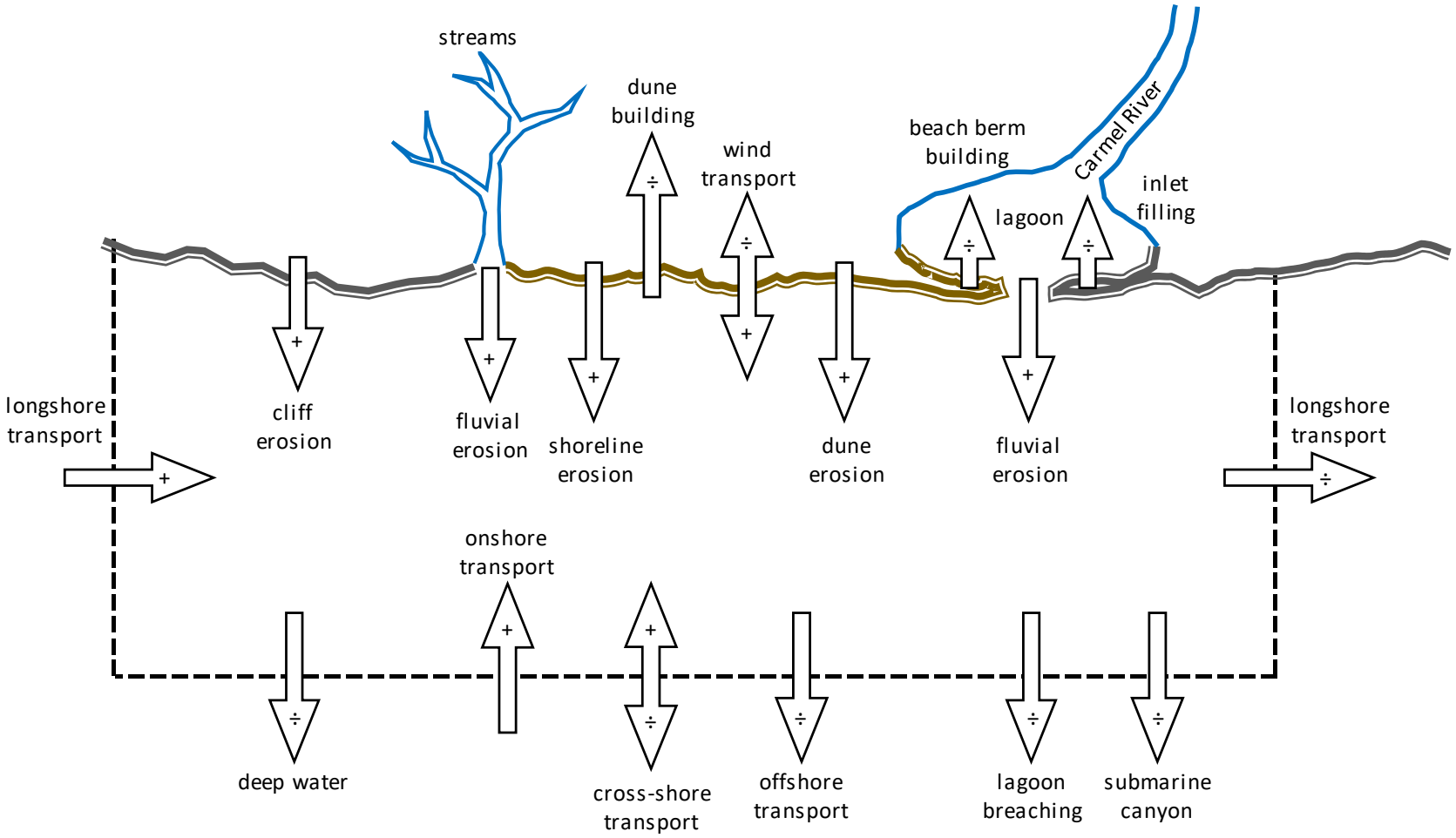

Figure 8-5: Littoral cell sediment sources and losses.

8.12. Sediment Input to Littoral Cell

The primary sources of sediment input to the cell include:

Cliff Erosion. Sediment created from erosion and weathering of the cliff formations along the coast and on the seabed. The erosive mechanisms include physical breakdown due to wave action, chemical breakdown, and due to biological processes. Refer to IMS (2007).

Fluvial sources. Sediment created from fluvial erosion conveyed to the littoral cell via gullies, streams, and rivers including Pescadero Creek, the Carmel River, and San Jose Creek.

Shoreline erosion. Sediment resulting from shoreline erosion is considered input to the littoral cell.

The Carmel River and lagoon comprises a separate system of sediment exchange within the littoral cell and a major source of sediment to the system. Sediment carried down the Carmel River provides input of sediment to the system. This source of sediment stems from fluvial erosion along the streambank and upland terrain within the drainage area of the river. The sediment load can vary significantly from year to year depending on several factors. Drought can reduce sediment output from the river, and upper portions of the watershed have historically been dammed off by the Los Padres Dam (1949). The San Clemente Dam (1921), and the Old Carmel River Dam (1880s). The latter two were removed around 2016 as part of the San Clemente Dam Removal Project. Increased sediment output from the Carmel River have been known to occur during wet years and following wildfires within the watershed.

8.13. Sediment Fluctuations

Wind transport of sand on the beach can contribute to sediment input to the littoral cell as well as loss of sediment from the cell. When wind-blown sand transport contributes to formation of dunes it is considered a loss from the system. When dunes are eroded due to wind or e.g. wave action it is considered an input to the system. Because the dune fields along Carmel Beach are relatively stable and not significantly expanding or eroding, the sediment exchange with the dune system can be considered a form of temporary storage of sediment within the littoral cell.

The Carmel River Lagoon also functions as a form of temporary storage of sediment within the littoral cell. During lagoon formation, seepage provides an input of sediment to the littoral cell. During breaching of the lagoon, sediment is also released into the system. Sandbar buildup resulting from wave action constitutes a loss of sediment from the system, but because these processes fluctuate, the overall sediment exchange with the Carmel Lagoon can be considered as temporary storage of sediment.

Cross-shore transport is another mechanism that fluctuates significantly seasonally and depending on the incident wave climate. Winter storm events often produce wave conditions that draw sediment out from the beach areas into deeper water. This movement of sediment can be considered as a temporary loss from the system. Swell waves tend to build up the beach profile. This onshore transport can be considered input of sediment to the system. Because these processes of sediment exchange

are dynamic and fluctuate seasonally, they can be considered as temporary storage or removal of sediment from the littoral cell.

8.14. Sediment Losses from Littoral Cell

Loss of sediment from the littoral cell is indicated by arrows pointing out from the cell shown in Figure 8-5.

One form of loss from the littoral cell includes sediment lost to deeper water. This process occurs when large winter storms draw sediment out from the beach areas into deeper water. Sediment that settles in water depths at the depth of closure may rarely if ever become re-mobilized and can be considered lost from the system. Another effect that contributes to this form of sediment loss is downslope sediment migration, which simply means that when sediment is mobilized, gravity will tend to move the sediment downhill. This effect is noticeable in areas offshore Pebble Beach, Stillwater Cover, Arrowhead Point, and Carmel Point. Refer to the areas outlined in purple in Figure 8-1 seaward of the closure depth contour (white contour line). The smooth appearance of these areas indicates a sandy substrate, as opposed to the irregular features on the seabed seen elsewhere, which are indicative of rocky substrate and/or outcrops of bedrock.

Breaching of the lagoon is another mechanism that can transport sand offshore into deep water past the depth of closure and/or into the submarine canyon.

The ultimate sink in the littoral cell system is the Carmel submarine canyon. Once sediment enters the canyon it will not return to the littoral cell.

Table 8-1 provides a sediment budget for the Carmel littoral cell. For simplicity, the analysis primarily captures major sediment contributions in the form of input from cliff and shoreline recession and streams. Losses account for sediment lost to deep water and lost to the submarine canyon. Temporary storage of sediment and seasonal sediment fluctuations are assumed to be quasi-steady and are not reflected in the breakdown. A cumulative total of sediment input and output is computed for shoreline reaches starting at Cypress Point, moving south along the shoreline to Point Lobos where the littoral cell ends.

Table 8-1: Carmel littoral cell sediment budget.

Area	Extent (yards)	Recession Rate (ft/yr)	Sediment Sources			Sediment Losses		Total
			Cliff Erosion (CY/yr)	Shoreline Recession (CY/yr)	Fluvial/ Streams (CY/yr)	Deep Water (CY/yr)	Carmel Canyon (CY/yr)	Cumulative Total (CY/yr)
Cypress Pt. to Pescadero Pt.	5,000	0.3	9,194					9,194
Pebble Beach	1,000	0.3	1,275					4,669
Stillwater Cove	1,000	0.3	1,755		3 a)	-17,400		627
Arrowhead Point	1,000	1.0	5,499					326
Carmel Beach	2,100	0.7		8,926	14 b)			9,265
Carmel Point	1,200	0.7	3,496			-12,000		761
Carmel River State Beach	1,000	1.0		7,379	61,931 c)		-23,000	47,071
Ribera Beach	800	0.3	1,540				-44,000	4,611
Monastery Beach	700	2.1		11,012	226 d)		-15,000	849
Granite Point	1,000	0.5	1,835			-1,800		885
Whaler's Cove	1,000	0.3	1,180			-1,200		865
Whaler's Cove to Point Lobos	2,500	0.3	4,519			-4,500		884
Total	**18,300**	**0.5 avg.**	**+30,293**	**+27,317**	**+62,174**	**-36,900**	**-82,000**	**+884**

a) Unnamed ravine/stream into Stillwater Cove.
b) Pescadero Creek.
c) Carmel River.
d) San Jose Creek.

In Table 8-1 cliff and shoreline recession rates were estimated based on USGS (2020). The sediment load for the larger streams, the Carmel River and San Jose Creek were estimated based on past studies, BH (2014b). The sediment load for Pescadero Creek and smaller unnamed streams were scaled based on the size of their respective watersheds.

Sediment losses to deep water and to the submarine canyon were estimated based on NOAA seabed survey data from 1933 to 2008, NOAA (2020b).

9. Beach Morphology

Figure 9-1 provides an overview of lagoon states (natural and management) over the period from 1991 to 2013, compiled based on data from BH (2014a) and James (2005). The horizontal yellow bars indicate periods of lagoon closure, i.e. with no outlet to the ocean. This period can start as early as April and May, but typically occurs over the summer months from July through November, at times extending into December and January. The blue squares indicate dates of mechanical lagoon breaching in order to reduce flood risk. This management action is initiated when the lagoon water level is high or projected to reach flood stage and typically takes place in from November through January. The dark green squares indicate times when natural lagoon breachings have been observed, from (2014a). The square in light green indicate dates of additional observations by Greg W. James reported in MPWMD (2005).

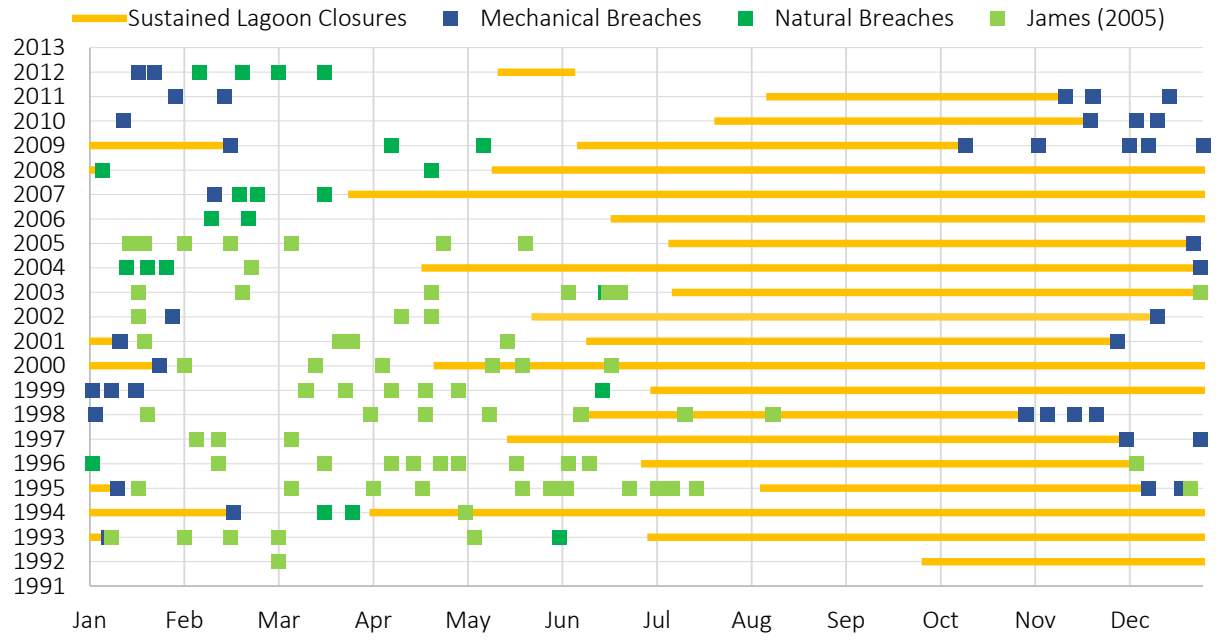

Figure 9-1: Overview of lagoon closures and breaches (1991-2013).

9.1. Wave Statistics and Lagoon Morphology

Wave statistics are summarized in the following and compared to the interannual morphology of the Carmel Lagoon. The wave statistics are grouped into:

1) North Pacific swell, persistent with seasonal variation, occurring 88% of the time on an annual basis.

2) Southern swell, seasonal and episodic, occurring 12% of the time on an annual basis.

3) Northwest wind-waves, persistent and episodic, occurring 70% of the time annually. Sea breeze occurring daily. Peak wind events exceeding 30 knots cumulatively occur 0.19% (16 hours/year).

4) Southwest wind-waves, infrequent and episodic occurring (16%) of the time annually with peak wind events exceeding 30 knots cumulatively occurring 0.21% of the time (18 hours per year).

For comparison, the following data is provided in the figures per the legend below:

Figure 9-2 shows the variation of North Pacific swell relative to the interannual stages of lagoon morphology and additional metrics such as the Carmel River discharge which is indicated by the black curve and the scale on the right. The percent occurrence of North Pacific swell is indicated on the vertical scale on the left and by month along the horizontal axis. The data shows that the occurrence of North Pacific swell can vary considerably between years – as low as 2% in the summer months of some years, and as high as 9% in January, March, and December in other years. It should be noted that the percent occurrence in a given year depends on the number of storms occurring over the North Pacific, which can vary from year to year. The average across all years (from 1991 through 2019) is indicated by the dark blue line.

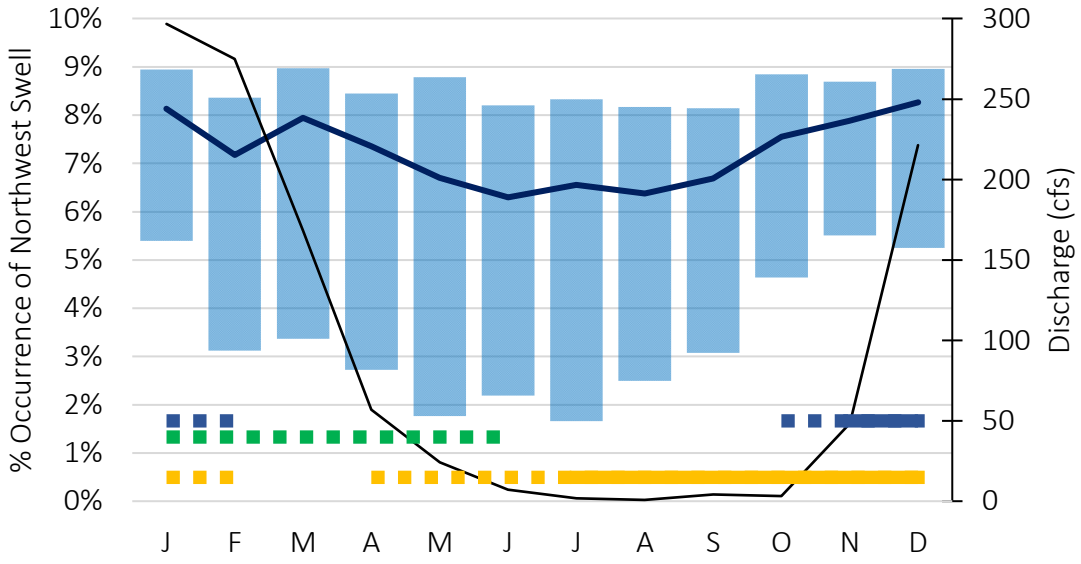

Figure 9-2: Patterns and occurrence of North Pacific swell.

The data shows that North Pacific swell occurs persistently but with lower frequency over the summer months, increasing in the winter months. The primary noticeable trend is perhaps that there is a lull in the percentage occurrence of swell over the period when the lagoon is closed, with an uptick in the months of November, December and January where most of the initial lagoon breaching takes place. It is therefore likely that North Pacific swell plays a role in closing lagoon breaches, which is known to happen when the Carmel River discharge decreases to around 10 cfs or less.

Figure 9-3 shows the interannual and seasonal variation of southern swell. It can be seen that swell from southerly directions can occur in any month of the year. The data also shows that there are years when no southern swell occurs in January through May, and in October through December, i.e. the lower bound of percent occurrence is zero or very small. The data shows a general trend of southern swell activity increasing over the summer months, which could indicate that southerly swell waves contribute to natural closing of the lagoon seasonally, i.e. southern swell frequency increases over the time when natural breaches cease to occur (green dots) and lagoon closure commences (yellow dots). Note that permanent closure of the lagoon has been found to occur when the outflow decreases to around 10 cfs or less. Per the black line in the figure, this typically happens around June to July on average.

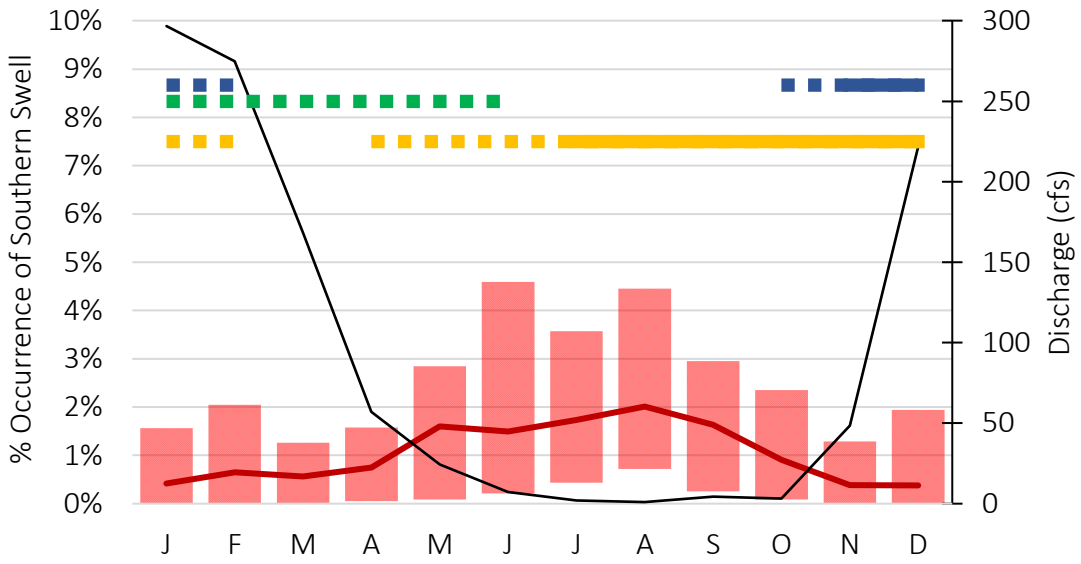

Figure 9-3: Patterns and occurrence of Southern swell.

Figure 9-4 shows the percent occurrence of northwest wind-waves interannually and seasonally. The average trend (dark blue line) shows a general increase in wind over the summer months, tapering off slightly over the winter months. October, as the only month, will have some years with very slight onshore wind (percentage lower bound is nearly zero).

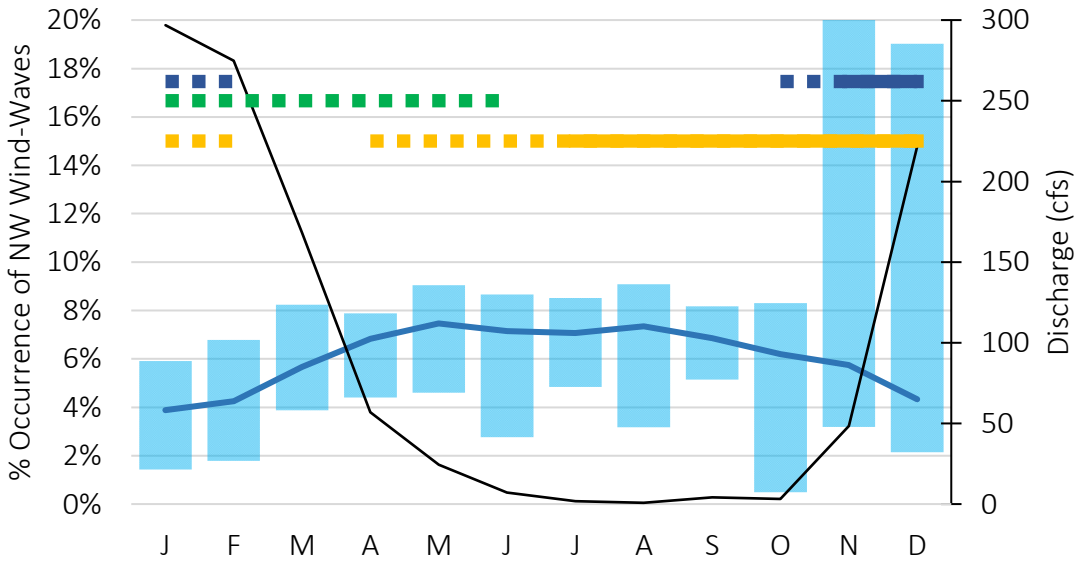

Figure 9-4: Patterns and occurrence of northwest wind-waves.

The most pronounced trend in the data is the substantial increase in wind events in the months of November and December. This trend coincides with the most frequent months of mechanical lagoon breaching, which also occur in November and December. Another apparent driver is the increase in outflow from the Carmel River, typically peaking in December through February. The increase in discharge from the Carmel River, which can cause the lagoon to rise rapidly has the most direct relation to when mechanical breaching of the lagoon takes place. The occurrence of northwest wind-wave events has the potential to significantly impact the morphology of the lagoon as these events can produce the following effects:

1) Strong southward sand transport, which can erode the beach and remove large quantities of sand from the sandbar in a short amount of time.

2) Northward sand movement along the northern end of the beach, which may promote lagoon migration to the north.

3) Southward sand transport along the central and southern part of the beach, which may promote lagoon migration to the south.

Figure 9-5 summarizes the interannual variation and seasonal variation of southwest wind-waves. The data shows a pretty consistent level of wind-wave events occurring over the months of January to December with a pronounced uptick in the frequency of wind events in December. All months of the year can have periods with little to no southerly wind, i.e. percentage lower bound is very small or zero (August is the only month which has had no southerly wind-wave events).

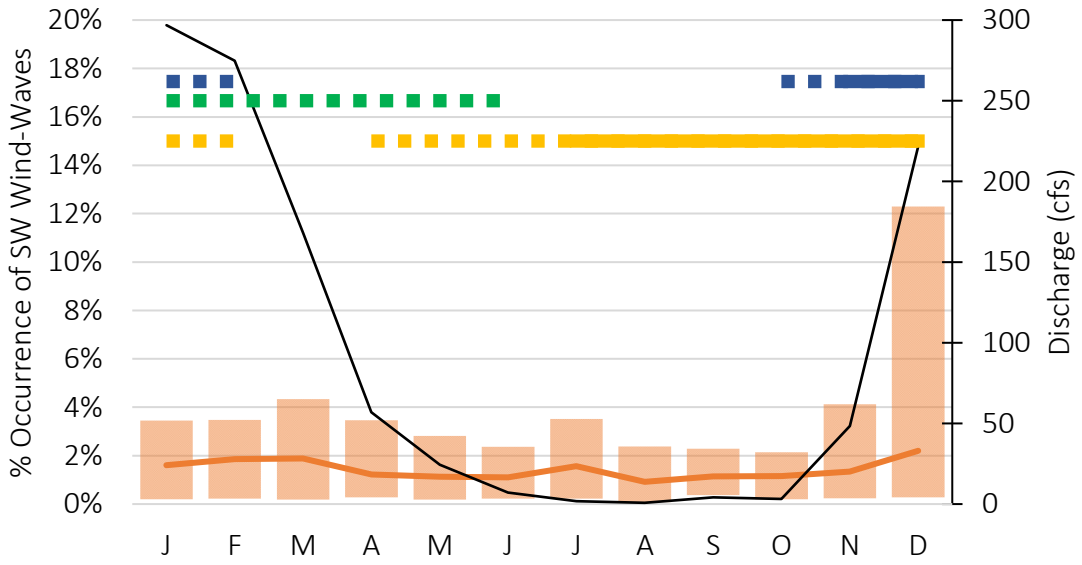

Figure 9-5: Patterns and occurrence of southwest wind-waves.

The increase in the frequency of wind-wave events does correlate with the common period of mechanical lagoon breaching in November and December, and shows that lagoon morphology can be impacted by these events during these times. The potential impact of southwest wind-wave events on lagoon morphology is:

1) Pronounced northward sand transport along the beach, which may drive lagoon migration to the north.

The conclusions from Figure 9-2 to Figure 9-5 are:

- Swell waves place sand on the beach with the wave runup and promote closures of lagoon breach channels when the Carmel River discharge diminishes to 10 cfs or less.
- North Pacific Swell can decrease over the summer months but also remain fairly persistent, while Southern swell increases over the summer months. These, in combination with Carmel River discharge decreasing to 10 cfs or less results in seasonal closure of the lagoon in June to July in average years.
- While swell waves play a key role in closing off the lagoon breaches, it is the discharge of the Carmel River that keeps the breach open. Closure of breach channels has been observed to occur primarily when the river discharge decreases to 10 cfs or less.
- The windiest months (November and December) coincides with the time when initial breaching of the lagoon often occurs. The enhanced transport associated with the wind driven waves means that a higher degree or breach channel migration should be expected in this period.

10. Lagoon and Beach Morphology

Figure 10-1 provides an overview of the processes that shape the CRSB sandbar and lagoon planform. Incident wave crests and wave troughs are indicated by the light blue solid/dashed lines. The crenulate shape of the bay and seabed contours cause incident waves to refract and diffract. Refraction causes incident waves to turn so the direction of wave propagation is approximately perpendicular to the seabed contours. Diffraction is spreading of wave energy and occurs in the lee of the headland (Carmel Point) at the north end of the beach.

Refraction causes the incident waves to converge on the headland at Carmel Point and the rock outcrop located at the south end of CRSB at the transition to Ribera Beach (black arrows in figure). Diffraction occurs primarily in the lee of the headland at Carmel Point. Because of the dispersal of wave energy in this area, the northern portion of CRSB is an area of low wave energy compared to the beach to the south, which is an area of relatively high wave energy.

Summer swell waves tend to build up the beach, while winter storm waves pull sand off the beach into deeper water. The typical summer beach extent is indicated by the solid red line, while the narrower winter beach planform is indicated by the dashed red line. Because of the wave diffraction effects at the north end of the beach and the low wave energy versus high wave energy zones, there is less variation of the beach width at the northern (on the order of 80 feet) end and more variation at the center and south end of the beach (on the order of 140 feet) between the summer and winter planforms.

The general Carmel River and lagoon planform is indicated by the solid blue line. Example paths showing migration of lagoon breaches are indicated by the dashed blue lines. The breaches can migrate south if the wave-driven littoral transport is southward (yellow arrows); and can migrate north if the direction of littoral transport is to the north. Migration of lagoon breaches occur when there is a significant outflow from the lagoon (which keeps the breach channel open), while the littoral transport tries to close the beach. If the outflow from the lagoon weakens, the littoral transport can close off the breach. Closure of a breach can occur due to littoral transport (along the shoreline in the plan view), and also due to vertical buildup of sand deposited with wave runup.

Northward lagoon migration has historically reached the northern end of the beach where it terminates at the rock outcrop at Carmel Point. Southward migration is limited by the rock outcrops at the south end of the beach. If the beach level is high, these outcrops are typically buried under the sand but appear when the beach level lowers.

The driver behind the lagoon water level rise each season is inflow from the river. This causes the planar extent of the lagoon to widen out over the sandbar as the water level rises.

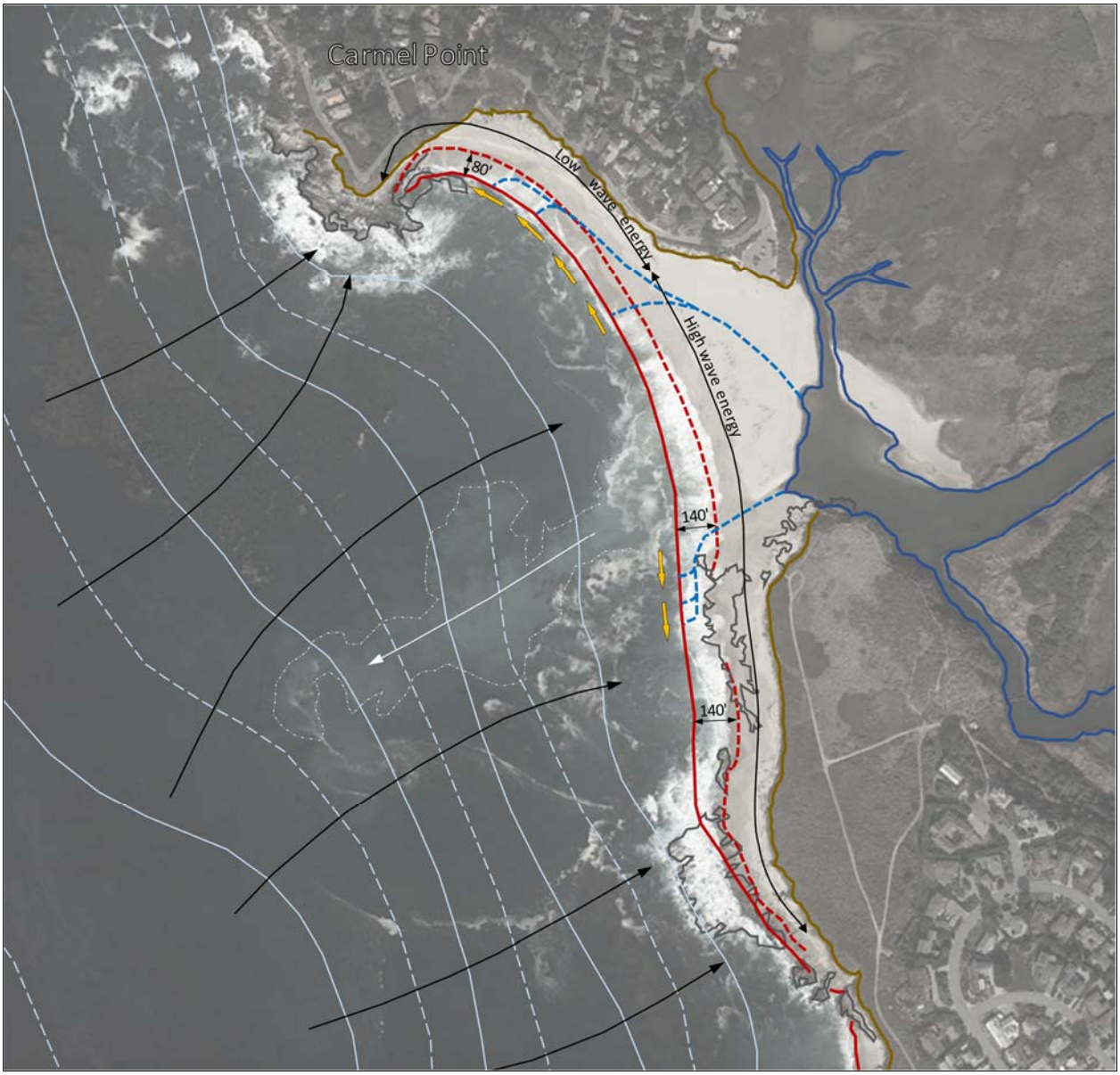

Figure 10-1: Overview of CRSB seasonal variation and lagoon morphology.

An effect that can promote breach migration northward or southward following its formation is believed to be incident wave action in combination with seepage outflow. An example of seepage outflow is indicated by the white dotted outline in Figure 10-1 and white arrow directed offshore.

The seepage outflow is likely present whenever the water level in the lagoon rises above the mean sea level and range of tides. A high lagoon water level can produce a significant outflow of water through seepage, which can produce migration of sand from the beach out to the ocean. The shedding of sand at the shoreline edge manifests in a large plume of sediment conveyed offshore towards the submarine canyon. Subject to the seepage flow through the beach, fines will tend to leach out first.

This process results in coarsening of the beach substrate, which enables the seepage flow to increase in magnitude. The removal of sediment at the shoreline by wave action and replacement of sand by wave runup is believed to further contribute to coarsening of the beach material where the seepage outflow occurs. This is the process by which wave action at the shoreline is able to affect lagoon migration at the back beach despite being separated by up to around 400 feet of beach width. This process indicates that lagoon migration is to a large extent driven by wave action and the direction of sand transport at the shoreline either northward or southward. This mechanism also explains why some years see formation of both a southerly and northerly spur off the lagoon, i.e. the direction of sand transport changed over the course of lagoon formation.

10.1. Beach Profile Variation

Erosion and accretion along the shoreline causes the sandbar to narrow and widen, respectively. As demonstrated earlier, there is a seasonal trend to this as well as irregular, episodic events.

Cross-shore transport of sediment can manifest in a number of ways as described in the following.

Figure 10-2 shows an example of shoreline recession due to erosion. The dashed and numbered lines indicate a progression over time. Erosion usually affects the entire height of the beach profile. When the profile is subject to erosion there is a volumetric loss of sand, while wave runup and rundown has the effect of smoothening the profile. If the wave runup elevation does not reach the crest of the sandbar, a near vertical scarp often develops (4) in Figure 10-2.

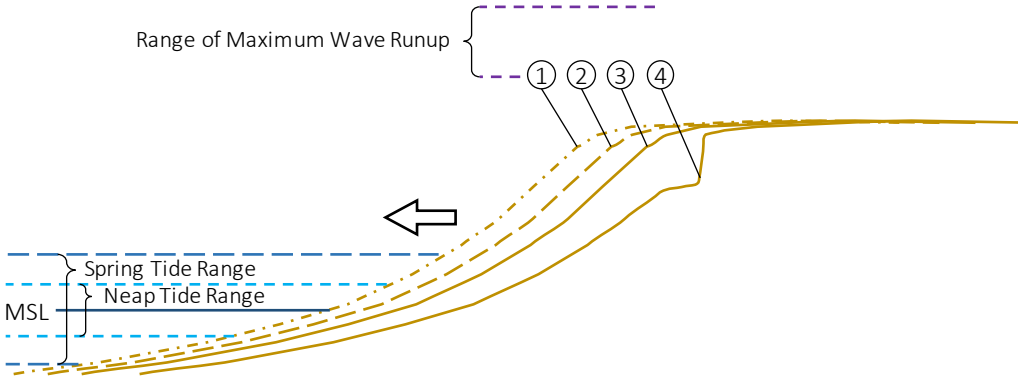

Figure 10-2: Beach erosion. Figure adapted from Weir (2006).

Figure 10-3 shows an example of vertical growth of the sandbar. In this case, the plan location of the shoreline is at an equilibrium, while sand deposited with wave runup produces vertical growth of the sandbar. Variations in the incident wave conditions can cause the beach face to flatten or steepen slightly as indicated in the figure. This mode of sandbar development usually also follows after lagoon breaching where the sandbar is eroded locally at the breach. In this case, both longshore sediment transport and cross-shore transport can work to close the breach, but it is primarily the vertical growth mode shown in Figure 10-3 that restores the sandbar to a new equilibrium elevation. In terms of the vertical buildup of the sandbar, both wave runup and tide levels can play a role. The historically highest

sandbar elevations recoded at CRSB have been a result of sand deposited during significant wave runup events in combination with high tides.

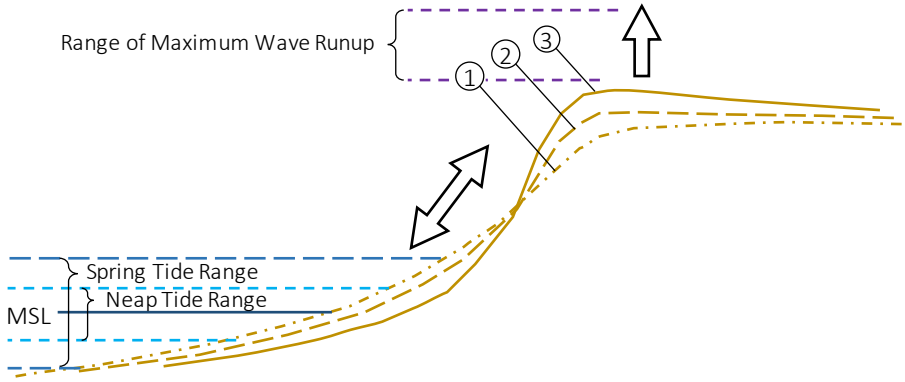

Figure 10-3: Sandbar vertical buildup. Figure adapted from Weir (2006).

Figure 10-4 shows a mode of horizontal sandbar growth. This can occur when wave runup does not overtop the sandbar and material transported by wave runup is instead deposited on the beach face resulting in seaward migration/widening of the sandbar. This mode of sandbar evolution can occur: 1) after the sandbar crest elevation has built up high; 2) during periods of milder wave climate with less wave runup; and 3) during neap tide cycles where the water level does not contribute much to the total wave runup elevation. During periods of neap tides the tide range is lower, as opposed to spring tides which exhibit the larger tide range (Figure 10-5).

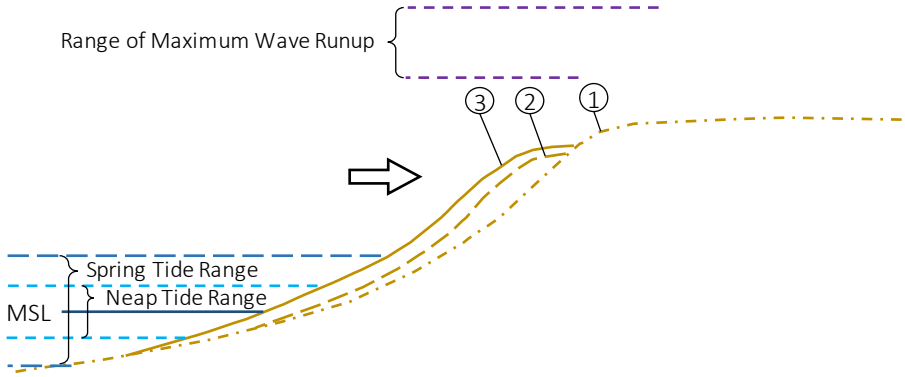

Figure 10-4: Sandbar widening. Figure adapted from Weir (2006).

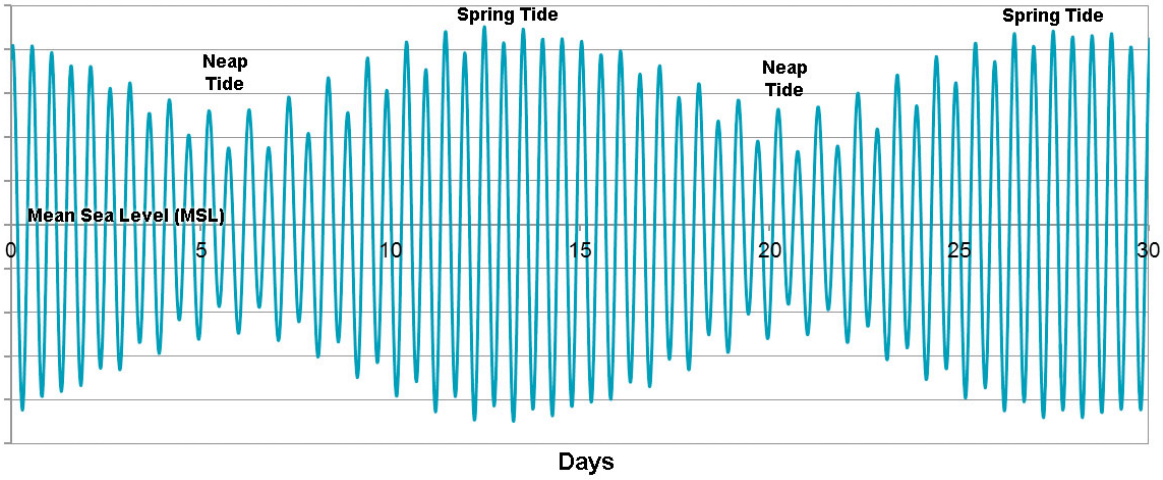

Figure 10-5: Monthly tide cycle of neap and spring tides.

Figure 10-6 shows an example of combined horizontal and vertical buildup of the sandbar, which occurs when incident waves are in a mode of accretion and able to overtop the sandbar.

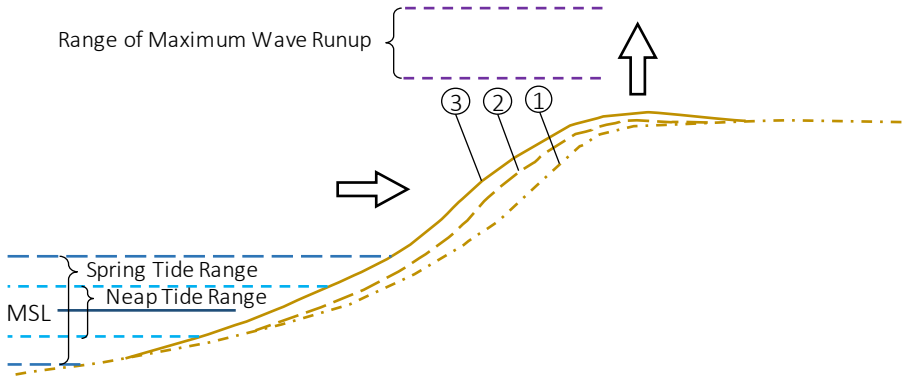

Figure 10-6: Sandbar horizontal and vertical growth. Figure adapted from Weir (2006).

10.2. Lagoon Breaching

Figure 10-7 shows mechanisms that can lead to breaching of the lagoon. From the ocean side, wave runup can erode the beach and wave overwash erode the sandbar to a point where the lagoon breaches. This mode of lagoon breaching is not common at CRSB, however, where wave runup tends to deposit sand and build up the sandbar. There have been a few cases where wave overtopping has filled up the lagoon without breaching it.

The most common mode of lagoon breaching is from the lagoon side when the lagoon water level rises to a point where it overtops the sandbar, or when the hydraulic head (active pressure) overcomes the weight of the sandbar (passive pressure).

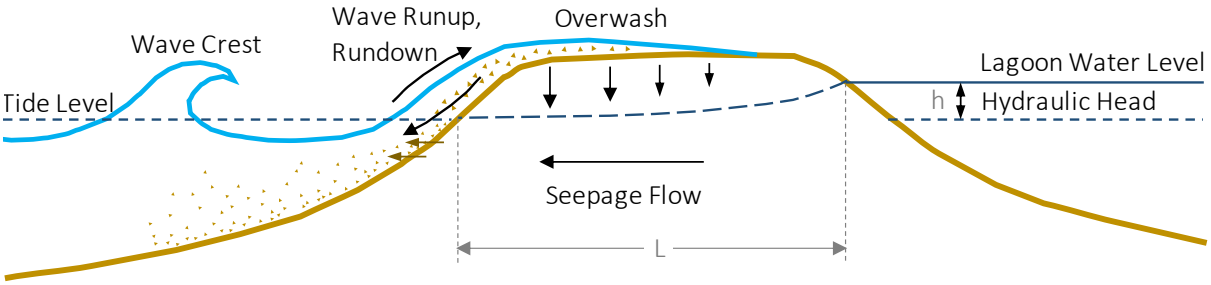

Figure 10-7: Parameters governing lagoon breaching. Figure adapted from Kraus (2008).

Close to the point of the lagoon breaching there is a significant seepage flow through the sandbar. The seepage can produce a couple of different effects that can affect when breaching occurs. One effect is removal of finer grained material over time where fines are winnowed out with the seepage flow. This mechanism is called suffusion. This process means that the porosity of the sandbar material can increase slightly over time (fines are removed), which theoretically reduces the resisting force of the sandbar, i.e. interstitial void space occupied by sand grains (with higher density) transitions to water-filled voids. However, washout of the fines also increases the permeability of the sand berm material so it can accommodate a higher hydraulic head before failing. A second effect of the seepage flow is that the pore pressure causes grains to separate at the beach face where the seepage flow enters the surf. This aids wave action in removal of sediment. The wave runup and rundown can have a filtering effect where smaller diameter material is removed and larger diameter material retained and deposited atop the sandbar (Figure 10-7). The net effect over time can be that the sandbar material transitions to larger diameter material.

Kraus (2008) describes the parameters governing breaching from the lagoon side, which occurs when the hydraulic head on the lagoon side is large enough to mobilize the weight of the sandbar damming up the breach channel. Kraus equates this balance as:

$$F_W \geq \kappa F_B$$

Where F_W is the hydrostatic force exerted by the water in the lagoon on the sandbar, given by:

$$F_w = \frac{1}{2}\rho g h \times hW$$

And the resisting force, F_B, being the weight of the sand on the sandbar given as:

$$F_B = (\rho_s - \rho)(1 - p)g \times hWL$$

In these equations, ρ is the density of water, ρ_s is the density of the sand, p is the porosity (about 0.4), and g is the gravitational acceleration. The hydraulic head, h, and the width of the sandbar, L, are as defined in Figure 10-7. The term hW is the hydraulic head h acting over the width of the lagoon breach channel, W. This term cancels out when equating F_W and F_B, which leads to the simplified expression for lagoon breaching when:

$$\frac{h}{L} \geq 2\kappa$$

The remaining factor, κ, is a site specific coefficient. For the Carmel Lagoon, Kraus (2008) estimated h/L on the order of 4 to 10%, i.e. κ = 2 to 5%. The κ accounts for uncertainties in the simplified breach criterion, which can include: 1) variation in hydraulic head due to tidal variation; 2) breaching promoted by seepage flow; 3) change in porosity; 4) change in grain size; 5) density difference between lagoon (fresh to brackish) and ocean water (saline); and 5) variation in the density of the sandbar material.

Lagoon breaching occurs when the hydraulic head exceeds the weight of the sandbar as described above, or if the lagoon water levels overtops the sandbar, which creates a channel that erodes the sandbar, providing for a further increase in erosion and flow until equilibrium is re-established.

11. Climate Change

Climate change can produce several potential impacts on the Carmel Lagoon. Climate change is predicted to produce a higher degree of irregularity in weather patterns with wider extremes. In recent years, California has experienced some of the driest years on record, and some of the wettest years as well. The increase in number and extent of wildfires in California can also have a potential impact on the lagoon system. Soil washing down from scorched areas within the watershed can cause a dramatic increase in the sediment load of the river.

In the following section, it is explored if sea-level rise can impact the lagoon system.

11.1. Sea-Level Rise

Table 11-1 summarizes select water level datums from Table 3-2 with adjustment for sea-level rise based on Table 3-4. The sea-level rise projection adopted for the analysis is the 1-in-200 chance projection with high emissions. This projection reflects a conservative outlook for climate change with limited efforts to curb emissions worldwide. The SWEL in the table is the 1% annual chance (1-year) still water level (without wave action). The BFE is the FEMA 1% annual chance coastal base flood elevation (including wave runup).

Table 11-1: Tidal datums with sea-level rise. Elevations in feet NAVD88.

Tidal Plane	Present	1-in-200 Chance Medium to High Risk Aversion Projection*		
		2030 (0.8' SLR)	2050 (1.9' SLR)	2100 (6.9' SLR)
Coastal BFE	+27.0	+27.8	+28.9	+33.9
Coastal SWEL	+8.2	+9.0	+10.1	+15.1
King Tide	+7.0	+7.8	+8.9	+13.9
MHW	+4.8	+5.6	+6.7	+11.7

* With high emissions.

Based on Table 3-4, the following rates of sea-level rise were determined as summarized in Table 11-2 projected by year, the amount of SLR, and the underlying rate of sea-level rise. The rate is given in feet per year and in inches per year for perspective. The data in Table 11-2 was applied to estimate potential SLR impacts at the CRSB, which is summarized in the three columns to the right in Table 11-2.

Table 11-2: Annual rate of sea-level rise.

Year	1-in-200 Chance SLR (feet)	Rate (feet/year)	Rate (inches/year)	Loss (CY/year) to Canyon	Loss (CY/year) due to SLR	Total Loss (CY/year)
2020	0.1	0.01	0.07	23,100	1,600	24,700
2030	0.8	0.05	0.56	23,100	2,200	25,300
2040	1.2	0.06	0.70	23,100	3,000	26,100
2050	1.9	0.07	0.84	23,200	4,000	27,200
2060	2.6	0.08	0.98	23,300	5,000	28,300
2070	3.4	0.09	1.12	23,400	6,300	29,700
2080	4.4	0.11	1.26	23,700	7,700	31,400
2090	5.5	0.12	1.40	23,900	9,400	33,300
2100	6.9	0.13	1.54	24,500	11,400	35,900

The *Bruun Rule*, devised by P. Bruun in 1962, relates shoreline erosion to sea level rise as shown in Figure 11-1 where R is shoreline recession, S is the amount of sea-level rise, L is the horizontal extent of the shoreline zone where active sediment transport occurs, B is the beach and dune height above mean sea level, and h is the closure depth beyond which significant sediment transport does not occur.

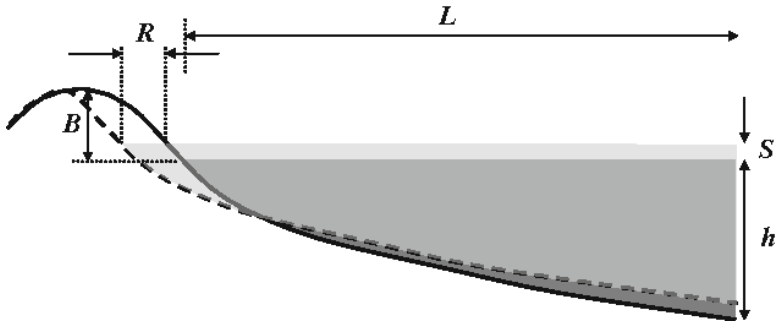

Figure 11-1: Schematic of Bruun Rule.

The Bruun Rule states that the sand deficit (dark gray area) needed to elevate the seabed to compensate for SLR can be balanced by shoreline erosion. The equation therefore predicts that sea-level rise can result in shoreline erosion and shoreline recession (R). However, this is for the case of a beach on the open coast which is different from the setting at Carmel. The CRSB is a crenulate-shaped beach formed due to wave diffraction between the headland (Carmel Point) and rocky downcoast shoreline along Ribera Beach (refer to Figure 10-1). Shoreline recession is therefore limited to the rate of cliff erosion, which is on the order of a few inches per year (refer to Section 5 and Figure 6-2).

The volume of sand needed to compensate for the deficit caused by SLR is instead supplied by the Carmel River. The three columns on the right side of Table 11-2 summarize the estimated annual loss of sediment to the Carmel Canyon, the loss associated with sea-level rise, and the sum of these as

the total annual loss. However, as the sediment supplied by the Carmel River is estimated to be on the order of 61,931 CY annually, the indication is that the CRSB can adapt to future sea-level rise.

Another outcome of the Bruun Rule shown in Figure 11-1 is that the beach elevation will rise in tow with sea-level rise. This occurs because the wave runup elevation increases with the rise in ocean level. The lagoon should therefore be expected to go through a similar transition.

In conclusion, the CRSB appears to be resilient to SLR hazards in the near-term as the Carmel River provides sufficient sediment annually to compensate for the sediment deficit caused by sea-level rise. However, it is also evident that the beach is dependent on the Carmel River sediment supply. So, to the extent that climate change alters the supply, the effect on the beach could be substantial.

12. Conclusions

The analysis has established the following sediment transport effects and drivers that affect the morphology of the CRSB lagoon.

12.1. Carmel Littoral Cell

The Carmel littoral cell is contained between Cypress Point and Point Lobos. The general littoral transport direction is from north to south. The main input of sediment to the system comes from: Breakdown and erosion of the granodiorite rock formations along the coast; The Carmel River provides sand to the Carmel River State Beach; and San Jose Creek similarly provides sand to Monastery Beach. The remaining creeks and streams in the area provide limited input of sand to the shoreline. The pocket beaches and crenulate bay shaped sections of shoreline: Stillwater Cove (SC), Carmel Beach (CB), Carmel River State Beach (CRSB), Monastery Beach (MB), and Whaler's Cove (WC) comprise quasi-stable littoral sub-cells. However, waves during winter storms can be large enough to induce longshore sand transport between these cells in a southward direction. Such storm events are infrequent and highly episodic.

CRSB can therefore be characterized as a quasi-stable littoral cell where the primary input of sand comes from the Carmel River and there is a secondary input of sand from Carmel Beach. Wave patterns at CRSB induce a circular pattern of sediment movement where the longshore transport at the shoreline is often in a northward direction, whereas the sediment transport direction in deeper water is in a southward direction. This circular pattern of sediment movement works to maintain the beach, although sand episodically moves southward past Ribera Beach towards Monastery Beach. The majority of sand volumes transported south are lost from the CRSB sub-cell and do not return. The magnitude of sand retained in the system at CRSB is therefore dependent on the wave climate from year to year, the occurrence of intermittent northwesterly wind-wave events (during which sand is lost from the sub-cell), and sand input from the Carmel River. The latter is the most important, as a decline in sediment output from the Carmel River will lead to depletion of sediment from the system; conversely an increase can aid in restoring the beach.

12.2. Carmel Canyon

The Carmel submarine canyon is a significant element of the Carmel Littoral Cell. Sand transport south along the coast is eventually lost to the submarine canyon in the area of Monastery Beach where the submarine canyon comes close to shore and is within the active portion of shoreline profile. Several mechanisms of sand loss to the submarine canyon have been identified, including: wave- and current-induced downslope migration of sand, submarine slope failures along the edge of the canyon, and rip currents. In the broader area from Pescadero Point down to CRSB large wave events during winter storms are capable of mobilizing sand to greater depths, which causes a loss of sand to the submarine canyon. Specific to CRSB, bursts of outflow from the Carmel River can wash sediment into the submarine canyon as well. The canyon acts as a sink for the littoral cell system, and sediment that enters the canyon is lost from the system.

12.3. Swell Waves

Swell waves approach the coast year-round. Swell waves originating from storm systems over the North Pacific primarily occur during the fall and winter months, while swell waves from storm systems in the Southern Hemisphere tend to occur over the summer months. Swell wave events follow a sequence where the longest waves roll in first followed by progressively shorter waves until the wave trains die out. Each episode of swell can last from hours to several days, depending on the magnitude and duration of the storm system of origin.

The Carmel submarine canyon has a pronounced effect on swell waves as they propagate from offshore waters to the shoreline. The canyon overall acts as a lens which focuses wave action along the cliffs from Cypress Point to Pescadero Point, at Point Lobos, and to a lesser degree focuses waves propagating towards Carmel Beach. Incident waves traveling along the canyon axis tend to disperse at the canyon heads in Carmel Bay, at CRSB, and at Monastery Beach, which produces a milder wave climate in these areas. The wave transformation caused by the canyon is to such a degree that incident swell waves end up having nearly the same angle of incidence at the shoreline irrespective of whether the swell arrives from northwesterly or southwesterly directions offshore. Wave transformation due to the submarine canyon is more significant the longer the wave periods of the incident waves, and therefore primarily affects swell waves.

12.4. Wind-Waves

The Carmel submarine canyon does not transform wind-waves to the same degree as swell waves. This is because the wave periods of wind-waves are significantly shorter than for swell waves. Waves associated with high winds from northwesterly directions can therefore cause intermittent bursts of sediment transport southward along the shoreline. These infrequent events can produce an exchange of sediment between the quasi-stable sub-cells of the system (SC, CB, CRSB, MB, and WC). Episodic wind events from southwesterly directions produce northward sediment transport along the shoreline. However, these events do not replenish sand to the littoral sub-cells, but rather tend to shift sand to the north within each sub-cell.

12.5. Wave Climate Interaction with Lagoon Breaching

Field observations have established that the primary agent in natural lagoon breaching is inflow to the Lagoon from the Carmel River. Swell waves have a key role in closing off lagoon breaches, but only when the discharge from the river decreases to 10 cfs or less. The primary role of swell waves is in building up the sandbar. Both swell waves and wind-waves can promote migration of lagoon breaches north or south depending on the incident wave direction; wind-waves probably more so than swell waves.

The frequency of swell wave and wind-wave action increases in November and December around the time when initial lagoon breaching often takes place. Because the wind/wave climate is episodic, it is not possible to predict if the lagoon breach will migrate north or south, and when an initial breach will

close. Swell waves combined with diminishing outflow from the Carmel River in the summer months result in seasonal closure of the lagoon in June to July in average years.

12.6. Sea-Level Rise

The CRSB and lagoon appear to be resilient to SLR hazards in the near-term as the Carmel River provides sufficient sediment annually to compensate for the sediment deficit caused by sea-level rise. However, it is evident that the beach is dependent on the Carmel River sediment supply. So, to the extent that climate change alters the sediment supply, the effect on the beach could be substantial.

References

AGU (2005). *Reflection and tunneling of ocean waves observed at a submarine canyon.* Authored by: Jim Thomson, WHOI-MIT Joint Program in Oceanography, Woods Hole, Massachusetts, USA and T. H. C. Herbers, Naval Postgraduate School, Monterey, California, USA. Geophysical Research Letters, Vol. 32, L10602, doi:10.1029/2005GL022834, 2005. American Geophysical Union. 0094-8276/05/2005GL022834.

BH (2014a). *The Geomorphic Role of Riverine Processes in Carmel Lagoon Water Surface Elevation and Sand Bar Breaching Dynamics for the Carmel River-Lagoon Biological Assessment Report.* Prepared for: Monerey County Resource Management Agency. Prepared by: Edward D. Ballman, P.E. and Anne E. Senter. Balance Hydrologics, Inc. January 2014.

BH (2014b). *San Jose Creek Watershed Assessment.* Prepared for: Monterey Peninsula Regional Park District, 60 Garden Court #325, Monterey, Ca 93940. Authored by: Denis Ruttenberg and Barry Hecht, Balance Hydrologics, Inc. and Danny Hagans and Tara Zuroweste, Pacific Watershed Associates. Prepared by: Balance Hydrologics, Inc., 800 Bancroft Way, Suite 101, Berkeley, CA 94710. Final report submittal. March 31, 2014.

CCRP (2020). *California Coastal Records Project.* An aerial photography survey of the California Coastline. https://www.californiacoastline.org/

DD&A (2016) *Carmel Lagoon Ecosystem Protective Barrier, Scenic Road Protection Structure, and Interim Sandbar Management Plan Project.* Draft Environmental Impact Report. SCH#2014071050. Prepared for: County of Monterey. Prepared by: Denise Duffy & Associates, Inc. December 2016.

Dean (1973). *Heuristic models of sand transport in the surf zone.* Conference on Engineering Dynamics in the Surf Zone, Inst. Of Eng., Sydney, N. S. W., Australia.

FEMA (2017). *Flood Insurance Study.* Monterey County, California and Incorporated Areas. FEMA, Federal Emergency Management Agency. Flood Insurance Study Number: 06053CV001B. Version Number: 2.3.2.1. Revised: June 21, 2017.

FEMA (2018). *Flood Insurance Rate Map.* Monterey County, California and Incorporated Areas. City of Carmel-By-The-Sea (Number 060196), Monterey County (Number 050195). Panel: 0316, Suffix: H. National Flood Insurance Program. FEMA, U.S. Department of Homeland Security.

IMS (2007). *Development of Sand Budgets for California's Major Littoral Cells. Eureka, Santa Cruz, Southern Monterey Bay, Santa Barbara, Santa Monica (including Zuma), San Pedro, Laguna, Oceanside, Mission Bay, and Silver Strand Littoral Cells.* Kiki Patsch, Gary Griggs. January 2007. Institute of Marine Sciences, University of California, Santa Cruz. California Department of Boating and Waterways. California Coastal Sediment Management Workgroup.

ISU (2020). *Worldwide Wind Roses - Graphics and Tabular Data.* NOAA, Climate.gov. Iowa Environmental Mesonet, Iowa State University of Science and Technology. Department of

Agronomy, 716 Farm House Ln, Ames, IA 50011. https://www.climate.gov/maps-data/dataset/worldwide-wind-roses-graphics-and-tabular-data

Kraus (2008). *Barrier beach breaching from the lagoon side, with reference to Northern California.* By: Nicholas C. Kraus, U.S. Army Engineer Research and Development Center (ERDC), Coastal and Hydraulics Laboratory,3909 Halls Ferry Road, Vicksburg, MS 39180 Nicholas.C.Kraus@usace.army.mil; Kiki Patsch, 2111 Bargamin LoopCrozet, VA 22932, kpatsch77@hotmail.com; and Sophie Munger, ERDC, Coastal and Hydraulics Laboratory, 3909 Halls Ferry Road, Vicksburg, MS 39180, Sophie.Munger@usace.army.mil. Article in Shore and Beach · January 2008.

MCPW (2014). *Carmel River Mouth Sand Bar Elevations.* Monterey County Public Works. Engineering Division, Survey/Minor Design Section. 312 East Alisal Street, Salinas, California 93901.

MG (2000). *Sediment distribution and transport along a rocky, embayed coast: Monterey Peninsula and Carmel Bay, California.* C.D. Storlazzi [a)], M.E. Field [b)]. [a)] UCSC/USGS Coastal Geology and Imaging Laboratory Co-operative, Department of Earth Sciences and Institute of Marine Sciences, A-360 Earth and Marine Sciences Building, University of California, 1156 High Street, Santa Cruz, CA 95064-1077, USA. [b)] UCSC/USGS Coastal Geology and Imaging Laboratory Co-operative, Coastal and Marine Geology Program, United States Geological Survey, A-316 Earth and Marine Sciences Building, University of California, 1156 High Street, Santa Cruz, CA 95064-1077, USA. Marine Geology. International Journal of Marine Geology, Geochemistry and Geophysics. Received 1 March 2000; accepted 28 July 2000.

MPWMD (2005). *Surface Water Dynamics at the Carmel River Lagoon Water Years 1991 through 2005.* Prepared by: Greg. W. James. Monterey Peninsula Water Management District. October 2005.

NDBC (2020. *National Data Buoy Center.* National Oceanic and Atmospheric Administration's Center of Excellence in Marine Technology. National Data Buoy Center, Bldg. 3205, Stennis Space Center, MS 39529.

NGS (2020). *VERTCON. Orthometric Height Conversion.* National Geodetic Survey. Communications and Outreach Branch, NOAA, N/NGS12, National Geodetic Survey, SSMC3 #9340, 1315 East-West Highway, Silver Spring, MD 20910-3282. https://www.ngs.noaa.gov/cgi-bin/VERTCON/vert_con.prl

NM (2020). *Nearmap.* High Resolution aerial imagery. 2019 Nearmap Ltd. / Nearmap US, Inc. https://www.nearmap.com/us/en

NOAA (2020a). *Tides and Currents*. Center for Operational Oceanographic Products and Services (CO-OPS), 1305 East-West Highway, Silver Spring, MD 20910-3281. Phone: (301) 713-2815. https://tidesandcurrents.noaa.gov/

NOAA (2020b). *Bathymetric Data Viewer.* Version: 2.19.0, last updated 5/18/2020, 9:23:13 PM. National Centers for Environmental Information, NOAA National Oceanic and Atmospheric Administration. https://maps.ngdc.noaa.gov/viewers/bathymetry/

NOAA (2020c). *Coastal LiDAR.* NOAA Office for Coastal Management. Data Access Viewer. https://coast.noaa.gov/dataviewer/#/

NPS (1968). *The Sediments in the Head of Carmel Submarine Canyon.* Thesis by: Steven Russell Wallin. United States Naval Postgraduate School. December 1968.

NPS (1972). *Sand Movement along Carmel River State Beach, Carmel, California.* Thesis by: Buford Fredrick Howell. September 1972. Naval Postgraduate School, Monterey, California.

NPS (2019). Morphology Changes to Carmel River State Beach in Relation to Waves and River Discharge. Thesis by: Jillian N. Coughlin, June 2019. Naval Postgraduate School, Monterey, California.

OPC (2018). *State of California Sea-Level Rise Guidance.* California natural resources agency, California Ocean Protection Council, 2018.

SPM (1984). *Shore Protection Manual.* Coastal engineering Research Center, Department of the Army, Waterways Experiment Station, 1984.

UCSB (2020). *Air Photos.* UCSB Library, University of California, Santa Barbara. FrameFinder web map app. https://mil.library.ucsb.edu/ap_indexes/FrameFinder/

USGS (2006). *National Assessment of Shoreline Change Part 3: Historical Shoreline Change and Associated Coastal Land Loss Along Sandy Shorelines of the California Coast.* Cheryl J. Hapke, David Reid, Bruce M. Richmond, Peter Ruggiero and Jeff List. Open-File Report 2006-1219. U.S. Department of the Interior. U.S. Geological Survey.

USGS (2020). *Coastal Change Hazards Portal.* https://marine.usgs.gov/coastalchangehazardsportal

Weir (2006). *Beach face and berm morphodynamics fronting a coastal lagoon.* Felicia M. Weir, Michael G. Hughes, Tom E. Baldock. Geomorphology 82 (2006) 331–346. Received 1 December 2005; received in revised form 19 May 2006; accepted 19 May 2006. Available online 20 July 2006.

Appendix A:

Wind Roses

January

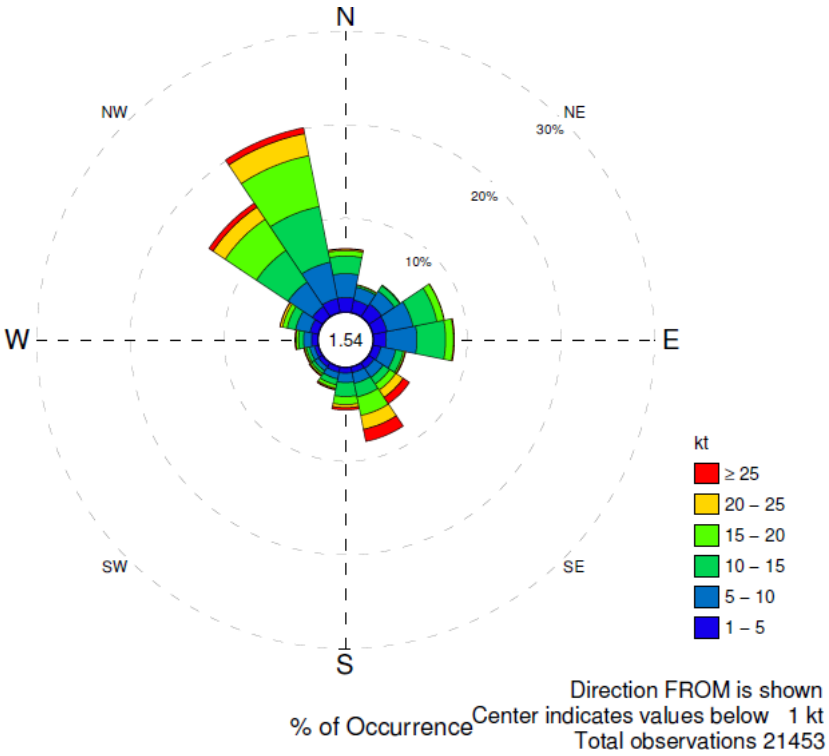

February

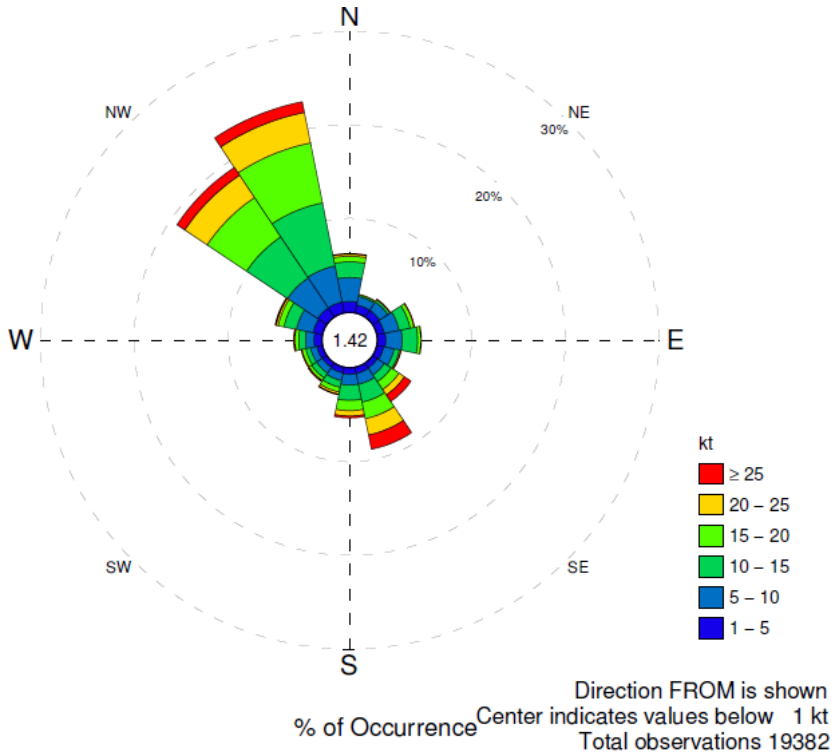

March

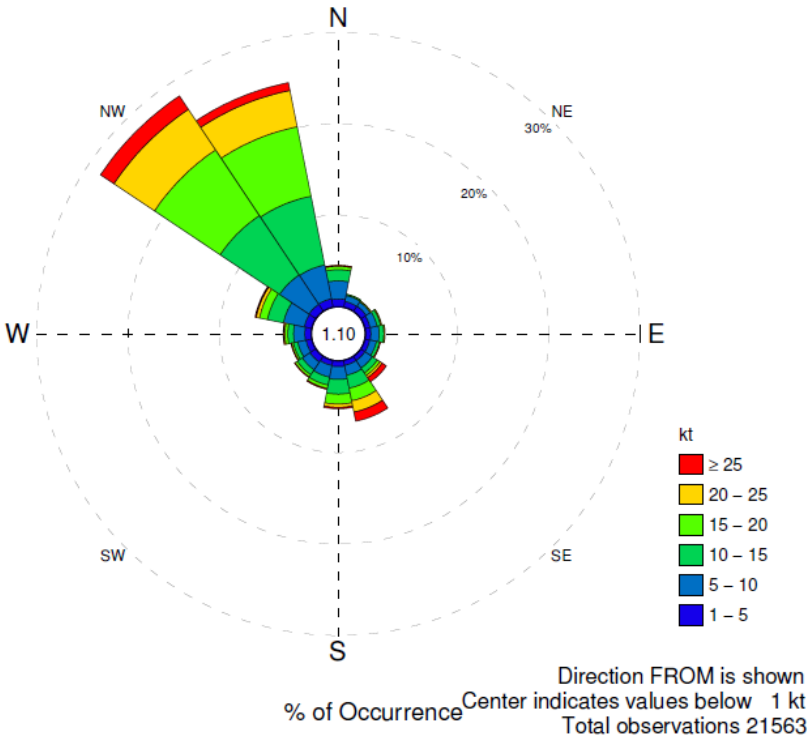
N
NW
NE
W
E
SW
SE
S
30%
20%
10%
1.10
kt
≥ 25
20 – 25
15 – 20
10 – 15
5 – 10
1 – 5
% of Occurrence
Direction FROM is shown
Center indicates values below 1 kt
Total observations 21563

April

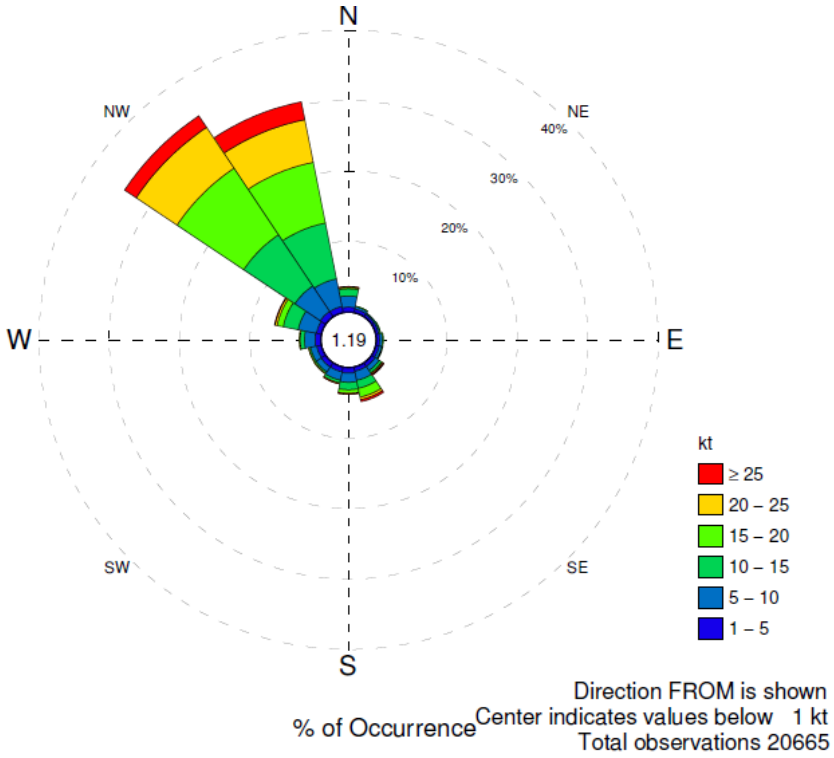
N
NW
NE
W
E
SW
SE
S
40%
30%
20%
10%
1.19
kt
≥ 25
20 – 25
15 – 20
10 – 15
5 – 10
1 – 5
% of Occurrence
Direction FROM is shown
Center indicates values below 1 kt
Total observations 20665

May

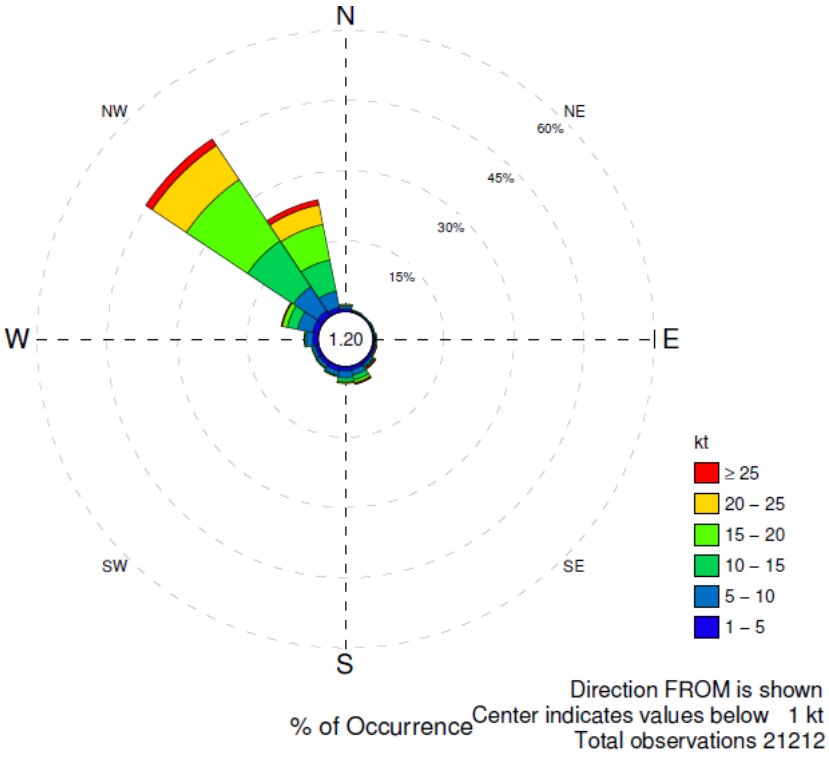
N
NE
E
SE
S
SW
W
NW
60%
45%
30%
15%
1.20
kt
≥ 25
20 – 25
15 – 20
10 – 15
5 – 10
1 – 5
% of Occurrence
Direction FROM is shown
Center indicates values below 1 kt
Total observations 21212

June

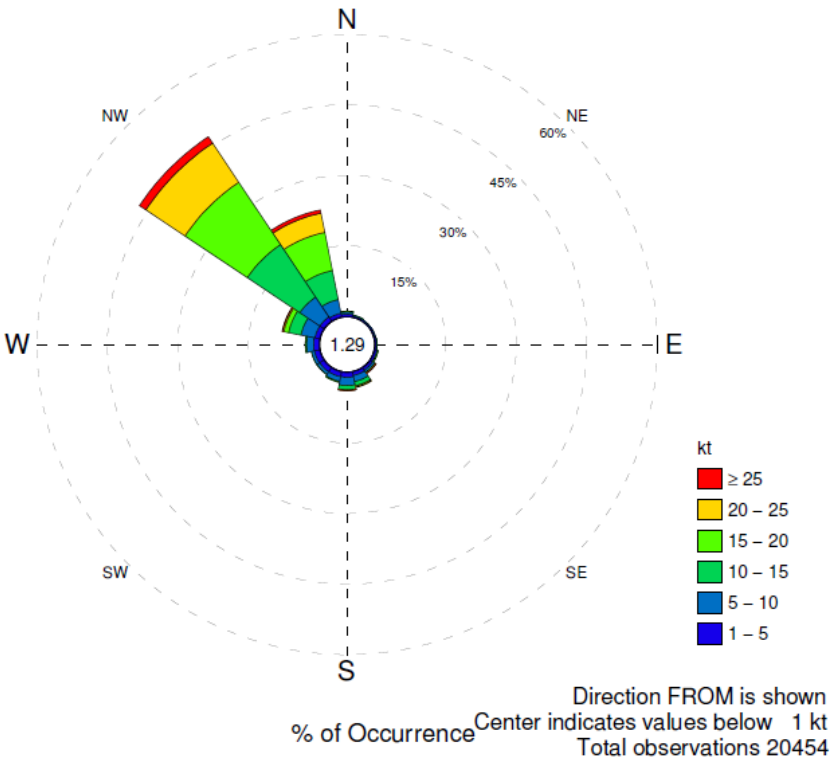
N
NE
E
SE
S
SW
W
NW
60%
45%
30%
15%
1.29
kt
≥ 25
20 – 25
15 – 20
10 – 15
5 – 10
1 – 5
% of Occurrence
Direction FROM is shown
Center indicates values below 1 kt
Total observations 20454

July

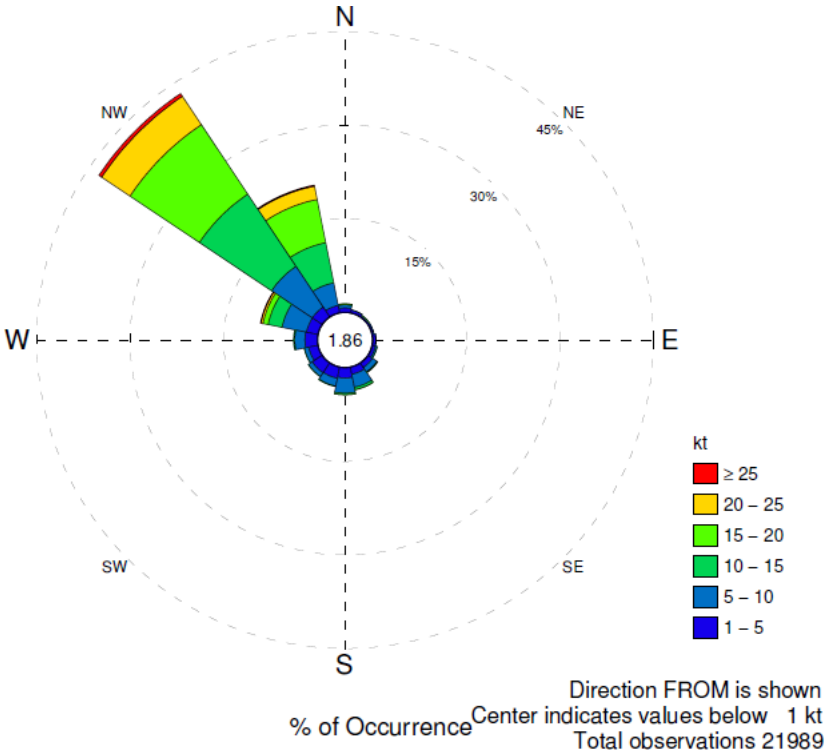
N
NE
E
SE
S
SW
W
NW
45%
30%
15%
1.86
kt
≥ 25
20 – 25
15 – 20
10 – 15
5 – 10
1 – 5
% of Occurrence
Direction FROM is shown
Center indicates values below 1 kt
Total observations 21989

August

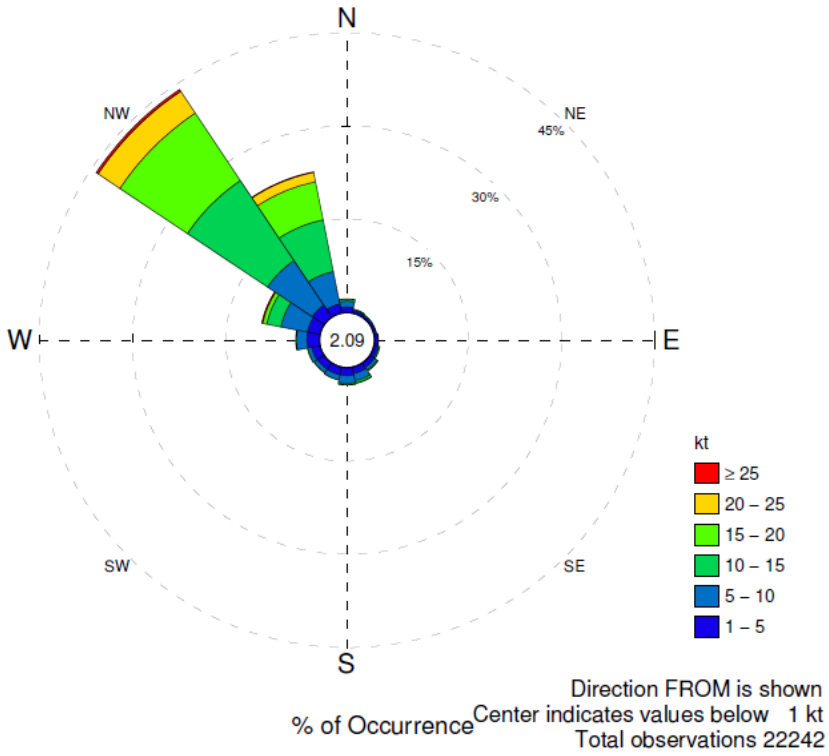
N
NE
E
SE
S
SW
W
NW
45%
30%
15%
2.09
kt
≥ 25
20 – 25
15 – 20
10 – 15
5 – 10
1 – 5
% of Occurrence
Direction FROM is shown
Center indicates values below 1 kt
Total observations 22242

September

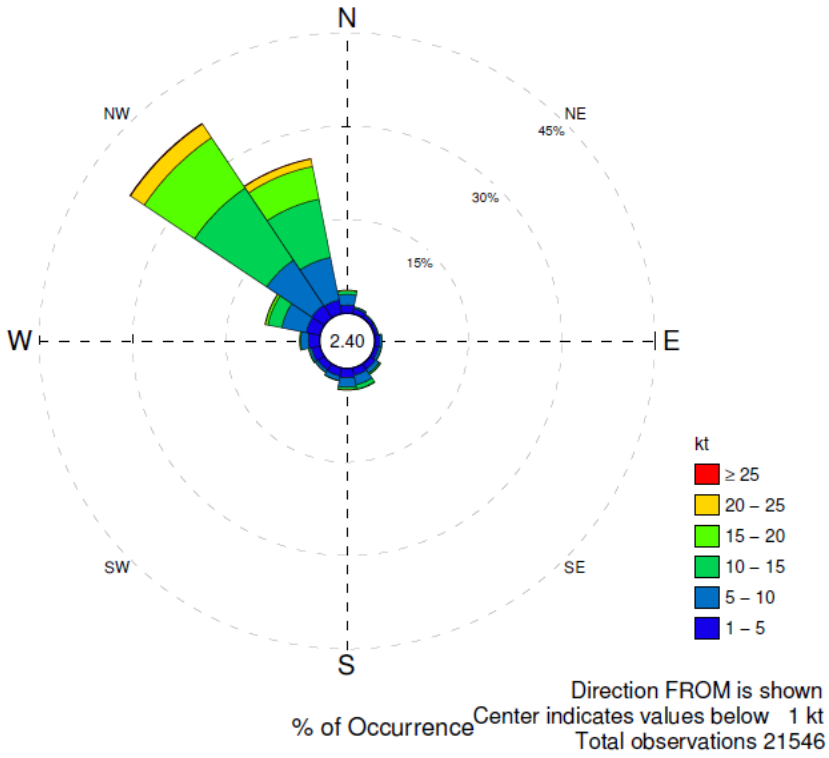

October

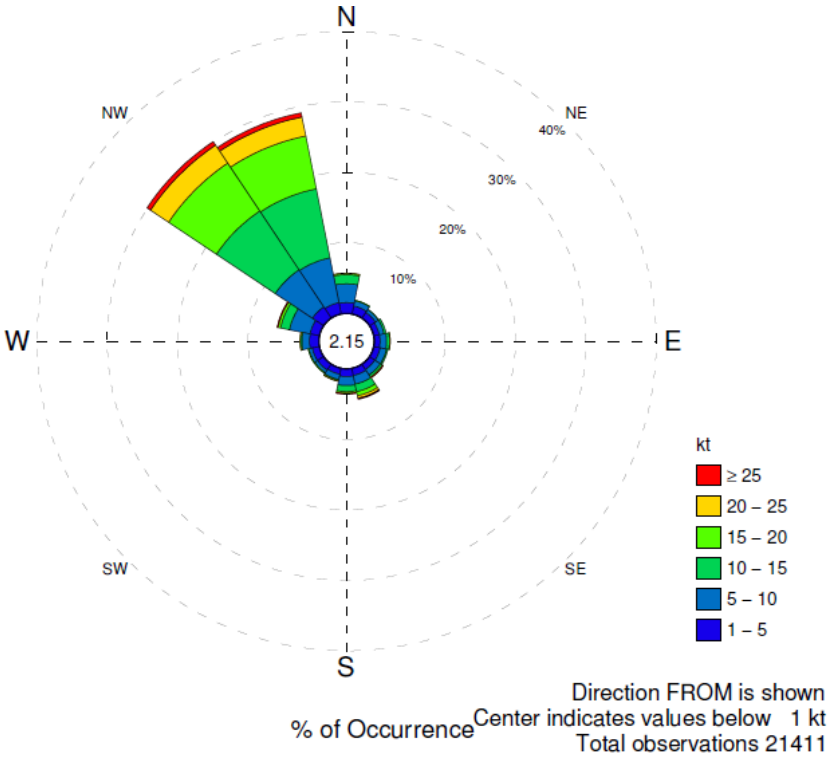

November

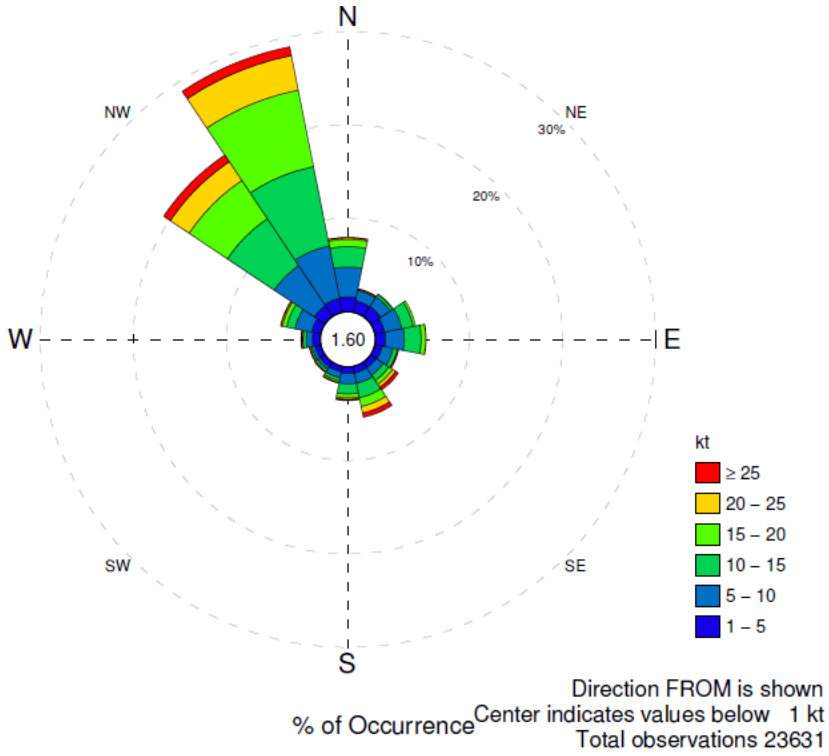

December

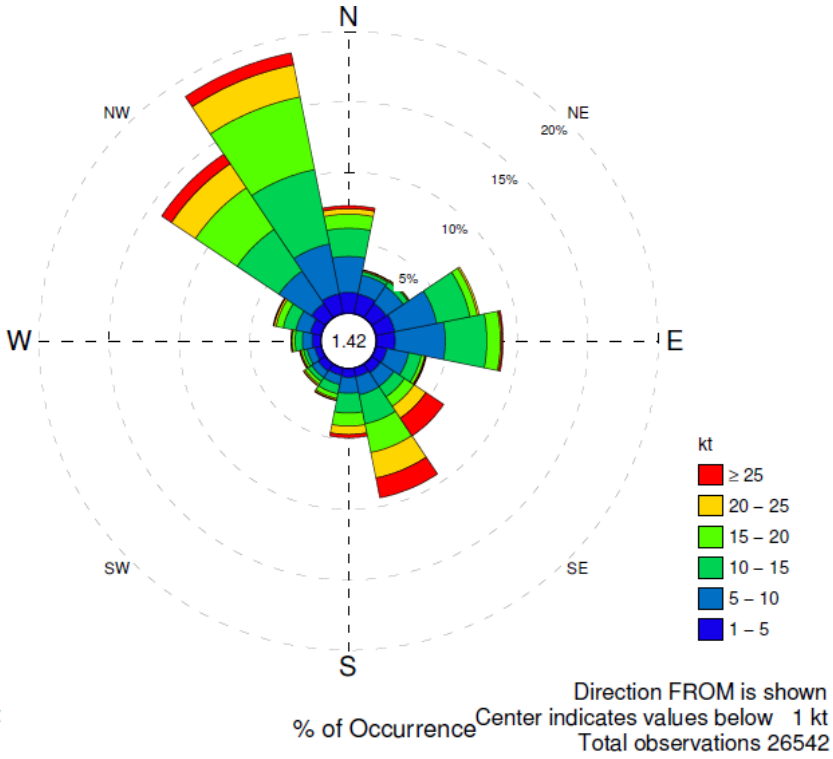

Appendix B:

Wentworth Classification Scale

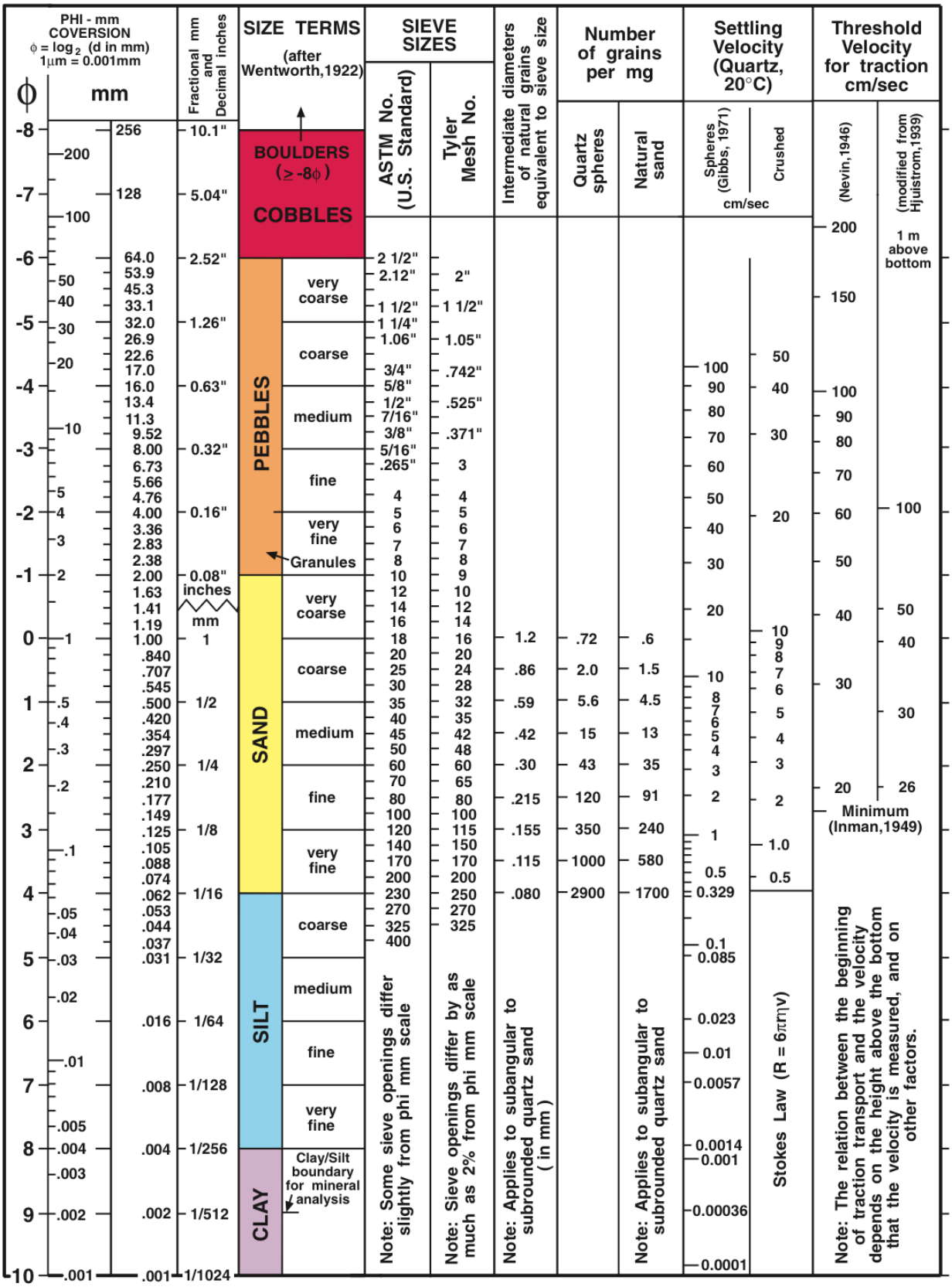
PHI - mm COVERSION
$\phi = \log_2$ (d in mm)
1μm = 0.001mm
ϕ
mm
Fractional mm and Decimal inches
SIZE TERMS
(after Wentworth,1922)
BOULDERS (≥ -8ϕ)
COBBLES
PEBBLES
very coarse
coarse
medium
fine
very fine
Granules
SAND
very coarse
coarse
medium
fine
very fine
SILT
coarse
medium
fine
very fine
CLAY
Clay/Silt boundary for mineral analysis
SIEVE SIZES
ASTM No. (U.S. Standard)
Tyler Mesh No.
Note: Some sieve openings differ slightly from phi mm scale
Note: Sieve openings differ by as much as 2% from phi mm scale
Intermediate diameters of natural grains equivalent to sieve size
Note: Applies to subangular to subrounded quartz sand (in mm)
Number of grains per mg
Quartz spheres
Natural sand
Note: Applies to subangular to subrounded quartz sand
Settling Velocity (Quartz, 20°C)
Spheres (Gibbs, 1971)
Crushed
cm/sec
Stokes Law (R = 6πηv)
Threshold Velocity for traction cm/sec
(Nevin,1946)
(modified from Hjulstrom,1939)
1 m above bottom
Minimum (Inman,1949)
Note: The relation between the beginning of traction transport and the velocity depends on the height above the bottom that the velocity is measured, and on other factors.

Appendix C:

Wave Transformation Coefficients

H_S (m)	H_S (ft)	T_P (s)	Wave Direction (from)								
			SSE	S	SSW	SW	WSW	W	WNW	NW	NNW
1.5	4.9	5.0	0.02	0.08	-	-	-	-	0.58	0.50	0.34
1.5	4.9	7.0	0.03	0.07	-	-	0.82	0.91	0.82	0.66	0.38
1.5	4.9	9.0	0.05	0.10	-	0.47	0.85	0.95	0.86	0.62	0.34
1.5	4.9	11.0	0.07	0.13	0.24	0.46	0.81	0.93	0.82	0.56	0.30
1.5	4.9	13.0	0.08	0.15	0.26	0.44	0.76	0.90	0.76	0.49	-
1.5	4.9	15.0	0.10	0.16	0.26	0.41	0.71	0.88	0.71	0.45	-
1.5	4.9	17.0	0.11	0.17	0.28	0.40	0.66	0.85	0.68	0.42	-
1.5	4.9	19.0	-	0.18	0.28	-	-	-	0.66	0.40	-
2.5	8.2	5.0	0.02	0.07	-	-	-	-	-	0.36	-
2.5	8.2	7.0	0.03	0.08	0.21	-	-	0.76	0.69	0.54	0.34
2.5	8.2	9.0	-	0.10	0.21	0.47	0.80	0.90	0.81	0.57	0.33
2.5	8.2	11.0	-	0.13	0.24	-	0.79	0.92	0.80	0.54	0.30
2.5	8.2	13.0	-	0.15	0.26	-	0.75	0.90	0.76	0.49	0.27
2.5	8.2	15.0	-	0.16	0.26	-	0.70	0.88	0.71	0.45	-
2.5	8.2	17.0	-	0.17	0.28	-	0.66	0.85	0.67	0.42	-
2.5	8.2	19.0	-	-	-	-	-	0.81	0.65	0.40	-
3.5	11.5	7.0	0.03	0.09	-	-	-	-	-	0.43	-
3.5	11.5	9.0	-	0.10	0.22	-	-	-	0.74	0.52	-
3.5	11.5	11.0	-	-	-	-	0.77	0.88	0.77	0.51	0.29
3.5	11.5	13.0	-	-	-	-	0.74	0.89	0.75	0.48	-
3.5	11.5	15.0	-	-	-	-	0.70	0.87	0.71	0.44	-
3.5	11.5	17.0	-	-	-	-	-	0.84	0.67	0.42	-
3.5	11.5	19.0	-	-	-	-	-	0.81	0.65	0.40	-
4.5	14.8	9.0	0.05	0.11	-	-	-	-	-	0.47	-
4.5	14.8	11.0	-	-	-	-	-	0.84	0.74	0.48	-
4.5	14.8	13.0	-	-	-	-	-	0.87	0.73	0.46	-
4.5	14.8	15.0	-	-	-	-	-	0.86	0.70	0.43	-
4.5	14.8	17.0	-	-	-	-	-	0.84	0.67	0.41	-
4.5	14.8	19.0	-	-	-	-	-	-	0.65	-	-
4.5	14.8	19.0	-	-	-	-	-	-	0.65	-	-

Ratio of nearshore significant wave height to offshore significant wave height, H_S/H_0.

H_S (m)	H_S (ft)	T_P (s)	Wave Direction (from)								
			SSE	S	SSW	SW	WSW	W	WNW	NW	NNW
1.5	4.9	5.0	1.34	0.64	-	-	-	-	1.11	1.11	1.12
1.5	4.9	7.0	1.04	1.04	-	-	0.99	0.99	0.99	0.98	0.98
1.5	4.9	9.0	1.02	1.01	-	1.00	0.99	1.00	0.99	0.99	0.99
1.5	4.9	11.0	1.01	1.00	1.00	0.99	0.99	0.99	0.99	0.98	0.99
1.5	4.9	13.0	1.01	1.00	1.00	0.99	0.99	1.00	0.99	0.99	-
1.5	4.9	15.0	1.00	0.98	0.98	0.97	0.98	0.98	0.98	0.98	-
1.5	4.9	17.0	1.01	1.02	1.02	1.02	0.98	0.97	0.97	0.99	-
1.5	4.9	19.0	-	0.98	0.97	-	-	-	1.01	1.00	-
2.5	8.2	5.0	1.36	1.02	-	-	-	-	-	1.17	-
2.5	8.2	7.0	1.28	1.27	1.06	-	-	1.05	1.05	1.04	1.03
2.5	8.2	9.0	-	1.02	1.01	1.00	1.00	1.00	1.00	0.99	0.99
2.5	8.2	11.0	-	1.00	1.00	-	0.99	0.99	0.99	0.98	0.99
2.5	8.2	13.0	-	1.00	1.00	-	0.99	1.00	0.99	0.99	1.00
2.5	8.2	15.0	-	0.98	0.98	-	0.98	0.98	0.98	0.98	-
2.5	8.2	17.0	-	1.02	1.02	-	0.98	0.97	0.97	0.99	-
2.5	8.2	19.0	-	-	-	-	-	1.00	1.01	1.00	-
3.5	11.5	7.0	1.30	1.27	-	-	-	-	-	1.08	-
3.5	11.5	9.0	-	1.03	1.02	-	-	-	1.00	1.00	-
3.5	11.5	11.0	-	-	-	-	0.99	0.99	0.99	0.99	0.99
3.5	11.5	13.0	-	-	-	-	0.99	1.00	0.99	0.99	-
3.5	11.5	15.0	-	-	-	-	0.98	0.98	0.98	0.98	-
3.5	11.5	17.0	-	-	-	-	-	0.97	0.97	0.99	-
3.5	11.5	19.0	-	-	-	-	-	1.00	1.01	1.00	-
4.5	14.8	9.0	1.29	1.05	-	-	-	-	-	1.01	-
4.5	14.8	11.0	-	-	-	-	-	0.99	0.99	0.99	-
4.5	14.8	13.0	-	-	-	-	-	1.00	0.99	0.99	-
4.5	14.8	15.0	-	-	-	-	-	0.98	0.98	0.98	-
4.5	14.8	17.0	-	-	-	-	-	0.97	0.97	0.99	-
4.5	14.8	19.0	-	-	-	-	-	-	1.01	-	-
4.5	14.8	19.0	-	-	-	-	-	-	1.01	-	-

Ratio of nearshore peak wave period to offshore peak wave period, T_P/T_{P0}.

H_S (m)	H_S (ft)	T_P (s)	Wave Direction (from)								
			SSE	S	SSW	SW	WSW	W	WNW	NW	NNW
1.5	4.9	5.0	1.58	1.39	-	-	-	-	0.91	0.86	0.82
1.5	4.9	7.0	1.58	1.38	-	-	1.02	0.96	0.91	0.85	0.80
1.5	4.9	9.0	1.58	1.38	-	1.11	1.02	0.96	0.90	0.84	0.79
1.5	4.9	11.0	1.58	1.38	1.23	1.11	1.02	0.95	0.89	0.83	0.78
1.5	4.9	13.0	1.59	1.39	1.24	1.12	1.02	0.95	0.88	0.82	-
1.5	4.9	15.0	1.59	1.39	1.24	1.12	1.02	0.94	0.88	0.82	-
1.5	4.9	17.0	1.60	1.40	1.25	1.12	1.03	0.94	0.88	0.81	-
1.5	4.9	19.0	-	1.40	1.25	-	-	-	0.88	0.82	-
2.5	8.2	5.0	1.58	1.39	-	-	-	-	-	0.86	-
2.5	8.2	7.0	1.58	1.38	1.24	-	-	0.96	0.90	0.85	0.80
2.5	8.2	9.0	-	1.38	1.23	1.11	1.02	0.95	0.89	0.84	0.79
2.5	8.2	11.0	-	1.38	1.23	-	1.02	0.95	0.89	0.83	0.78
2.5	8.2	13.0	-	1.39	1.24	-	1.02	0.95	0.88	0.82	0.77
2.5	8.2	15.0	-	1.39	1.24	-	1.02	0.94	0.88	0.82	-
2.5	8.2	17.0	-	1.40	1.25	-	1.02	0.94	0.87	0.81	-
2.5	8.2	19.0	-	-	-	-	-	0.94	0.88	0.82	-
3.5	11.5	7.0	1.58	1.39	-	-	-	-	-	0.84	-
3.5	11.5	9.0	-	1.38	1.23	-	-	-	0.89	0.83	-
3.5	11.5	11.0	-	-	-	-	1.02	0.95	0.88	0.83	0.78
3.5	11.5	13.0	-	-	-	-	1.02	0.95	0.88	0.82	-
3.5	11.5	15.0	-	-	-	-	1.02	0.94	0.87	0.82	-
3.5	11.5	17.0	-	-	-	-	-	0.94	0.87	0.81	-
3.5	11.5	19.0	-	-	-	-	-	0.94	0.87	0.81	-
4.5	14.8	9.0	1.58	1.38	-	-	-	-	-	0.83	-
4.5	14.8	11.0	-	-	-	-	-	0.95	0.88	0.83	-
4.5	14.8	13.0	-	-	-	-	-	0.94	0.88	0.82	-
4.5	14.8	15.0	-	-	-	-	-	0.94	0.87	0.82	-
4.5	14.8	17.0	-	-	-	-	-	0.94	0.87	0.81	-
4.5	14.8	19.0	-	-	-	-	-	-	0.87	-	-
4.5	14.8	19.0	-	-	-	-	-	-	0.87	-	-

Ratio of nearshore wave direction to offshore wave direction, α/α_0.